Heat Release Rates

26

Vytenis Babrauskas

Introduction

Calculations of fire behavior in buildings are not possible unless the heat release rate of the fire is known. This chapter on heat release rates provides both theoretical and empirical information. The chapter is organized so that theory and basic effects are considered first, then a compendium of product data is provided, which is arranged in alphabetic order.

Definitions

The essential characteristic that describes quantitatively *How big is the fire?* is the heat release rate. This is so important that it has been described as the single most important variable in fire hazard [1]. The heat release rate (HRR) of a burning item is measured in kilowatts (kW). It is the rate at which the combustion reactions produce heat. The term "burning rate" is also often found. This is a less specific term, and it may either denote the HRR or the mass loss rate. The latter is measured in units of kg s^{-1}. It is best to reserve 'burning rate' for non-quantitative fire descriptions and to use either HRR or mass loss rate, as appropriate. The relationship of these two quantities can be expressed as:

$$HRR = \Delta h_c \times MLR \qquad (26.1)$$

where h_c is the effective heat of combustion (kJ kg^{-1}) and MLR is the mass loss rate (kg s^{-1}). Such an equation implies that HRR and MLR are simply related by a constant. This is not in general true. Figure 26.1 shows the results obtained from a test on a 17 mm sample of Western red cedar. It is clear that the effective heat of combustion is not a constant; it is roughly 12 MJ kg^{-1} for the first part of the test, but increases to around 30 MJ kg^{-1} during the charring period at the end of the test.

In principle, the effective heat of combustion can be determined by theory or by testing. In practice, if the effective heat of combustion is not a constant, then experimental techniques normally involve directly measuring the HRR, rather than using Equation 26.1.

Measuring the HRR, Full-Scale

The simplest case is when full-scale HRR can be directly measured. This can be grouped into two types of techniques:

- Open-burning HRR calorimeters
- Room fire tests.

Open-burning HRR calorimeters were developed in the early 1980s at NIST by Babrauskas and colleagues [2] and at FMRC by Heskestad [3]. The operating principles of these calorimeters are described in Chap. 27. Based on this work, a large number of different test

V. Babrauskas (✉)
Fire Science and Technology Inc.

M. Hurley (ed.), *SFPE Handbook of Fire Protection Engineering*,
DOI 10.1007/978-1-4939-2565-0_26,

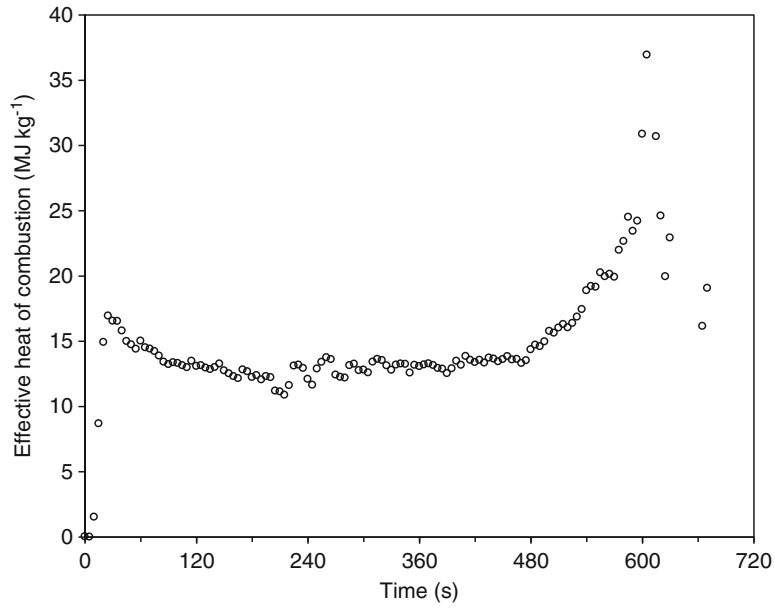

Fig. 26.1 Effective heat of combustion for 17 mm thick Western red cedar, tested at an irradiance of 65 kW m^{-2}

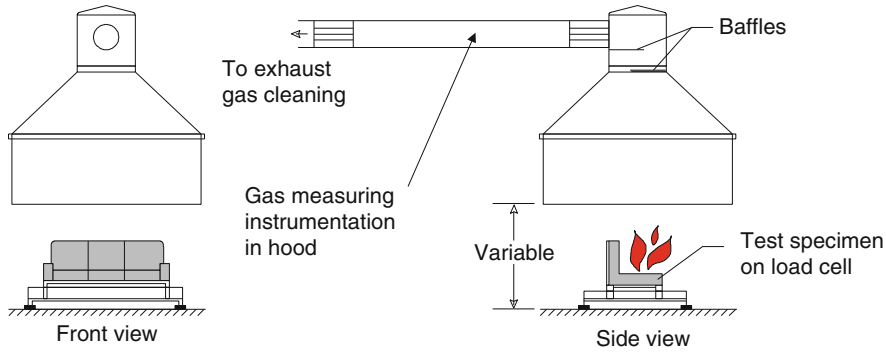

Fig. 26.2 NORDTEST NT FIRE 032 calorimeter

standards have been issued, for example [4–8]. A discussion of a number of other standards can be found [9].

The NORDTEST furniture calorimeter [7] is shown in Fig. 26.2. Open-burning HRR measurements are simpler to make since a test room does not need to be constructed. The HRR within a room and under open conditions are, clearly, identical at very low HRR. What happens at higher values of HRR depends on the situation at hand. If the fire is so large that room flashover can be reached (about 1.5–1.75 MW if ventilation is through a single normal-sized door opening) then actual room HRR values post-flashover can be drastically different from their open-burning rates. This is due primarily to additional radiant heat flux contribution from the hot gas layer and the hot room surfaces, although ventilation effects can also play a role.

For upholstered chairs, extensive studies have shown that room effects are only at the 20 % level up to a 1 MW fire [10]. The same study, however, showed that for mattresses, a room presence effect shows up at much lower HRR values. For liquid pools, the HRR is strongly

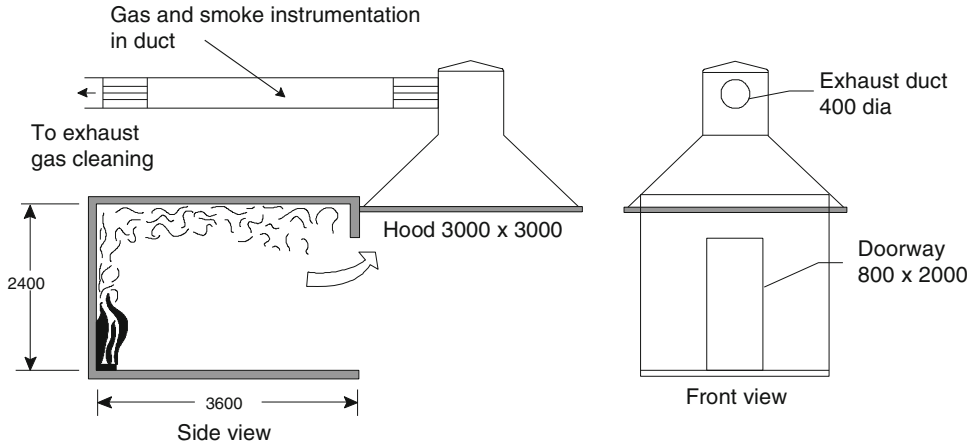

Fig. 26.3 ISO 9705 room HRR test

affected by the surrounding room [11]. For most other commodities, this issue has not been studied.

The degree by which the room affects the HRR is largely determined by how 'open' the fuel package itself is. A liquid pool on the floor has a view factor of 0 to itself and 1.0 to the room. By contrast, the reason that chairs tend to be little-affected by the room is that the chair 'sees' its own surfaces to a significant extent, rather than being fully-exposed to the room. Some useful error analyses of large open calorimeter measurements have been reported [12]; a theoretical discussion of the 'ideal' large scale calorimeter has also been presented [13].

Room fire tests should be commissioned when room effects are anticipated to be strong, or when a more precise estimate is needed. Apart from cost, there is a drawback to room fire testing. This is because the

HRR measured in a room fire cannot be extrapolated to any rooms with larger ventilations. Open-burning HRR data could, by contrast, be applicable to such well-ventilated rooms.

The development of the modern room HRR test took place at several institutions, including Fisher and Williamson at the University of California [14], Lee at NIST [15], and Sundström at the Swedish National Testing and Research Institute [16]. Room test standards include [17, 18] and also [4, 5]. A typical standard room fire test, ISO 9705 is shown in Fig. 26.3; a similar room fire test is ASTM E 2257 [19]. This test equipment is available for commercial testing in North America, Europe, Asia, and other places.

Measuring the HRR, Bench-Scale

To measure the HRR in a bench-scale test is nowadays an easy task. Most commonly, the Cone Calorimeter [20] developed at NIST by Babrauskas will be used (Fig. 26.4). These instruments are available at commercial and research laboratories worldwide. The procedures for conducting Cone Calorimeter tests are described in ASTM E 1354 [21] and ISO 5660 [22]. Other HRR calorimeters, such as the Ohio State University apparatus or the Factory Mutual Research Corp. Flammability Apparatus are also in use at some laboratories. A textbook is available which discusses many of the details of HRR measuring technology [23]. Thus, the modeler can assume that if at least enough material is available to run several small samples (100 mm × 100 mm, in the case of the Cone calorimeter), an empirical HRR curve can be obtained by running bench-scale tests.

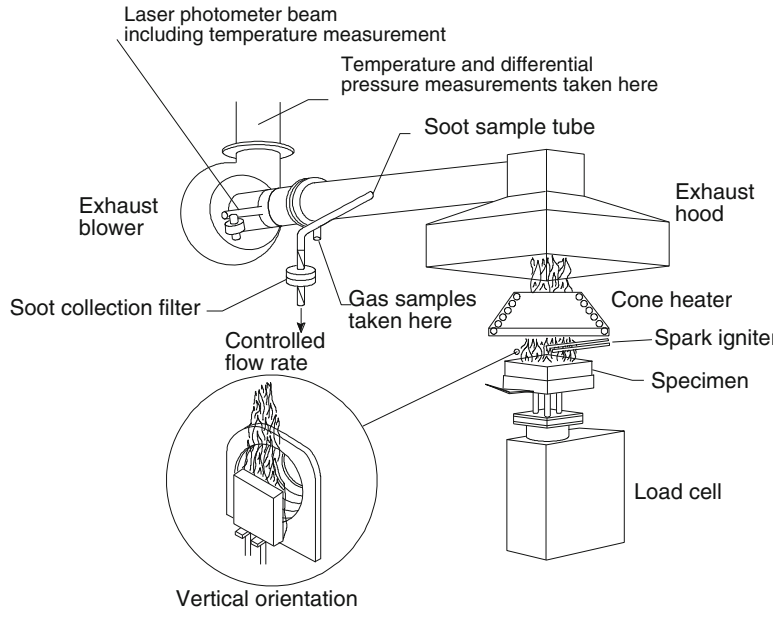

Fig. 26.4 The cone calorimeter

Measuring the HRR, Intermediate-Scale

The newest experimental technology for determining the HRR is intermediate-scale calorimetry. Various earlier efforts have been made, but the first instrument to receive standards support is the ICAL, developed at Weyerhaeuser [24] (Fig. 26.5). It has been standardized as ASTM E 1623 [25]. This test method accommodates 1.0 m by 1.0 m specimens, which allows for complex or highly non-homogenous constructions to be tested. However, since the data are still not of full scale, some additional analysis is needed to be able to utilize the test data in fire modeling.

Modeling Implications for Using Full-Scale HRR Data

If access is available to full-scale HRR data, then the task of defining the fire is on a solid basis. Even here, however, there are a number of problems and caveats. Apart from the obvious issue that the available full-scale data must be known to describe the specific fuel source in question (and not some possibly very differently performing 'similar' item), there are some additional concerns. Supposing one finds full-scale test results on one's exact commodity, can the data simply be used unquestioningly? The answer, of course, is not. There are two main issues:

- The available data may be open-burning calorimetry data. One must then determine if there is an enclosure effect to be accounted.
- The available data may be room fire data, but the test enclosure may not correspond to the room for which modeling is to be done.

The first of these issues was briefly touched on above already. The availability of quantitative guidance is lacking. For upholstered chair fires in a room of about the size of the ISO 9705 room, one can estimate a 20 % augmentation over the open-burn rates when considering fires in the 100–1000 kW range. For mattresses, the effect is large and without adequate guidance. For liquid pools, a pool sub-model must be specifically present in the fire model used, since no simple approximation is adequate. For wood cribs, there are formulas for guidance [26], although of course wood cribs are hardly a feature of most real fires. For other combustibles, neither data nor guidance is available.

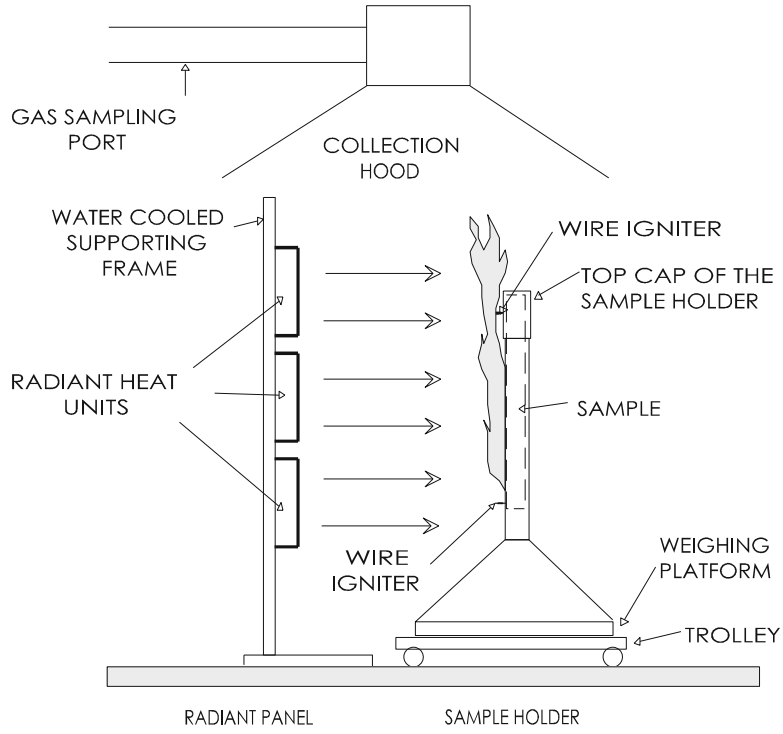

Fig. 26.5 Intermediate scale (ICAL) calorimeter

A very similar problem is faced when the modeler has available full-scale HRR data, but the test was run in a room of rather different size or ventilation conditions than is the intended application. Only two studies on this topic have been published in the literature. Kokkala and colleagues compared [27] some room wall/ceiling linings in a large room to the values obtained in the ISO 9705 room. Also, during the CBUF project some furniture fires were done in rooms of two scales [10]. Neither of these studies looked at this issue comprehensively enough to yield numerical guidance.

Some European designers have proposed that 250 or 500 kW m^{-2} of floor area is an appropriate peak value of HRR according to which to design buildings of almost any kind [28]. It is not clear how these values were obtained, but one must consider whether they are conservative. Figure 26.48 gives HRR data for one pallet and half a pallet loads of some elastomer pellets. While these are 'industrial' materials, nonetheless substances of similar heat of combustion and state of aggregation can readily be found in shops, storage rooms, and various other places in diverse building types. The test data showed that the whole-pallet test had to be extinguished at about 4500 kW m^{-2}; the fire was still growing, and its ultimate HRR would have been higher.

Growth curves for the FM data listed in Table 26.8 are not available; nonetheless the peak values of roughly 2,000–20,000 kW m^{-2} are sobering. Goods of this kind cannot occupy anywhere close to 100 % of the floor area, of course, but even assuming coverage at ¼ to ½, the actual HRR values are enormous. Now, there are clearly occupancies where it is impossible to introduce high fuel loads—swimming facilities may be an example. But other facilities, even if designed to be spartan in actual use (e.g., ceremonial lobbies) may sustain large fuel loads during construction, remodeling, expansion, and similar activities.

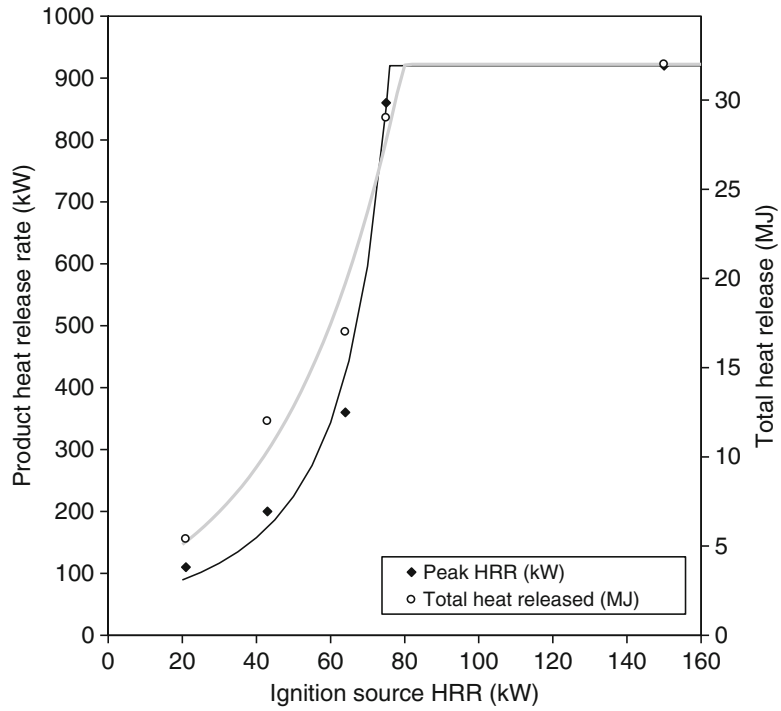

Fig. 26.6 Effect of ignition source on the HRR of PVC foam wall coverings

Effect of Ignition Source on Full-Scale HRR

Full-scale tests for HRR usually do not impose an *overall* radiant heat flux and are ignited with localized flame sources. But locally, the heat fluxes from various ignition sources will differ both in their magnitude and in the size of the area subjected to the heat flux. Most plastic commodities that do not contain fire retardants (and are not made from an intrinsically-FR plastic) can be ignited with very small flame sources, often no bigger than a paper match. FR commodities, however, will resist ignition from small flames, but may be ignited from a large-flame ignition source. Commonly, such products show an all-or-nothing behavior. That is, ignition sources below a certain size will cause essentially no heat release from the test article, while a larger ignition source may cause a large fraction of, if not the total, combustible mass of the article.

For example, it was shown [29] that a television cabinet made from a plastic fire retarded to the extent of obtaining a V-0 classification in the UL 94 [30] test gave no heat release when using a 10 kW burner, but burned well when exposed to a 30 kW burner. Dembsey [31] conducted room tests on rooms partially lined with a PVC-foam wall covering. His results are shown in Fig. 26.6. Note that the curve is very steep and could be represented reasonably by a step-function. Apart from a few examples, this type of data, unfortunately, is very rarely available for practical commodities of engineering interest.

Effects of Other Variables

Some *thermoplastic materials* have a highly pronounced tendency to melt and flow. Consequently, commodities made from these materials, when burning, will often exhibit object burning above the floor and an accompanying pool fire at the floor, formed by the melt material. Sherratt and Drysdale [32] studied the problem in intermediate scale, by burning vertical polypropylene sheets above various floor materials.

Major differences were found both in the peak HRR and in the time-resolved HRR curve, depending on the floor type. The differences were largely attributable to thermal characteristics (thickness, density, thermal conductivity, etc.) of the floor materials. Upholstered furniture using plastic foam padding often burns with a secondary pool fire underneath, however, this behavior occurs only in some cases.

Modeling with Bench-Scale HRR Data

If full-scale data on HRR are available, then these are simply used in the fire model. In many cases, however, such data are not available, often due to cost of testing or unavailability of large size specimens. In such cases, it is desirable to be able to use bench-scale data, denoted as and measured in units of kW m^{-2}. With the bench-scale HRR, there are two main questions: (1) can it be predicted from some more fundamental measurements? and (2) how can the full-scale HRR be predicted from the bench-scale HRR?

Predicting Bench-Scale HRR from Fundamental Considerations

The former question has been of considerable interest to fire researchers, but practical engineering methods are not yet at hand. This task is often described as creating a 'pyrolysis model,' since the degradation of a material when it is exposed to heat is known as pyrolysis. When a material heats up, degrades, ignites, and burns, some very complicated physical and chemical phenomena are taking place. In addition to a change of phase, there is often flow of moisture simultaneously with heat flow.

The material may undergo several different types of phase changes during the decomposition process, each accompanied by changes in density and porosity. Bubbles may be created within the bulk of the material and migrate to the surface. These may be accompanied by molten flow ejection at the surface. Oxygen may or may not directly interact with the surface to create a glowing combustion.

The chemical reactions being undergone are commonly several in number and occurring at different temperature regimes. Finally, the material may undergo large-scale cracking, buckling, or sloughing. Each of these physical phenomena may significantly affect the rate of specimen decomposition. From even this very brief description, it is clear that computing the pyrolysis of a material may be a difficult task. Thus, today for any fire hazard analysis purposes, HRR is invariably measured, rather than being computed from more fundamental theory.

Readers wishing to look more closely at the type of modeling needed to represent the pyrolysis process can refer to the dissertation of Parker [33] as a good example of how charring materials need to be treated. Some half-dozen other dissertations have been written on the same topic. Melting type materials have proven to be even more interesting as a subject of advanced research. Several hundred of papers have been published on various aspects of modeling the pyrolysis behavior of just one common material, poly(methylmethacrylate). References [34–40] can provide an introduction to this research.

Predicting Full-Scale HRR from Bench-Scale Data: Overview

Prediction of full-scale HRR is probably the single most important engineering issue in successful modeling of fires. Schematically, we may write that:

$$\dot{q} = \int \dot{q}'' dA \tag{26.2}$$

This representation does not fully reveal the difficulties involved. More explicitly,

$$\dot{q}(t) = \int \dot{q}''(t, x, y, z) dA(t) \tag{26.3}$$

This makes more clear that the instantaneous per-unit-area HRR is a function of time and also of the location of the burning element. The instantaneous burning area, A(t), is also a function of time. In addition, while we have not written this explicitly, $\dot{q}''(t)$ depends on the heating boundary conditions to the element. This quantity usually identified as the *heat flux* or *irradiance* incident upon the element. The latter term is commonly used since in full-scale fires the heating is dominated by the radiant component.

By examining the nature of dA(t), we can also identify the role of flame spread in characterizing the HRR of full-scale fires. A bench-scale HRR test specimen is usually ignited nearly-instantaneously over its entire surface. Full-scale fire, by contrast, nearly always exhibit finite spread rates. The flame spread velocity in a full-scale fire can be identified with the movement of the boundaries of the flame-covered area dA(t). Flame spread may occur in several directions over walls, ceilings, floors, and over individual surfaces of discrete commodities burning in a space. Consequently, it can be seen that tracking flame spread and dA(t) is a major undertaking. This task, by its nature, is incompatible with zone-type of fire models, since it presumes that a mechanism is in place to track very small surface elements. Such mode line is variable with CFO models [41] the quality of production is dependent on fuel type and the user needs to verify the permanent details.

Our approach will have to be restricted to identifying some of the attempts which have been made to simplify the problem in order to make it tractable for zone modeling. Simplifications are not yet possible for the 'general' case. Instead, we must examine specific combustibles, for which appropriate flame spread representations have been established. This is illustrated in a number of the sections below. Before we do this, however, it is important to examine in more detail some of the variables which influence the HRR.

Predicting Full-Scale HRR from Bench-Scale Data: The Role of Irradiance

Engineering variables such as HRR, ignitability, flame spread, etc. are sometimes viewed as material fire properties. This is a useful view, but it must be kept in mind that such 'properties' are not solely properties defined by the physical/chemical nature of the substance. Instead, they are also determined by the boundary conditions of exposure. The boundary conditions can be divided into two types: (1) intended, and (2) unintended. The intended boundary conditions include irradiance (since the heat fluxes in room fires are dominated by the radiant component, the terms irradiance and imposed heat flux are used interchangeably) and thickness. Unintended boundary conditions, sometimes known as *apparatus-dependencies*, include such factors as edge effects, perturbations due to non-uniform heating, drafts and uncontrolled air velocities, etc. The latter are usually small if a well-designed test apparatus was used for measuring the response of the specimen.

The most significant intended boundary condition is the heat flux imposed on the specimen. This variable is crucial and no reduced-scale HRR results have meaning without knowing the irradiance. A test apparatus can impose a very wide range of specimen irradiances. For example, the Cone Calorimeter is capable of irradiances from zero to 100 kW m^{-2}. For the user of the data, the crucial question becomes what irradiance to select when requesting a test. There are no simple answers to this, but we summarize here the main conclusions of an extensive study [42].

The major consideration in the selection of the test irradiance must come from a knowledge of heat fluxes associated with real fires. In theory, this could range from zero to an upper value which would be $\varepsilon\sigma\left(T_f^4 - T_o^4\right)$, where ε = emissivity (–), σ = Stefan-Boltzmann constant (5.67 10^{-11} kW m^{-2} K^{-4}), T_f = flame temperature (K), and T_o = ambient temperature (K). But the

$\varepsilon \approx 1$ for larger flames, and the ambient temperature contribution is insignificant, since $T_o << T_f$.

The adiabatic flame temperature for most organic fuels [43] is approximately 2300 K. This would give a maximum irradiance limit of some 1500 kW m^{-2}. This limiting value is, of course, nearly 10 times the actual maximum that is found in building fires of normal types. Thus, it is evident that the theoretical bounds to possible heat fluxes do not offer any guidance for testing. Instead, it is necessary to look at experimental data on heat fluxes found in actual building fires. We divide this into several types of building fires to be examined. More detailed data on heat fluxes from various objects and ignition sources is contained in the *Ignition Handbook* [44].

(a) **Heat fluxes in the vicinity of ignition sources**

First, we must be clear by what is meant by 'ignition source.' The innate definition of the term does not have limits—a burning building can be the ignition source to its neighboring building, as can a fire bomb. For discussion here, however, ignition sources can be limited to those that are small with respect to a fully-developed room fire. Since the latter will be in the range of over 1 MW, the range of fires considered to be ignition sources might be taken as $<$ ca. 300 kW.

A NIST study examined various ignition sources, ranging from 5 W to over 300 kW [45]. The sources included both realistic igniting objects (cigarettes, matches, burning paper lunch bags, etc.) and schematic ones (small gas burners and wood cribs). It was found that, as the power output of the ignition source increased, the peak heat flux generally did not increase. Instead, only the area covered by the peak heat flux progressively increased. For flames ranging from a 0.3 kW Bunsen-type burner to a 50 kW wastebasket, the peak fluxes were remarkably constant at 30–40 kW m^{-2}. Thus, for HRR from objects being ignited with a small ignition source, a test irradiance of 35 kW m^{-2} can be selected. There are some unusual sources having a much higher flux, and these are discussed elsewhere [42].

For larger burners, such as used in room fire tests, higher heat fluxes may have to be assumed. For porous square-faced gas burners, the wall heat flux was found to depend on the burner face size [46]. In some cases, fluxes up to 65–80 kW m^{-2} were noted, although for most cases fluxes of 30–50 kW m^{-2} are considered appropriate [47].

At the extreme, ignition can occur due to a high velocity jet, such as from a failure on an oil-drilling rig. There, heat fluxes in the vicinity of 150–300 kW m^{-2} have been observed [48]. Such situations, however, are very specialized. For ignitions from small wood cribs or other solid-fuel ignition sources, it can be estimated that the heat flux to adjacent objects in the same 35 kW m^{-2} range as for small flaming sources. The picture is more complicated, however, for the heat flux from these sources to the object underneath. These heat fluxes may be much higher [42], but they are highly non-uniform and difficult to model.

(b) **Heat fluxes in preflashover room fires**

After ignition, the combustibles in a room can be considered to be exposed to preflashover conditions. Heat fluxes occurring in preflashover room fires will vary widely. Away from the initial source of fire there will be essentially no heating at all. Near a small initial fire source, heat fluxes of the sort described in the preceding section will be seen. With increasing fire spread and involvement, a hot gas layer will build up below the ceiling. The heat fluxes will be significantly hotter within this layer than in lower spaces. Söderbom [49] found values typically $<$ 45 kW m^{-2} at the center of the ceiling during preflashover fires. The value at the floor level is, of course, always $<$ 20 kW m^{-2} prior to flashover, since attaining 20 kW m^{-2} at floor level is one definition of flashover [50]. Since there is surprisingly little general guidance on this point, the user will have to make some assumptions or *ad hoc* calculations.

(c) **Heat fluxes on burning walls**

Heat fluxes from burning items of larger types have, in general, not been studied in enough detail to be systematically known. The notable exception is for upward flame spread on vertical

surfaces. For this configuration, a number of studies have explored the heat fluxes from the flame to the yet-unignited portion of the surface.

Hasemi studied this problem in detail [51] and provided correlations. For his experiments, peak values of ca. 25 kW m^{-2} were seen for the region downstream of the ignited area, but before the tip of the flames; beyond the flame tip, fluxes were no longer constant, but dropped off further downstream. Additional similar data have also been presented in a summary form [52]. Work by Kulkarni and co-workers has enlarged the diversity of material types to have been studied [53]. The value of 25 kW m^{-2} is seen from these more extensive studies to be the lower bound of where data are clustered—most of the data are in the interval from 25 to 45 kW m^{-2}. Thus, a value of 35 kW m^{-2} might better capture the mean behavior.

A 35 kW m^{-2} heat flux, then, can be used to characterize the peak level of heating to a vertical surface element from its own upstream flame, just prior to its ignition. This value will need to be increased if the material is so situated as to be in a hot gas layer that is accumulating in the upper reaches of the room. Apart from the data of Söderbom, discussed above, this additional heating has not been studied in detail.

(d) **Heat fluxes in post-flashover room fires**

The maximum temperatures actually seen in post-flashover room fires are ca. 1100 °C. A perfect black-body radiator at that temperature would produce heat fluxes of approximately 200 kW m^{-2}. Actual heat fluxes measured in post-flashover room fires can come close to this value, but are usually somewhat lower. For instance, examining the extensive room burn data of Fang [54], one finds the following ranges of experimental results shown in Table 26.1.

Table 26.1 Heat fluxes measured in postflashover room fires

	Heat flux (kW m^{-2})		
	Ceiling	Walls	Floor
Maximum	106–176	116–229	119–143
Average	68–147	91–194	–

One might reasonably conclude that a heat flux of ca. 150 kW m^{-2} would be needed to properly represent the environment of the post-flashover room fire. Today's bench-scale HRR apparatuses, however, can only go to about 100 kW m^{-2} or less. Interestingly, the inability to realistically create the heat fluxes of the post-flashover fire has not been seen to be a problem in fire testing. Often, the situation is avoided in its entirety by assuming that the maximum burning rate that will occur within the room is consistent with the available oxygen supply [55]. Nonetheless, if for more detailed fire modeling the HRR of individual items in the post-flashover fire would be required, such high heat flux values would be required.

The Dependence of the HRR on the Heat Flux

In the simplest case, the relationship of the HRR to the irradiance is very simple, as shown in Fig. 26.7. Here, we see that the HRR depends in a linear manner on the irradiance. The curve does not pass through the origin due to the existence of flame flux. The total heat flux seen by the specimen can be viewed as comprised of two components: the external irradiance, and the flux from its own flame. Only if the flame flux were zero would the curve pass through the origin. Otherwise, the x-axis intercept is equal to (minus) the flame flux.

Flame flux is very difficult to measure experimentally, as decomposing materials tend to foul the instrumentation and invalidate the readings. A value of ca. 35 kW m^{-2} has been reported for the flame flux of PMMA burned in the horizontal orientation in the Cone Calorimeter [56]. In another study, estimates of flame flux were made for several plastics burned in a similar manner [57]. These showed 30, 25, and 14 kW m^{-2}, respectively, for nylon, polyethylene, and polypropylene. The furniture research program CBUF [10] determined that the flame fluxes in the Cone Calorimeter associated with fabric/foam composites are in the range 20–25 kW m^{-2}. Finally, some data are

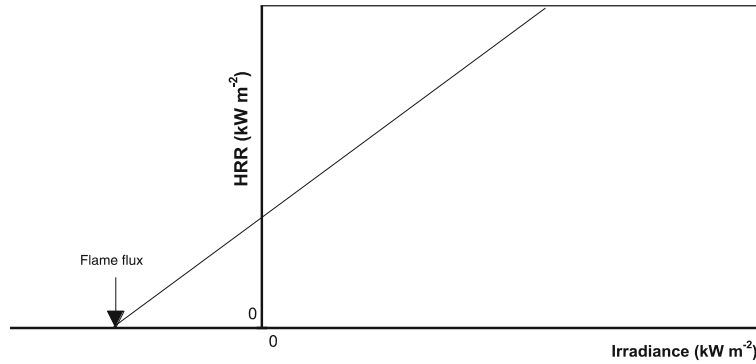

Fig. 26.7 The simplest form of HRR dependence on irradiance

available [58] for liquids in containers of similar size as a Cone Calorimeter specimen holder. Flame fluxes of about 10–15 kW m^{-2} are seen for alcohols and about 15–20 kW m^{-2} for some hydrocarbons (heptane, methylmethacrylate, toluene, styrene).

The value appears to depend only slightly on the chemical nature of the fuel. Gore et al. [58] specifically determined that this value does not increase with increasing fuel sooting tendencies. All of the above data refer specifically to the horizontal specimen orientation. There is very little data for the vertical orientation, although Janssens deduces that for wood products the vertical-orientation flame flux is ca. 10–15 kW m^{-2}, of which only about 1 kW m^{-2} is due to radiation [59].

With regards to linearity, the following very broad generalization can be made: for many products, over a substantial heat flux range, the HRR is linearly proportional to the heat flux. This generalization, however, will be seen to have only limited utility, since it is rarely known *a priori* whether or not it will be obeyed. Furthermore, there is a distinct tendency for most materials and products to deviate from linearity at very high and at very low heat fluxes.

This behavior is best illustrated by an example. Some data obtained by Sorathia and co-workers [60] on advanced composites are shown in Fig. 26.8. It is clear that the results are somewhat linear, but not precisely so. Some old, but still suggestive data were obtained in the 1970s by Parker [61]. His results for a number of fire-retardant grades of polyurethane foam are shown in Fig. 26.9. Of the five formulations shown, three show somewhat linear behavior, whereas two clearly do not. For most categories of specimens, however, substantially linear behavior can be seen.

Predicting Full-Scale HRR from Bench-Scale Data: The Effect of Thickness

The same material may be used in different applications in varying thicknesses. Thickness does affect the HRR response. In general, a thin material will show a spike of HRR, whereas a thick product will commonly (but not always) show some quasi-steady period of burning. This variable has not been extensively explored, and there is not much guidance available. Figure 26.10 shows results from Paul [62] on a thermoplastic, PMMA. This illustrates that near-steady burning behavior can be seen when the thickness approaches ca. 20 mm. Some similar data on polyethylene [63] have been published, but the maximum thickness specimens examined in that study, 10 mm thick, did not reach steady burning.

Data for medium-density wood fiberboard obtained by Tsantaridis [64] are shown in Fig. 26.11. If tested over the standard substrate (lightweight mineral fiber blanket), wood-family materials show a second HRR peak which corresponds to the accelerated burning when the specimen becomes nearly burned through.

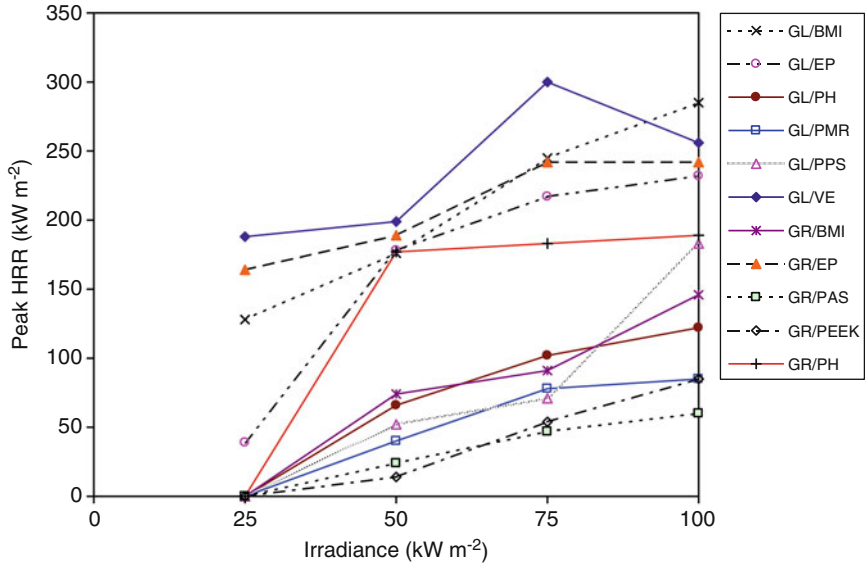

Fig. 26.8 Response to irradiance of some advanced composite materials. Reinforcements: *GL* glass, *GR* graphite. Resins: *BMI* bismaleimide, *EP* epoxy, *PAS* polyaryl sulfone, *PEEK* poly(ether ether ketone), *PH* phenolic, *PMR* monomer-reactant polyimide, *PPS* polyphenylene sulfide, *VE* vinyl ester

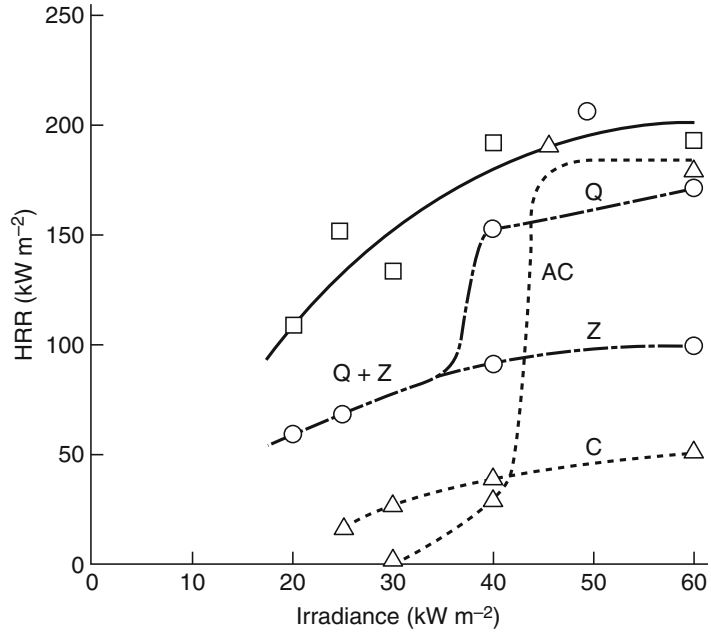

Fig. 26.9 HRR of FR polyurethane foams, as measured in the NBS I calorimeter by Parker

For foams, by contrast, no reasonable amount of thickness will normally show steady-state burning. Of special interest are polystyrene foams. These are normally very low density foams of around 16 kg m^{-3}. When exposed to heat, PS foams tend to collapse their cell structure and become a thin liquid film. This occurs before ignition takes place. Thus, after ignition what is burning is a thin coating on whatever was the substrate. This is the reason why the HRR of PS foams tends to be so apparatus-dependent that it is hard to discern

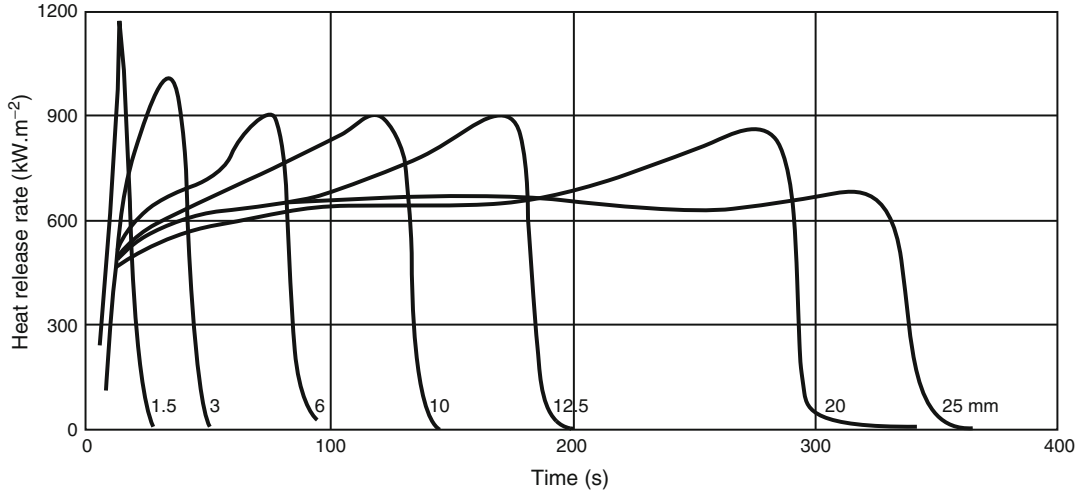

Fig. 26.10 Effect of thickness on the HRR for PMMA (heat flux = 35 kW m^{-2})

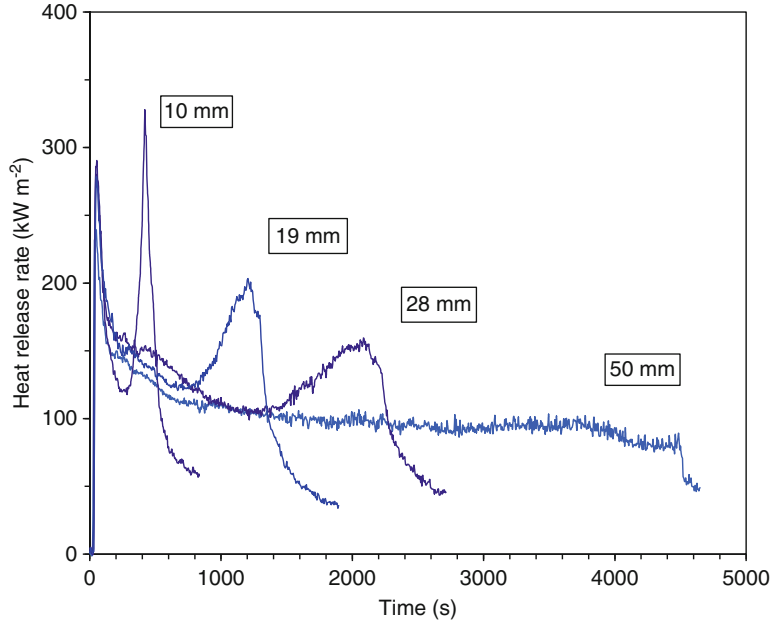

Fig. 26.11 Effect of thickness on the HRR for medium-density fiberboard (heat flux = 50 kW m^{-2})

any 'intrinsic' response of the material at all: its performance is totally dominated by the specimen-holder and edge conditions [65].

Predicting Full-Scale HRR from Bench-Scale Data: The Effect of Orientation

Routine testing in the Cone Calorimeter is specified by the ASTM standard to be done only in the horizontal orientation. This is because (1) many products show serious testing difficulties (e.g., melting) when tested in the vertical orientation. (2) Conversely, the vertical orientation does not provide 'a better simulation' of the burning of vertical objects. This is because there is no direct connection between flame fluxes in a bench-scale test and in a real-scale fire. The actual fluxes occurring in a real-scale fire are determined by many factors, including

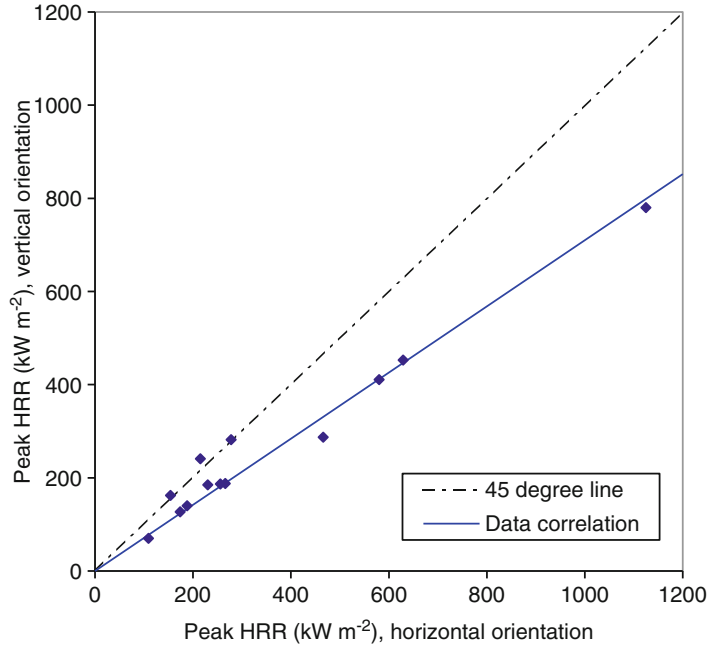

Fig. 26.12 Orientation effect on the peak HRR, as determined from two Cone Calorimeter round robins

size of room, thickness of hot gas layer, flame spread occurring over other surfaces, etc. None of these are subject to the control of the bench-scale apparatus but, rather, must be specifically modeled.

Orientation effects will also make a difference during the bench-scale testing of specimens. Even though routine testing is done only in the horizontal orientation, a small body of work exists where both orientations were explored. This is best illustrated by the results of two round robins which were conducted on the Cone Calorimeter, one under the auspices of ASTM and one under ISO. The data were taken at two irradiances, 25 and 50 kW m^{-2}, and the results are briefly summarized in the Appendix to ASTM E 1354 [20]. Such results are especially valuable since the values tabulated are the 'best estimate' values and are not subject to the specific errors of any one particular laboratory. A comparison for the peak HRR is shown in Fig. 26.12, while the comparison for the 180 s average value of HRR is given in Fig. 26.13. In both cases, the data points plotted represent all of the data analyzed within the two round robins for which horizontal and vertical orientation results were obtained on a product.

For the peak HRR, a least-square regression gives that:

$$\dot{q}''_{pk}\ (V) = 0.71\ \dot{q}''_{pk}\ (H) \qquad (26.4)$$

While for the 180 s average HRR, the corresponding relation is:

$$\dot{q}''_{180}\ (V) = 0.72\ \dot{q}''_{180}\ (H) \qquad (26.5)$$

Both can be adequately approximated by the general relation that:

$$\dot{q}''\ (V) = 0.7\ \dot{q}''\ (H) \qquad (26.6)$$

This clearly verifies that the thin, boundary-layer type flames occurring in the vertical orientation provide a lower heat flux than the pool-like flames in the vertical orientation.

Predicting Full-Scale HRR from Bench-Scale Data: Other Controlling Variables

Numerous other variables can, in principle, affect the HRR of specimens. This can include local velocities, scale and intensity of turbulence, etc. For room fire modeling purposes, such effects

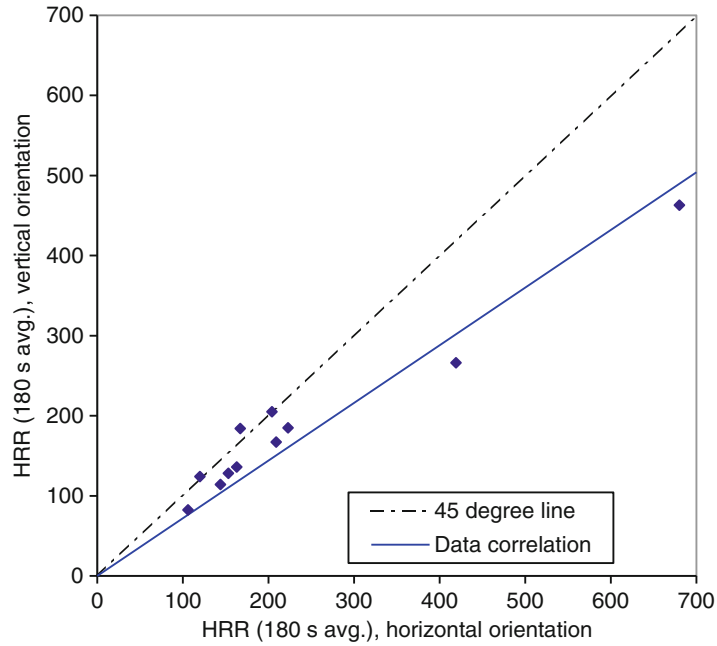

Fig. 26.13 Orientation effect on the 180-s-average HRR, as determined from two Cone Calorimeter round robins

can be assumed to be small. Two effects which are often of specific interest, however, are scale and vitiation effects. Scale effects are, in principle, normalized out when the per-unit area variable is computed. These effects will not be zero, however.

One factor affecting them is the flame flux found in the bench-scale test apparatus. This will have some scale effect. The studies in this area are not extensive. A study using a custom Cone Calorimeter with 200 mm × 200 mm specimen size tested horizontally found only a very small scale effect, when compared to standard Cone data [66]. A comparison between the ICAL and the Cone Calorimeter for a series of wood products showed that systematic differences were surprisingly small, despite the 10× difference in linear dimension of the specimens [67]. Note, however, that in this case the specimens were tested in the vertical orientation. In such orientation, the specimen flames are thin and there is little variations with scale. Of additional guidance is a study by Orloff [68] where a vertical 3.56 m high PMMA slab was burned. The mass loss rate, per unit area was found to be:

$$\dot{m}'' = 5.32 + 3.97x \qquad (26.7)$$

where x is the vertical distance (m). Note that this result implies that there is but little variation for specimens with height < 0.5 m, but significant increases for very large specimens.

In the case of objects burning in the horizontal orientation, large 'pool' flames surmount the specimen. The flux from such flames will vary greatly with scale. Guidance provided for estimating burning rates of pools (addressed later in this chapter) can be directly applied to this case.

HRR for Real Products

For many objects and commodities, published HRR are not available, thus, laboratory tests will have to be run if an answer is needed. For some commodities, however, exemplar data have been published and are available to the public. The tabulated test data can be very useful as generic representatives of items constructed of these materials, and with this general geometry.

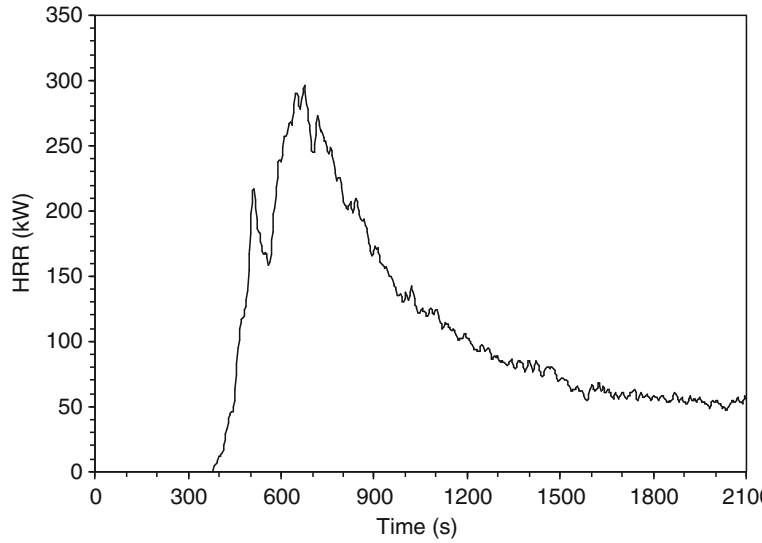

Fig. 26.14 HRR of a small air conditioner with a plastic housing

Where the analysis is intended to evaluate a specific product, that product should be tested in a suitable calorimeter and the data then used in the analysis. It must be strongly emphasized that in no case should generic database information be used when the purpose of the analysis is to seek regulatory approval for a product or to demonstrate the performance of a specific product in a court of law. In all such cases, actual laboratory testing on the item in question must be done.

In the case of a few product categories, methods are available for estimating large-scale HRR on the basis of bench-scale HRR data. The question then becomes: where can bench-scale HRR data be found? For a few product categories, some data are provided in the sections below. For the user interested in a more comprehensive look at bench-scale HRR data, the textbook *Heat Release in Fires* [23] and the Cone Calorimeter Bibliography [69] are good sources. Also, Chap. 36, "Combustion Characteristics of Materials and Generation of Fire Products," provides some data on pure chemicals.

For convenience, the sections below are arranged alphabetically by type of product. However, many of the ideas are an offshoot of pioneering studies on pool fires. Thus, it is recommended that the user first read through the section on "pools" before progressing to other product categories.

Air Conditioners

Beard and Goebeldecker [70] tested a small European in-room air conditioner 466 × 406 × 855 mm high. The unit had an ABS plastic housing, polystyrene foam inside, and a mass of 35 kg, of which 26 kg remained post-test; the total HR was 212 MJ (Fig. 26.14).

Audio Equipment

EFRA [70] tested two bookshelf-size micro-stereo systems, each comprising a receiver and a pair of stereo speakers. The receiver enclosures were made HIPS plastic, but one system had fiberboard speaker cabinets (P), while the other had HIPS cabinets (G). The systems were both very small, with the mass before test being only 4.1 kg (specimen G) and 4.9 kg (specimen P). Figure 26.15 shows the HRR results for the two tests.

Bedding

Ohlemiller et al. [71] tested inert beds (twin-size) with 12 different bedding combinations, with the peak HRR values found ranging from 38 to 200 kW. Detailed HRR curves are shown in Fig. 26.16 for one bedding combination. This

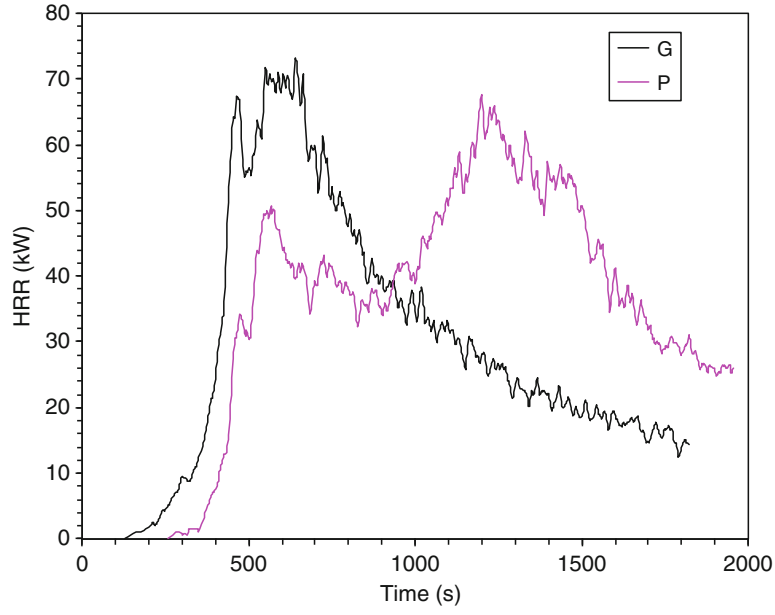

Fig. 26.15 HRR values for two small stereo systems

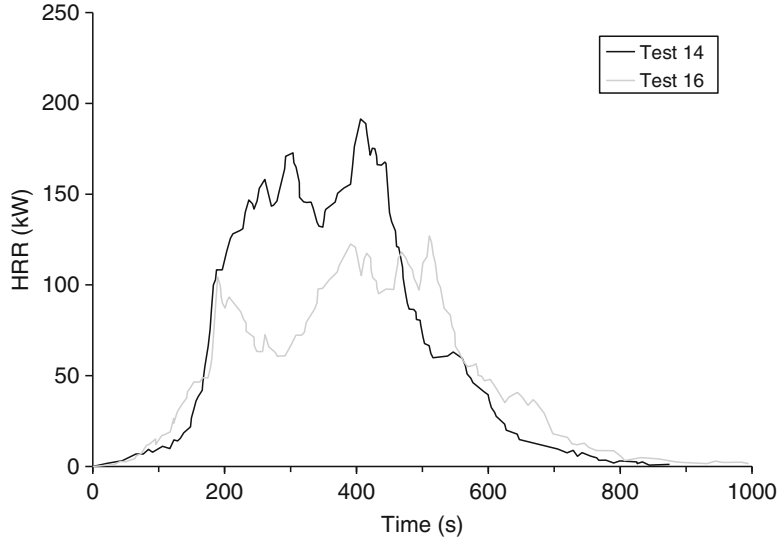

Fig. 26.16 HRR results for two replicate tests for a bedding set on an inert, twin-size bed

combination involved 2 polyester/cotton sheets, a mattress pad, a pillow, an acrylic blanket, and a medium-weight comforter. The HRR (average for the replicates) was exceeded by only one other combination, which gave values about 5–10 kW higher. The latter comprised two polyester/cotton sheets, a mattress pad, a pillow, a polyester blanket and a medium-weight comforter. The pillows were filled with polyester fiber filling in for both combinations and were covered with a polyester/cotton pillow case. Detailed HRR curves were not published for other combinations. The lowest peak HRR values were for a combination with two sheets and a pillow only, which showed 38 and 73 kW for the two replicates.

NRCC [72] conducted four tests on bedding and got peak HRR results up to 388 kW.

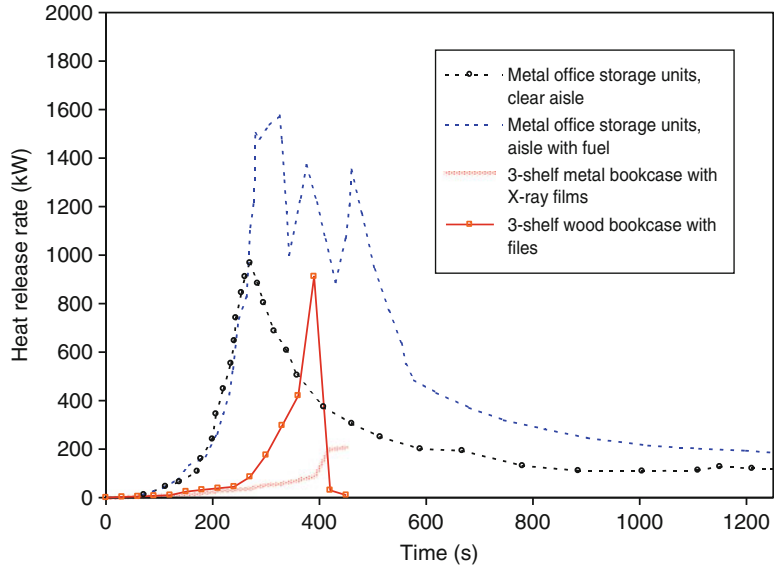

Fig. 26.17 HRR of storage units

Bookcases, Casegoods and Storage Units

In most cases, for storage furniture the fire hazard is created by the contents, not by the furniture item itself. An exception is modular storage units made of thermoplastic materials, which tend to burn very vigorously [73], but quantitative HRR data have not been published. Storage furniture made of wood or wood covered with thin layers of thermosetting plastic tend to resist ignition unless filled with combustible contents. Some data are illustrated in Fig. 26.17. The metal office storage units tests [147] arrangement involved two tiers of shelving with an 0.76 m aisle in between. Each test contained 480 kg of paper fuel load in shelving units totaling 1.67 m^2 of floor area. For the configuration with fuel in the aisle, only 3 kg was placed in the aisle, but this extra fuel provided a major difference in fire severity. The data on X-ray film shelves and wooden bookcase are from Ref. 170. For storage of paper files, it is known that the arrangement is more important than the quantity of fuel. Especially, storing files in cardboard boxes so that they can exfoliate exacerbates burning. Exfoliation occurs when paper folders are placed parallel, rather than perpendicular to the front of the shelf. When fire attacks the front, folders progressively fall out and burn in the aisle. While well-known, this effect has not been documented with HRR testing.

Boxes and Packaging

Full-scale tests were run at Western Fire Center [74] to measure the HRR of fruit/berry baskets (i.e., small plastic containers), packaged in cardboard shipping cartons, and assembled into pallet loads. In each case, no fruit goods were actually included, the boxing material being packaged as would be delivered from the manufacturer. For all tests, only a single pallet was used. Identification of materials is given in Table 26.2, while HRR results are given in Fig. 26.18. Southwest Research Institute [75] tested pallets similar to Sample A, but assembled as a $2 \times 2 \times 2$ array of pallets. This test gave a peak HRR of 8695 kW and the results are shown in Fig. 26.19.

Carpets and Other Floor Coverings

Carpets which are in the room of fire origin are not likely to contribute significantly to fire

Table 26.2 Packaged fruit cartons tested in shipping pallets

Sample	Overall dimensions of pallet load (m)	Mass before test (kg)	Mass after test (kg)	Peak HRR (kW)	Eff. heat of comb. (MJ/kg)
A	0.75 × 1.14 × 1.83	393	307	4923	17.3
B	1.02 × 1.26 × 1.83	308	222	3553	14.0
C	0.99 × 1.19 × 1.87	421	393	3044	12.1
D	1.33 × 0.80 × 1.17	430	344	896	11.9
E	1.18 × 1.07 × 2.29	461	319	3894	11.0
F	1.00 × 1.22 × 2.00	254	192	4280	13.9

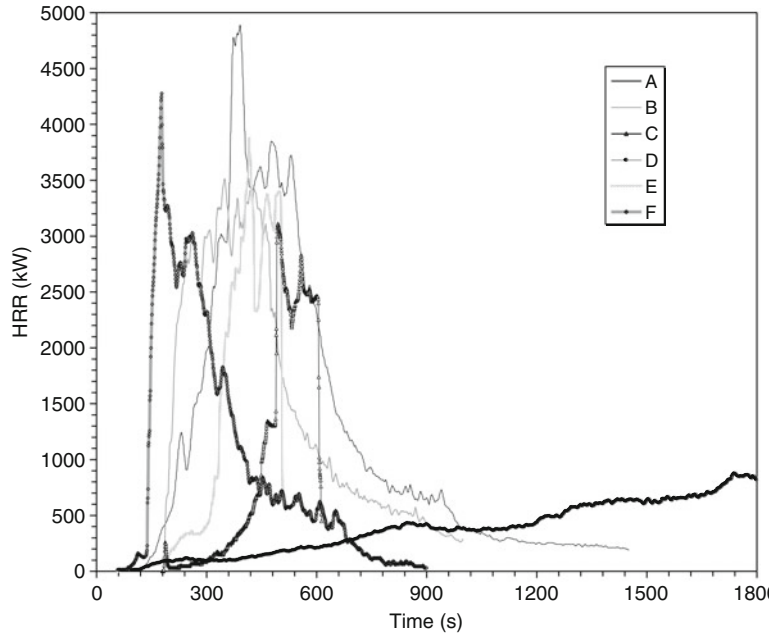

Fig. 26.18 HRR of single pallet-loads of packaged fruit/berry baskets

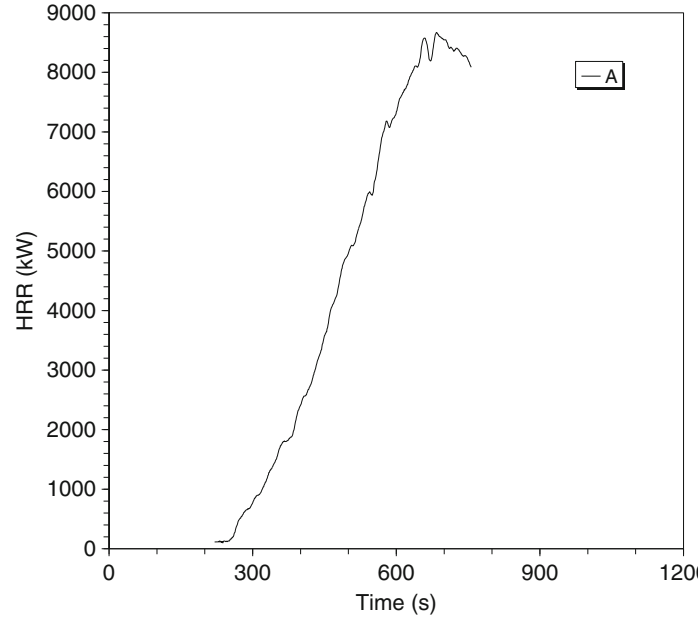

Fig. 26.19 HRR of a 2 × 2 × 2 pallet array of packaged fruit/berry baskets

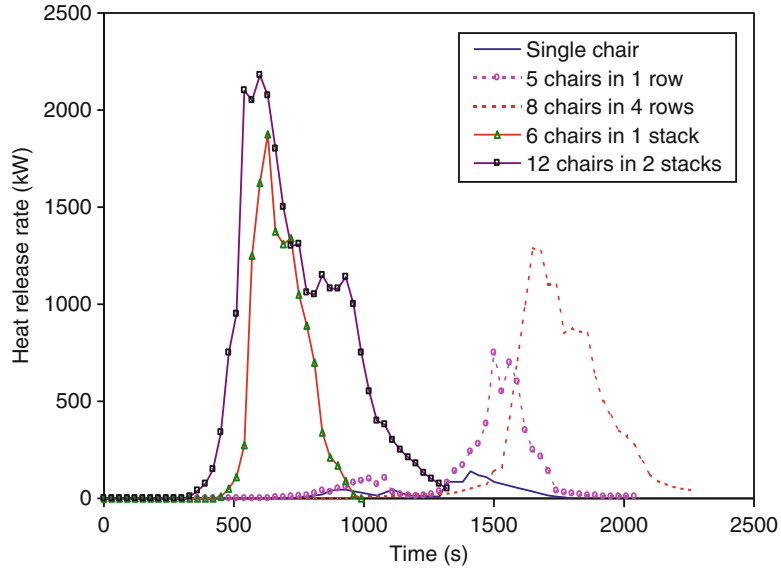

Fig. 26.20 HRR of stackable chairs, polypropylene with steel frame, no padding

growth. This has been demonstrated experimentally [76]. It is also consistent with modeling considerations: the floor area is convectively cooled and has normally the smallest view factor to the hot regions, which tend to be in the upper regions. The same material may be much more hazardous if installed on wall surfaces, although it must be pointed out that commercial textile wall coverings are normally similar, but not identical to carpeting.

The hazard from floor coverings arises when an unsuitable product is used in a corridor, especially if this is an escape path. In such situation, very rapid flame spread and high HRR can result due to the fact that the corridor floor covering becomes involved due to a room fire feeding it. Not only carpeting, but solid materials such as linoleum and wood parquet flooring are also subject to becoming fully involved down the length of a corridor. A recent study has quantified this behavior and has also provided a predictive method [77]. It is shown that floor coverings with a peak HRR of less than 200 kW m^{-2}, measured in the Cone Calorimeter under an irradiance of 25 kW m^{-2} tend not to show accelerating flame spread down a corridor.

Some carpeting materials can present a rapid fire spread hazard when installed on stairs. A residential carpet installed over a stairway has been measured to produce a peak HRR of 3 MW [78]. The test carpet was 80 % acrylic/20 % nylon; no other types of carpeting were explored.

Chairs, Stackable

Stackable chairs are most commonly used in hotels and banqueting facilities. These chairs typically have metal legs and frame and only a small amount of combustible padding or structural material. Thus, a single chair can be expected to represent negligible hazard. However, when not in active use, they are stored in tall piles and many of these piles may be aggregated together. The hazard of even a single pile of modest height can be notable. Figure 26.20 illustrates some typical data on non-upholstered, molded chairs [169]. Figure 26.21 illustrates some data on lightly-upholstered chairs [79]. For the latter, the effect of radiant augmentation from burning in a corner is also illustrated.

Clothing Items

Two men's jackets (anoraks) were tested by SP [10] as potential ignition sources. One was a

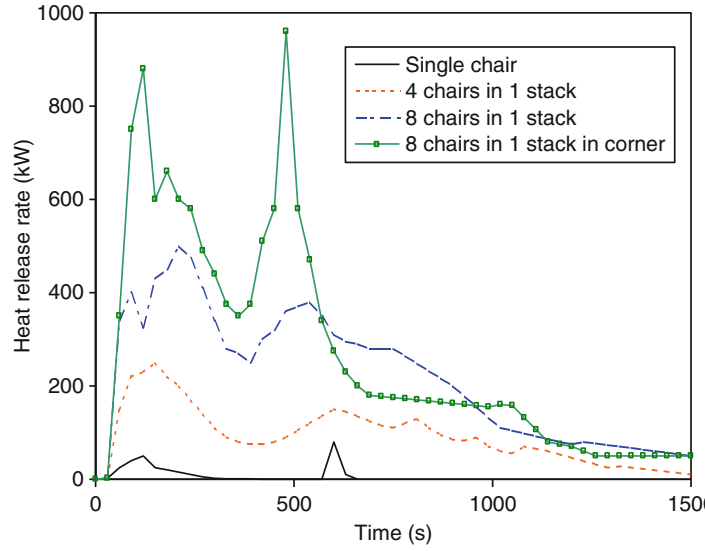

Fig. 26.21 HRR of metal-frame, upholstered stacking chairs

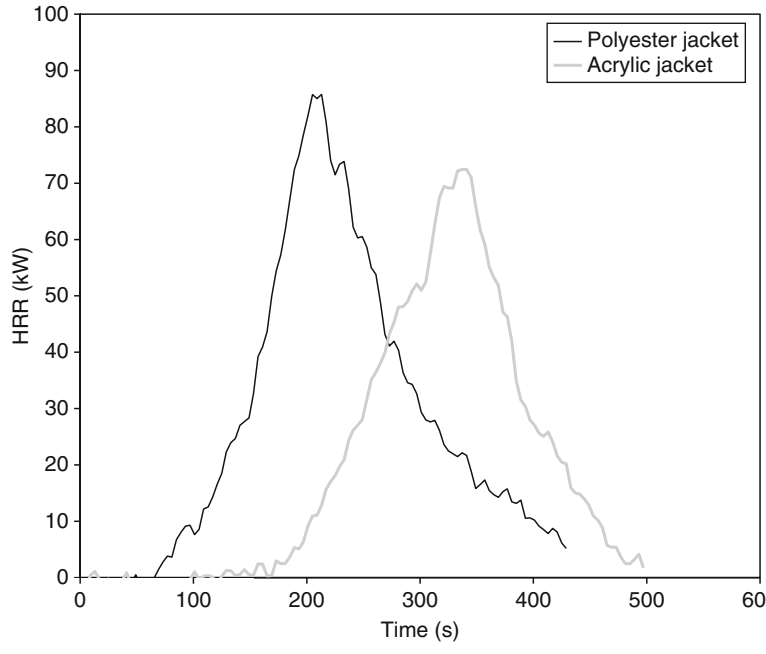

Fig. 26.22 HRR of men's jackets (laid loose)

'polyester' jacket with an outer fabric comprising 65/35 cotton/polyester, an inner fabric of 100 % polyamide, and a filling of 100 % polyester wadding. The total weight was 739 g. The second jacket tested was an 'acrylic' jacket with a fabric of nylon/Taslan and a filling of 100 % acrylic wadding. The total weight was 618 g. The HRR of these jackets are shown in Fig. 26.22. Stroup et al. [80] measured the HRR of racks of men's suits, such as might be found in a retail shop. Each rack held 48 suits, made of polyester and wool and arranged in two rows vertically. The

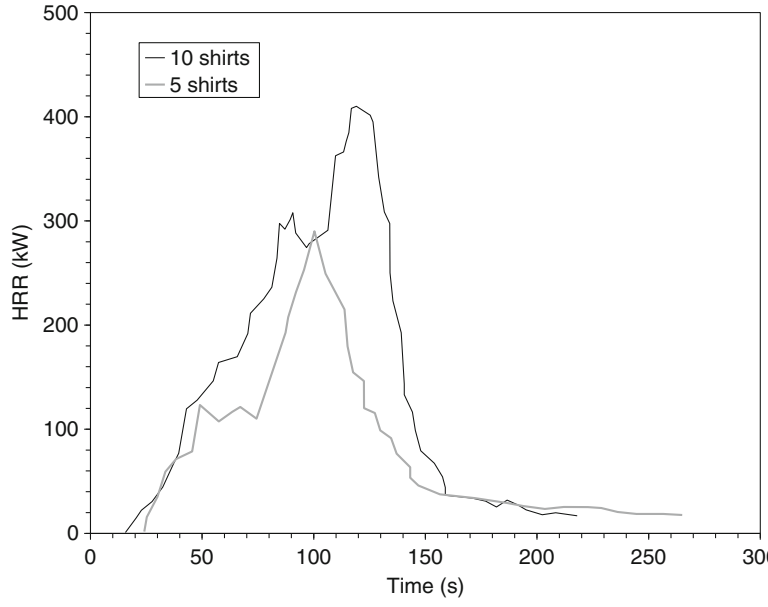

Fig. 26.23 HRR of hanging, cotton shirts

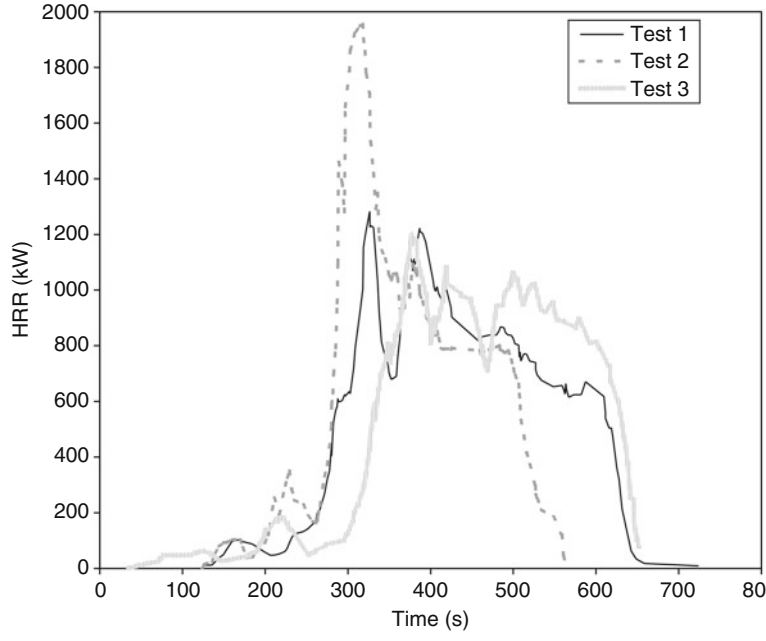

Fig. 26.24 HRR of racks of men's suits; the rack was 1.8 m long (arranged as two rows side-by-side)

results of three replicate tests are shown in Fig. 26.24. There is a lot of scatter, since the suits fall as they are burning. Japanese results [81] were reported for cotton shirts, hanging on a rack. These results are given in Fig. 26.23. The authors also tested a single hanging cotton shirt, which gave a peak HRR of 70 kW, and a pile of 10 folded shirts, which only showed a peak of 35 kW. Additional data are given under "Shop displays" later in this chapter.

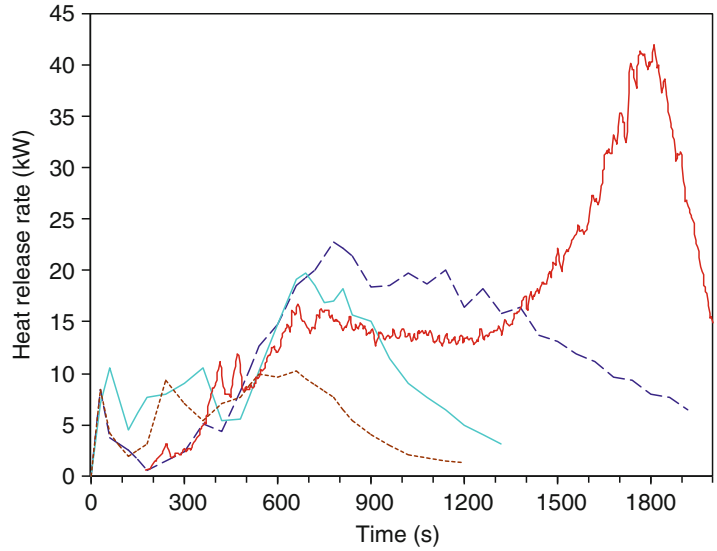

Fig. 26.25 HRR of coffee makers

Coffee Makers

The HRR of several coffee makers weighing 0.8–1.4 kg is shown in Fig. 26.25 [70, 169]. The material for the unit showing the highest HRR was identified as polypropylene [70], the others were not specified.

Computers and Electronic Equipment

Here are given results on HRR testing of computers and electronic equipment, set up as intended to be used. Additional results are given under *Industrial commodities* for packaged goods.

Computer CPUs. Two computer CPUs were tested by SP [82]. One was made by IBM, using a plastic facing rated V0 according to UL 94 [30]. This could not be ignited from a small ignition source. The second unit, of HP manufacture, could be ignited by a small ignition source and its HRR is shown in Fig. 26.26.

Computer keyboards. Bundy and Ohlemiller [83] tested at NIST three polystyrene computer keyboards weighing 580 g. These were ignited with a needle flame and the results are shown in Fig. 26.27.

Computer mice. Edenburn [84] tested two brands of computer mice. Both were ignitable by a needle flame and one brand showed a peak HRR of 3.6 kW and a total heat release of 1.20 MJ. The second brand was tested in the Cone Calorimeter with an applied external heat flux. Using a 25 kW m^{-2} flux, a peak HRR of 5.0 kW was found and a heat release of 1.35 MJ; at a 50 kW m^{-2} heat flux, a peak HRR of 6.1 kW and a heat release of 1.45 MJ were found.

Computer monitors. Bundy and Ohlemiller [83] tested at NIST a series of 480 mm (19 in.) computer monitors of the CRT type. Three ignition sources of progressively greater intensity were used: a needle flame, a burning polystyrene keyboard, and a radiant panel providing a heat flux of 21 kW m^{-2} onto the specimen (Table 26.3). Selected results are shown in Figs. 26.28, 26.29, 26.30, 26.31, and 26.32.

Computer printers. Three computer printers were tested by SP [85]. All were of the personal type, manufactured by Epson, HP, and Lexmark; the results are given in Fig. 26.33. The printers were tested without paper or toner.

Computer tapes. A test was conducted on a set of open steel shelves holding 90 computer

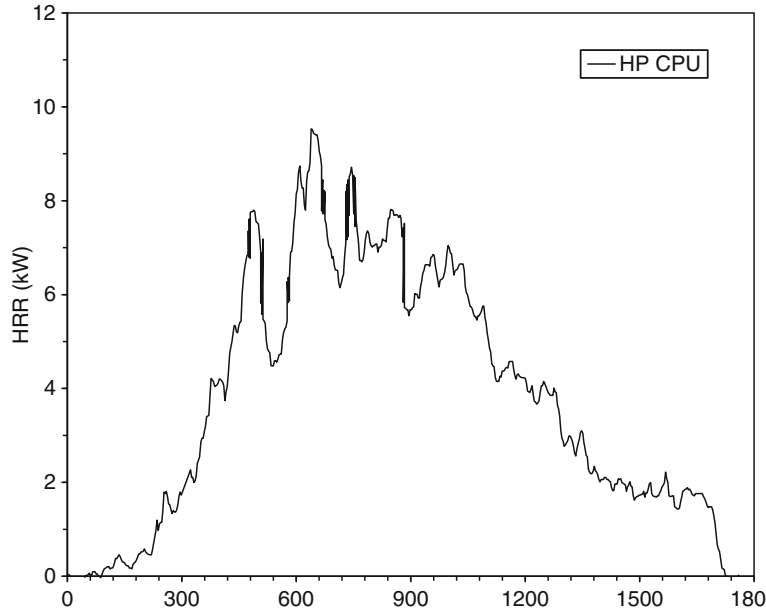

Fig. 26.26 HRR of computer CPU tested by SP

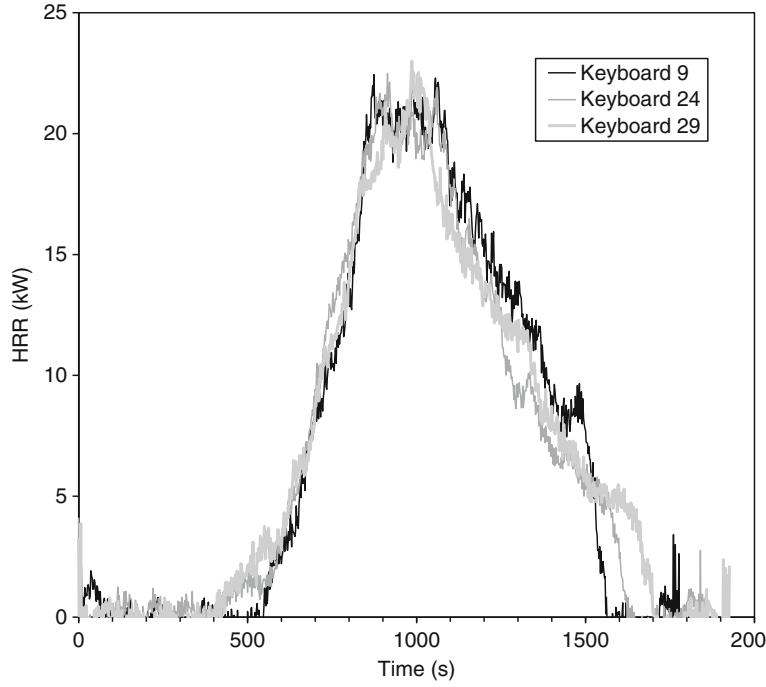

Fig. 26.27 HRR of polystyrene computer keyboards tested at NIST

tapes [86]. The tapes were 300 mm diameter and the total mass of 99 kg was distributed on four shelves, two tiers deep. The results are given in Fig. 26.34.

Racks with computer equipment. Zicherman and Stevanovic [87] tested stainless steel mesh-type racks containing computer and electronic equipment. The rack size was

Table 26.3 Computer monitors tested at NIST

Specimen ID	Material	UL 94 rating	Test #	Ignition source	CRT	Peak HRR (kW)	Total mass loss (g)
7	ABS	V0	6	Needle flame	No	DNI	
7	ABS	V0	11	Needle flame	No	DNI	
7	ABS	V0	6a	Keyboard	No	43.6	797
7	ABS	V0	11a	Keyboard	No	31.3	831
7	ABS	V0	27	Keyboard	Yes	34.5	830
7	ABS	V0	13	Radiant panel	No	0.0	24
7	ABS	V0	15	Radiant panel	No	0.0	23
7	ABS	V0	23	Radiant panel	No	25.2	765
1	PC	V0	7	Needle flame	No	DNI	
1	PC	V0	8	Needle flame	No	DNI	
1	PC	V0	7a	Keyboard	No	45.8	768
1	PC	V0	8a	Keyboard	No	120.2	2048
1	PC	V0	28	Keyboard	Yes	54.7	
1	PC	V0	31	Keyboard	No	54.4	1626
1	PC	V0	18	Radiant panel	No	124.0	1504
1	PC	V0	20	Radiant panel	No	117.2	1441
18	HIPS	V1	2	Needle flame	No	DNI	
18	HIPS	V1	10	Needle flame	No	DNI	
18	HIPS	V1	2a	Keyboard	No	114.5	1483
18	HIPS	V1	10a	Keyboard	No	88.8	1607
18	HIPS	V1	25	Keyboard	Yes	72.4	
18	HIPS	V1	16	Radiant panel	No	87.7	1267
18	HIPS	V1	21	Radiant panel	No	94.2	1329
13	PP	V2	5	Needle flame	No	DNI	
13	PP	V2	12	Needle flame	No	DNI	
13	PP	V2	5a	Keyboard	No	205.1	2469
13	PP	V2	12a	Keyboard	No	198.5	2545
13	PP	V2	30	Keyboard	Yes	180.0	3303
13	PP	V2	17	Radiant panel	No	192.6	1776
13	PP	V2	22	Radiant panel	No	166.2	1849
3	HIPS	HB	1	Needle flame	No	207.2	2401.0
3	HIPS	HB	4	Needle flame	No	199.8	2478.0
3	HIPS	HB	26	Needle flame	Yes	143.8	3309.0
3	HIPS	HB	14	Radiant panel	No	239.2	2475
3	HIPS	HB	19	Radiant panel	No	189.8	2413

1.73 m high, 0.92 m wide, and 0.61 m deep, with each rack having six shelves. The top shelf contained a CRT monitor and a personal computer, the next four shelves each contained two small data acquisition units (each fully metal-cased), while the bottom shelf held a dot-matrix printer and a 75 mm high stack of computer paper. A keyboard and a power strip were hung from the top shelf. Three tests were run on replicate units. A barbeque lighter was used to ignite the computer monitor in Test 1, the stack of paper in Test 2, and likewise the paper in Test 3. Test 3 differed from the others in that each of the top five shelves also contained a 0.60 × 0.90 cardboard sheet, which was treated with an antistatic treatment. The sheets were located directly on top of each shelf and underneath the electronic equipment. The HRR results are shown in Fig. 26.35. They have an important

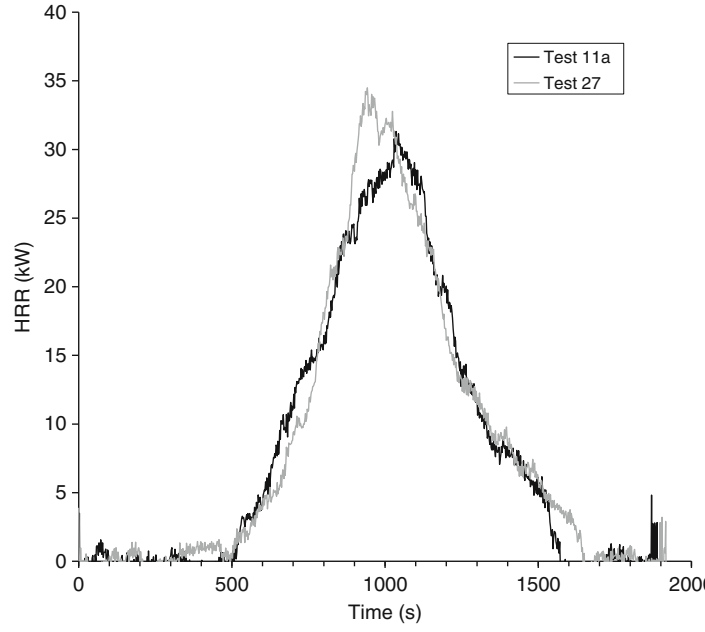

Fig. 26.28 HRR results of ABS monitors, rated UL 94 V0

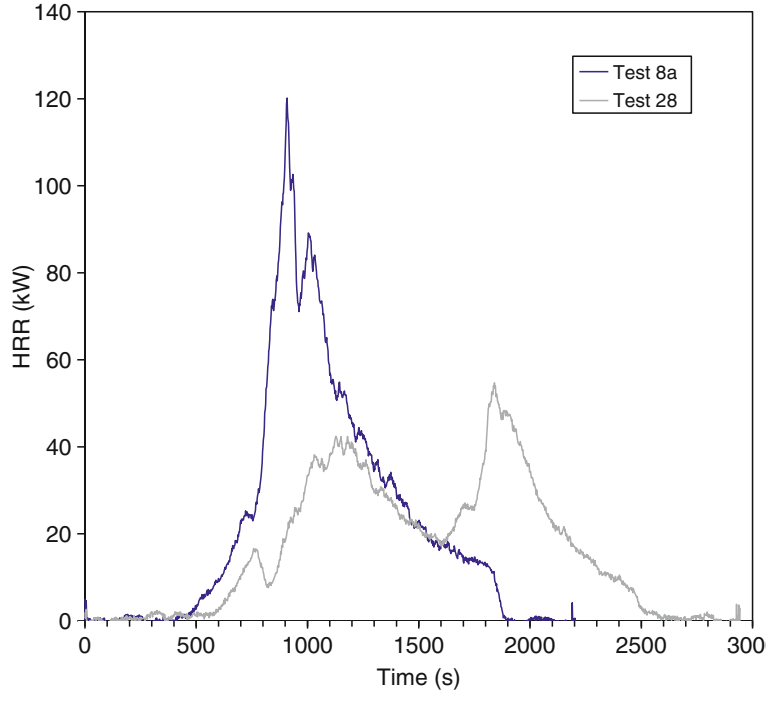

Fig. 26.29 HRR results of polycarbonate monitors, rated UL 94 V0

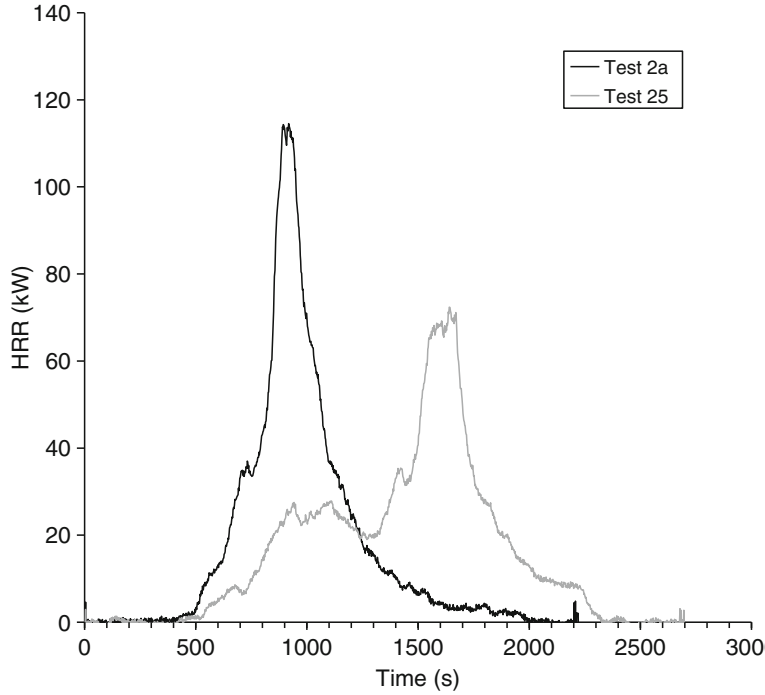

Fig. 26.30 HRR of high-impact polystyrene (HIPS) monitors, rated UL 94 V1

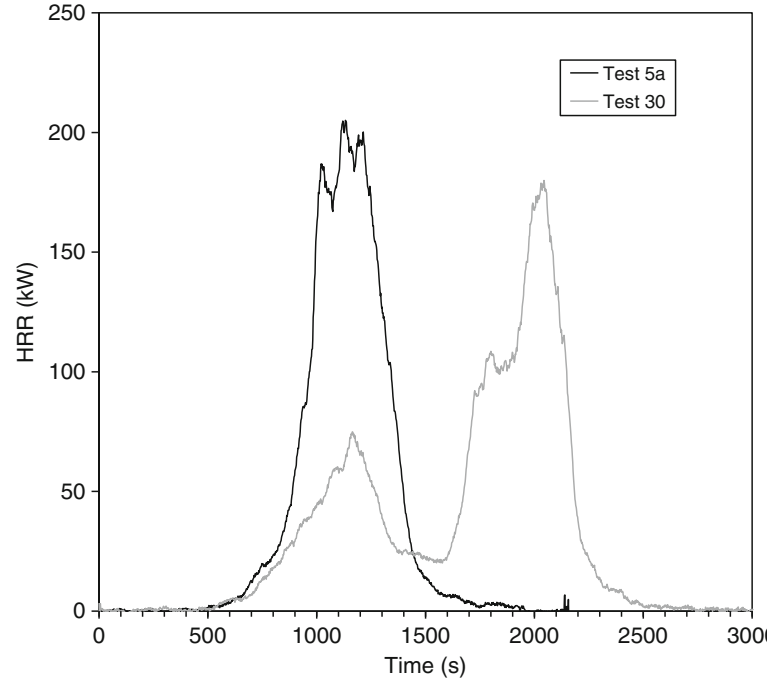

Fig. 26.31 HRR of polypropylene computer monitors, rated UL 94 V2

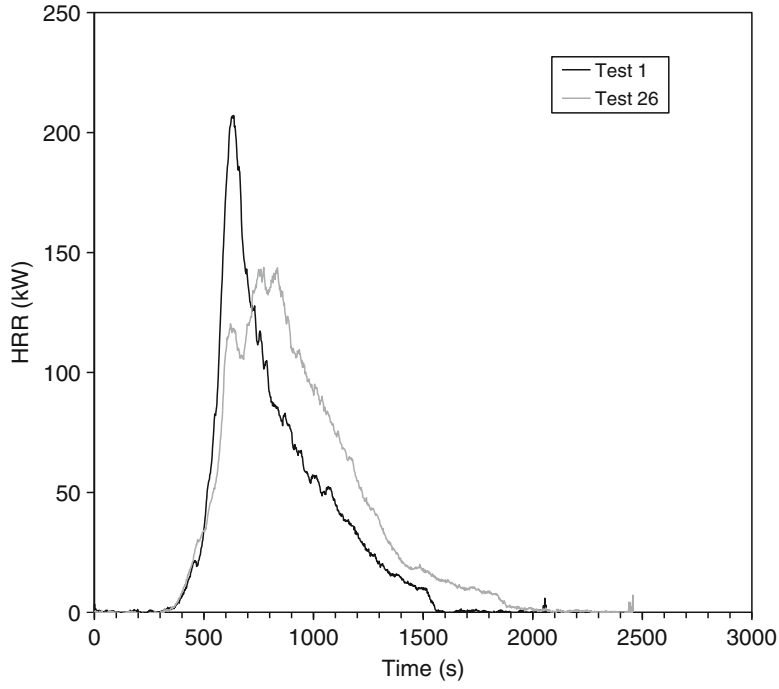

Fig. 26.32 HRR of high-impact polystyrene (HIPS) monitors, rated UL 94 HB

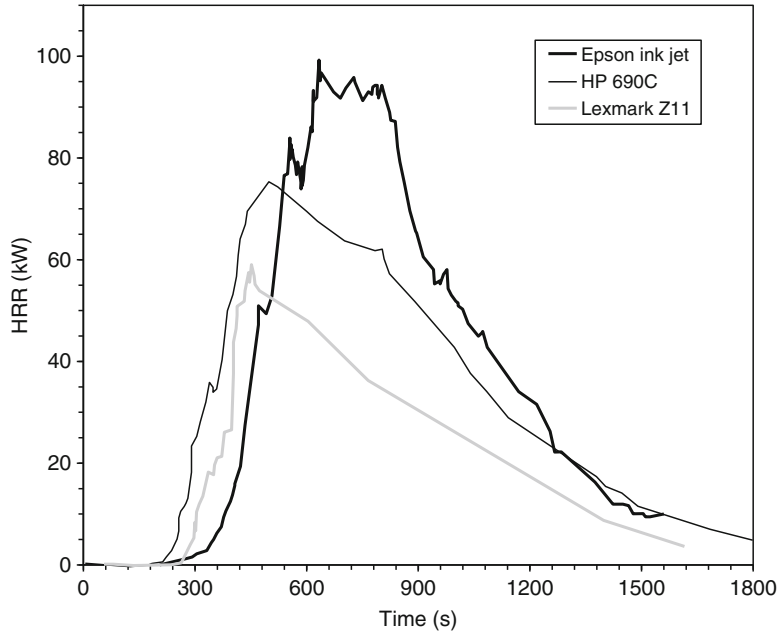

Fig. 26.33 HRR of two, personal-type printers tested at SP

instructive value in demonstrating that minor changes in the fuel loading or fuel arrangement can have drastic influences on the HRR. In this case, introducing the cardboard sheets raised the peak HRR from 155 kW (Test 2) to 528 kW (Test 3). Conversely, changing the ignition location had a major effect on the time of the peak, but essentially no effect on the HRR peak value (146 kW in Test 1, 155 kW in Test 2).

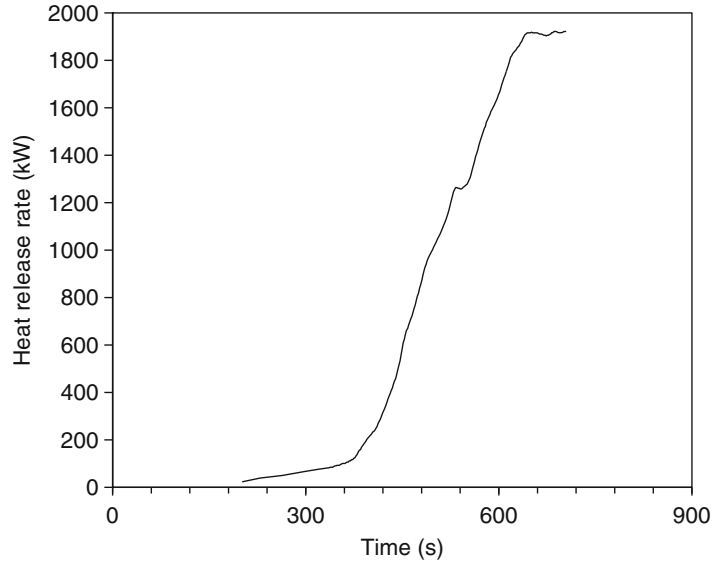

Fig. 26.34 HRR of a rack of computer tapes

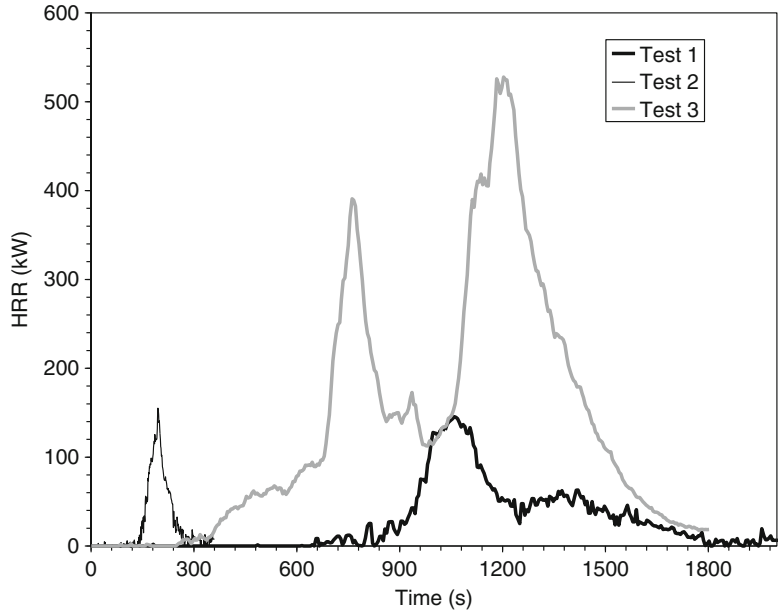

Fig. 26.35 HRR of computer equipment racks

Miscellaneous electronic equipment cabinets. Babrauskas et al. [88] tested two types of plastic business machine cabinets. The cabinets were tested as pairs (two identical units) and ignited with a 50 kW burner. The cabinets had 3 mm wall thickness and each pair of cabinets weighed 3.5 kg. The HRR results are shown in Fig. 26.36.

Two series of tests on steel cabinets used for housing nuclear power-plant control electronics were conducted by VTT [89, 90]. These showed HRR peaks of 100–200 kW. The authors also proposed computation formulas for predicting the HRR level to cause internal cabinet 'flash-over' and for burning to reach a ventilation limit [91]. Such computations are based on the

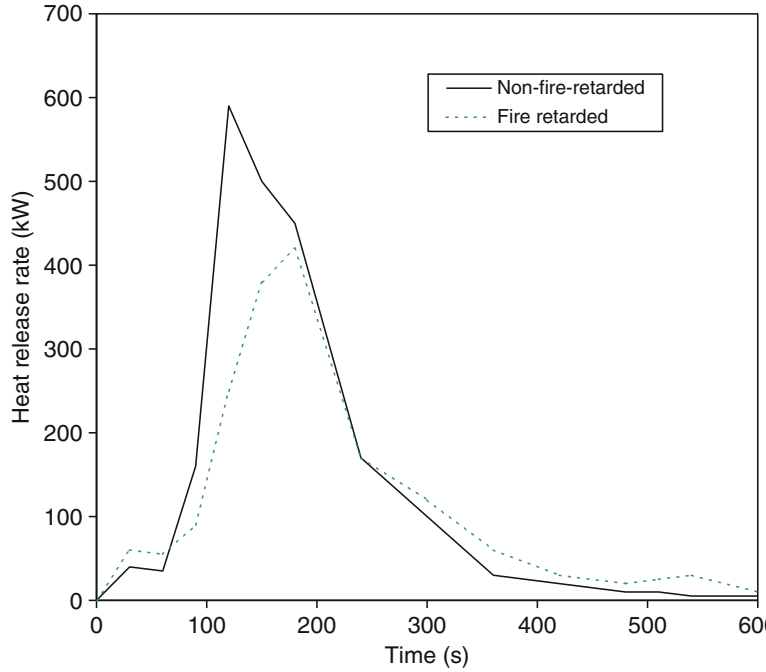

Fig. 26.36 HRR of business-machine cabinets made from polyphenylene oxide

assumption that air flow occurs only through fixed cabinet openings. In such cases, the peak HRR (or, a quasi-steady-state plateau) can be computed and actual testing would not be needed. However, some cabinets may react to fire by effectively increasing their air inflow area, e.g., if doors warp open or fall from the cabinet. Researchers at Institut de Radioprotection et de Sûreté Nucléaire (IRSN) extended the VTT theory and conducted numerous validation experiments [92]. They found that, in most cases, predictions based on ventilation-controlled burning were quite closely borne out by experiments. In a few cases, fires did not develop sufficiently to cause internal flashover, and the theory conservatively over-predicts the HRR for such instances. With an extremely flammable fuel (PMMA), but one which is probably unrealistic for actual industrial electronics cabinets, they did note that actual HRR can exceed the prediction, since some of the pyrolysis gases which lack sufficient oxygen to burn inside the cabinet can leave the cabinet and burn as a fire plume outside. However, since industrial electronics equipment is usually selected with at least some attention being paid to avoidance of excessive flammability behavior, in their tests with actual electronic equipment—as opposed to PMMA—they did not find any instances of such external burning.

Cribs (Regular Arrays of Sticks)

Cribs here are taken to mean regular, three-dimensional arrays of sticks. Each stick is of a square cross-section and of a length much greater than its thickness. The sticks are placed in alternatingly oriented rows, with an air space separating horizontally adjacent sticks. (See Fig. 26.37). Wood crib burning rates have been studied longer than any other product, with early data available from the 1930s [93]. Different analysis formulas have been presented over the years by numerous authors. Here we present a method of analysis [26] based largely on the voluminous experimental data of Nilsson [94] on wood cribs and the functional form suggestions of Yamashika and Kurimoto [95]. The scant available data on plastic cribs are from Harmathy [96] and Quintiere and McCaffrey [97]. The conditions of most interest

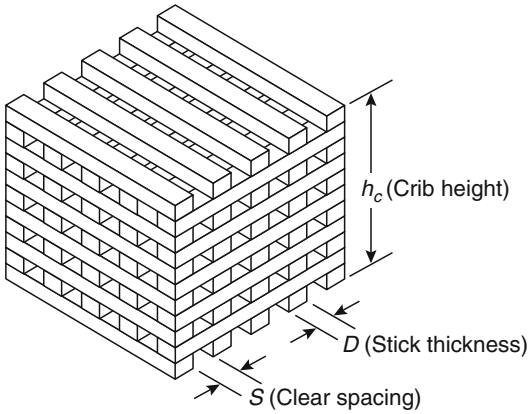

Fig. 26.37 General arrangement of a wood crib

are when cribs are ignited instantaneously, as with the use of a small amount of combustible liquid underneath. The first group of equations below represents this case. There is occasionally an interest in a crib fire where only one end of a crib is ignited, and a slow fire propagation is seen. An analysis for this situation has also been made [98]. A similar analysis is also available for the center-ignited, fire-spreading crib scenario [99].

For cribs ignited uniformly overall, the burning rate can be governed by one of three conditions: (1) the natural limit of stick surfaces burning freely; this limit applies to cribs with wide inter-stick spacings; (2) the maximum flow rate of air and combustion products through the air holes in the crib; this governs for tightly packed cribs; and (3) the maximum oxygen that can be supplied to the room; this effect is discussed separately. The numerical expressions are as follows:

Fuel surface control:

$$\dot{m} = \frac{4}{D} m_o v_p \left(1 - \frac{2 v_p t}{D}\right) \tag{26.8}$$

or

$$\dot{m} = \frac{4}{D} m_o v_p \left(\frac{m}{m_o}\right)^{1/2} \tag{26.8a}$$

with

Table 26.4 Fuel type versus regression velocity v_p for cribs

Material	v_p
Wood	$2.2 \times 10^{-6} D^{-0.6}$
Polymethylmethacrylate	$1.4 \times 10^{-6} D^{-0.6}$
Thermosetting polyester	$3.1 \times 10^{-6} D^{-0.6}$
Rigid polyurethane foam	$3.8 \times 10^{-6} D^{-0.6}$

$$m = m_o - \sum_i^t \dot{m}_i(t_i)\Delta t \tag{26.9}$$

Crib porosity control:

$$\dot{m} = 4.4 \times 10^{-4} \left(\frac{S}{h_c}\right)\left(\frac{m_o}{D}\right) \tag{26.10}$$

Room ventilation control:

$$\dot{m} = 0.12 A_v \sqrt{h_v} \tag{26.11}$$

The *least* of Equations 26.8, 26.10, or 26.11 is to be taken as the governing rate (Equation 26.11 is discussed later in this chapter). Equation 26.8a is necessary instead of the simpler Equation 26.8 when a switch of burning regime occurs during the course of the fire, e.g., the burning changes from porosity control to fuel surface control at some point. This can happen since Equation 26.8 or (26.8a) is a time-dependent expression. Thus, a crib may start burning under porosity or room ventilation-controlled conditions, then later switch to fuel surface control.

In the above equations, D is the stick thickness, m_0 is the crib initial mass, t is the time since ignition, h_c is crib height, S is the clear spacing between sticks, and room ventilation variables are A_v, the ventilation opening area, and h_v, the ventilation opening height. The fuel surface regression velocity, v_p, depends on the stick thickness and on the fuel type, as shown in Table 26.4. The experimental data for the plastic materials are extremely scant, however, so the values should be viewed as indicative rather than quantitative.

For the case of the center-ignited crib, the burning regimes are divided according to whether at a particular time the flame spread has reached the edge of the crib. This time is defined as t_0.

$$t_o = 15.7n \tag{26.12}$$

where n = the number of sticks per row. For time $t < t_o$, the following relation holds [99]:

$$\dot{m} = 0.0254\, m_o \frac{v_p t^2}{n^2 D} \tag{26.13}$$

For $t > t_o$, Equations 26.8 through 26.11 are used. The heat release rate is determined from Equation 26.1. For plastics, the heat of combustion is commonly fairly constant and can be taken from tabulations or from Cone Calorimeter testing. For wood cribs, commonly the heat of combustion is taken to be 12×10^3 kJ kg^{-1}. However, as illustrated in Fig. 26.1, the heat of combustion of wood is a varying function of time. A better procedure would be to either predict the HRR of wood cribs directly, without going through Equation 26.1, or else to be able to have recourse to a realistic value of Δh_c (t). Neither of these possibilities have currently been developed.

Room Fire Effects Experimentally, it has long been observed [94] that, unlike a pool fire, which can burn in a room in a highly fuel-rich manner, a wood crib does not burn more than approximately 30–40 % fuel rich. Conditions more fuel rich than that are not sustained, presumably, because of the highly vitiated air being supplied to the crib under those conditions. The stoichiometric fuel pyrolysis rate can be estimated as [11]

$$\dot{m}_p(st) = \frac{1}{r} \cdot 0.5 A_v \sqrt{h_v} \tag{26.14}$$

where the stoichiometric air/fuel mass ratio, r, for wood can be taken as $r = 5.7$. Comparing, then, the maximum pyrolysis rate given by Equation 26.11 with the stoichiometric rate given by Equation 26.14, it can be seen that a limit of approximately 37 % fuel rich is reached when Equation 26.11 becomes the governing limit to the burning rate. Similar limits may possibly exist for other classes of combustibles, but experimental data are only available for wood cribs.

Curtains

Thermoplastic curtains often do not sustain any appreciable burning when ignited by a flame. Instead, a small piece ignites, but it falls off and the rest of the material still in place does not burn. The dropped-down material will usually continue burning, but its HRR will be trivial. There is no systematic study available that would elucidate under what conditions curtains will burn in place (and release a significant amount of heat), versus burning only to a trivial extent.

Even if curtains ignite and burn in place, the heat content and HRR are generally moderate, but curtains can contribute to the severity of a fire by quickly propagating fire over large surfaces. Moore has done the most extensive study of curtains and draperies [100]. His test specimens were ignited with a match along the bottom. The results are summarized in Table 26.5 and Fig. 26.38. His results show primarily the effect of fabric weight. Lightweight fabrics, of weight around 125 kg m^{-2}, can show heat release rate peaks almost as high as heavy ones (around 300 kg m^{-2}); however, their potential to ignite surrounding objects is much smaller, as demonstrated in Fig. 26.38. These conclusions hold for both thermoplastic and cellulosic materials, but not for constructions using foam backings, for which insufficient data were available. Whether the curtain was in the closed or in the open position seemed to make little difference. The reason for the more severe fire performance of the heavyweight curtains was largely due to their increased burning time, which was typically about twice that for the lightweight curtains. Additional data on the HRR of curtains have been published by VTT [156] and by SP [101].

Yamada et al. [102] conducted full-scale tests on curtains of 0.9–1.2 m width and 2.0 m length. They tried 10, 30 and 50 kW square burners and found that generally at least the 30 kW burner needed to be used if full flame development was to be reached. Polyester curtains, both FR and non-FR, melted and failed to show a sustained

Table 26.5 HRR data for curtains. Nominal curtain size: two curtains each, 2.13 m high by 1.25 m wide. Wall area covered: 2.13 m high by 1.0 m wide (in closed position)

Type of fiber	Weight (g/m^2)	Configuration	Peak HRR (kW)	Number of wall and ceiling panels ignited[a]
Cotton	124	Closed	188	1
Cotton	260	Closed	130	7
Cotton	124	Open	157	0
Cotton	260	Open	152	7
Cotton	313	Closed	600	3
Rayon/cotton	126	Closed	214	0
Rayon/cotton	288	Closed	133	6
Rayon/cotton	126	Open	176	0
Rayon/cotton	288	Open	191	2
Rayon/cotton	310	Closed	177	8
Rayon/acetate	296	Closed	105	4
Acetate	116	Closed	155	0
Cotton/polyester	117	Closed	267	1
Cotton/polyester	328	Closed	338	5
Cotton/polyester	117	Open	303	0
Rayon/polyester	367	Closed	658	2
Rayon/polyester	268	Closed	329	7
Rayon/polyester	53	Closed	219	0
Cotton/polyester	328	Open	236	7
Polyester	108	Closed	202	0
Acrylic	99	Closed	231	0
Acrylic	354	Closed	1177	8
Acrylic	99	Open	360	0
Acrylic	354	Open	NA	7
Cotton/polyester/foam	305	Closed	385	1
Rayon/polyester/foam	284	Closed	326	0
Rayon/fiberglass	371	Closed	129	5
Rayon/fiberglass	371	Closed	106	5

[a]Maximum possible number of panels to ignite = 10

fire, as did FR cotton and FR rayon. Acrylic, modacrylic, non-FR rayon and non-FR cotton showed sustained burning, attaining 100–250 kW peak HRR values when subjected to the 50 kW ignition source.

Decks

The California Office of State Fire Marshal reported some HRR tests [103] done on outdoor decks, comparing wood, wood/plastic composite, and various all-plastic constructions. For samples sized 0.61 × 0.61 m, a redwood deck gave a peak HRR of 12 kW. Wood/plastic composites ranged between 10 and 394 kW, while all-plastic products ranged from 10 to 1055 kW.

Desks

Chow et al. [104] measured the HRR of a small wooden office desk. The desk was 0.6 × 1.2 × 0.8 m high The ignition source

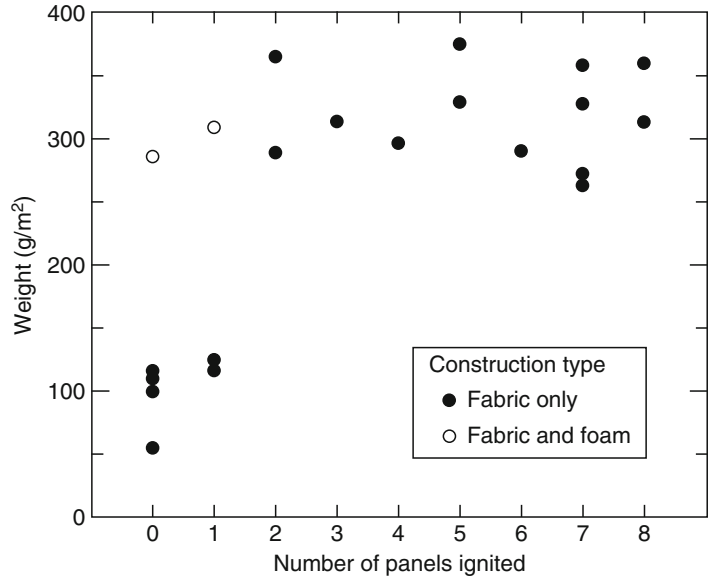

Fig. 26.38 Effect of fabric weight on number of curtain panels ignited

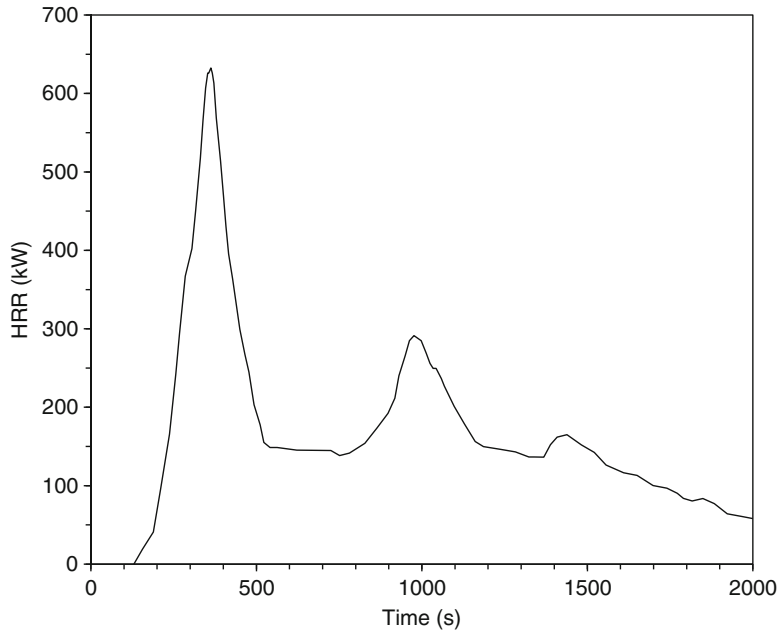

Fig. 26.39 HRR of a wooden desk tested by Chow et al.

was a pool of 0.5 L gasoline which, by itself, produced a peak HRR of 40 kW. These results are shown in Fig. 26.39.

Dishwashers

VTT tested [105] European dishwashers using a propane burner of 1 kW. The specimens are described in Table 26.6, while test results are shown in Fig. 26.40. These results must *not* be applied to appliances used in North America, since European appliance styles are different from North American ones and also because local standards are such as to permit appliances of greater flammability in Europe. HRR data on North American dishwashers are not available.

Dressers

A test of a wooden dresser has been conducted by NIST [106], see Fig. 26.41.

Dryers

Results for a small European clothes dryer (40 kg) have been published [70]. Even though use of plastics in North American clothes dryers has been increasing, nonetheless it would appear that the unit was more typical of the European market than the American one. In the test (Fig. 26.42), 11 kg of mass was lost and 253 MJ of heat was released.

Table 26.6 European dishwashers tested by VTT

Specimen	D1	D2
Initial mass (kg)	35.6	47.5
Mass loss (kg)	6.1	8.4
Peak HRR (kW)	476	347
Total heat (MJ)	165	206

Electric Cable Trays

Cable tray fires present almost an endless plethora of combinations of cable materials, tray construction, stacking, ignition sources, etc. Only a very few of these have been explored. The most systematic studies available are those from Tewarson et al. [107] and Sumitra [108]. A useful engineering analysis of their data has been prepared by Lee [109]. Lee provided a basic correlation of Tewarson's and Sumitra's data (see Fig. 26.43), which shows that the peak full-scale heat release rate $\dot{q}_{fs}$ (kW m^{-2}) can be predicted according to bench-scale heat release rate measurements:

$$\dot{q}_{fs} = 0.45\dot{q}''_{bs} \cdot A$$

where $\dot{q}''_{bs}$ is the peak bench-scale HRR (kW m^{-2}), measured under 60 kW m^{-2} irradiance, and A is the exposed tray area actively pyrolyzing (m^2). The active pyrolysis area, in turn, is estimated from Fig. 26.44, which gives dA/dt as a function of $\dot{q}''_{bs}$. Thus, at any given time, t,

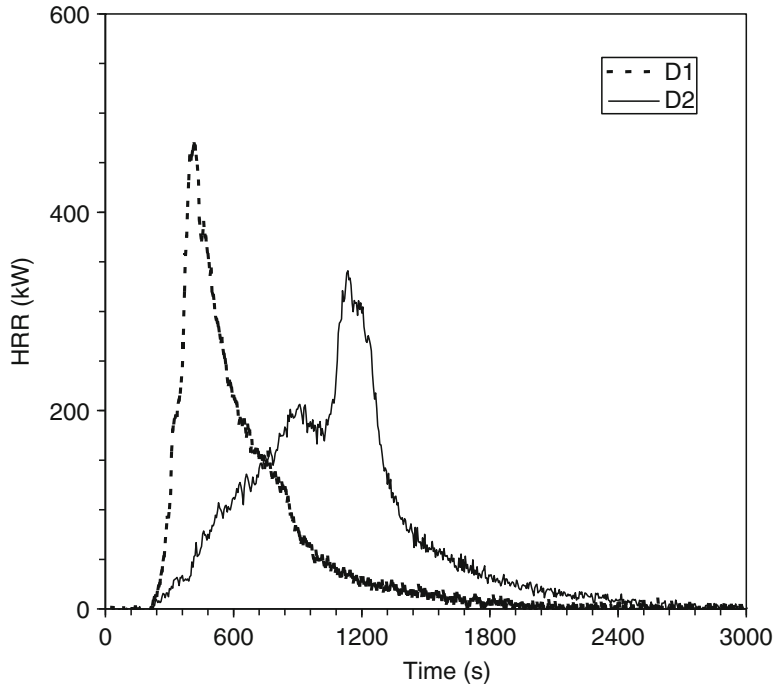

Fig. 26.40 HRR of European dishwashers tested by VTT

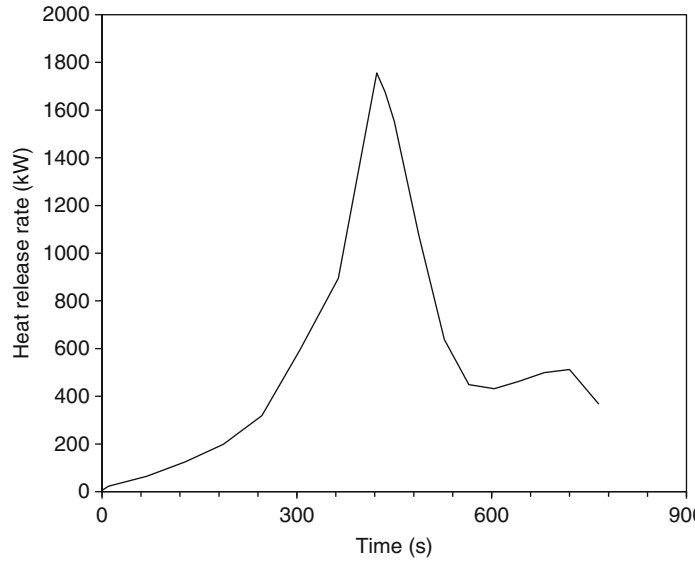

Fig. 26.41 HRR of wooden dresser

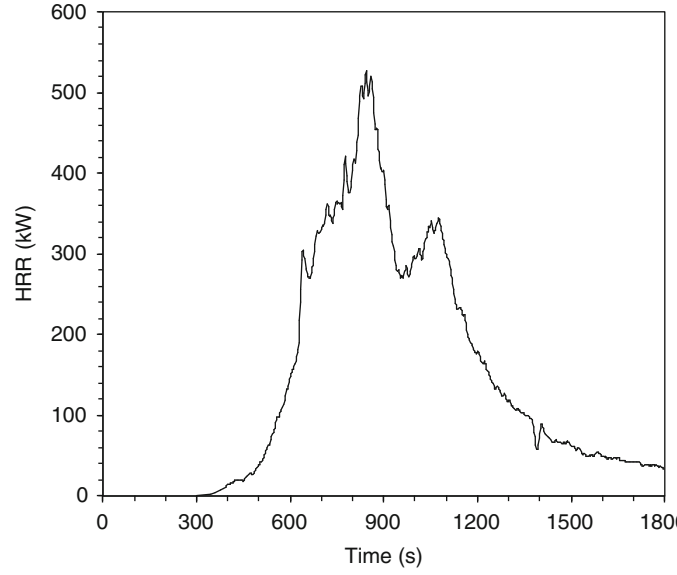

Fig. 26.42 HRR for a small European clothes dryer

$$A(t) = A_o + \frac{dA}{dt} \cdot t$$

Finally, Table 26.7 gives a selection of measured values of $\dot{q}''_{bs}$ for various cable types.

Foodstuffs

SP reported on a test [110] to simulate the burning of snack foods in a shop. Retail bags of two types of snacks were tested in a single test—potato chips and cheese nibbles. A total fuel load of 275 kg was set up in a tightly-packed, three-shelf high shelving unit, 5.4 m long. The HRR results are shown in Fig. 26.45. Visual observations indicated that potato chips burned more vigorously than cheese nibbles.

NIST [111] ran two full-scale tests on bags of potato chips on a rack with open-wire-mesh shelves. Each shelf had 20 bags of potato chips. The bags were arranged five across and four

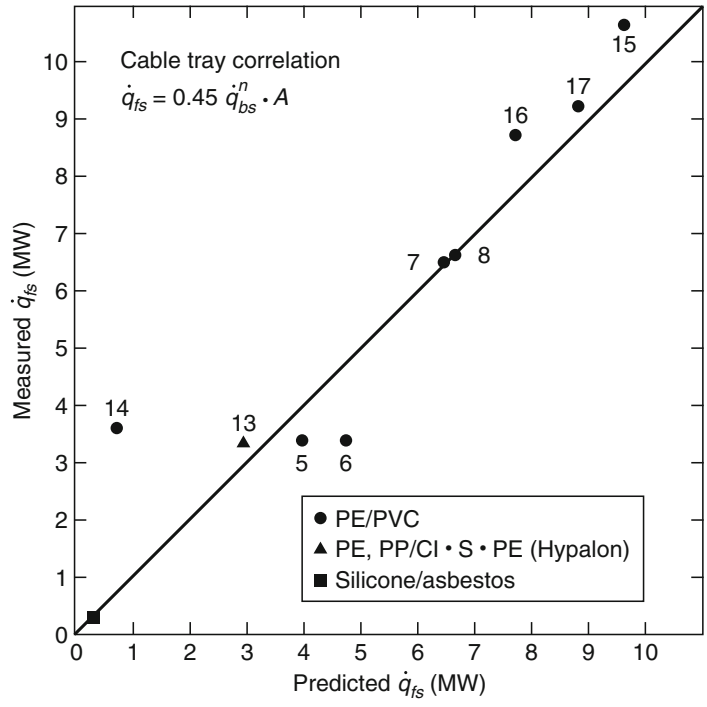

Fig. 26.43 HRR prediction for cable trays (numbers at data points identify full-scale tests)

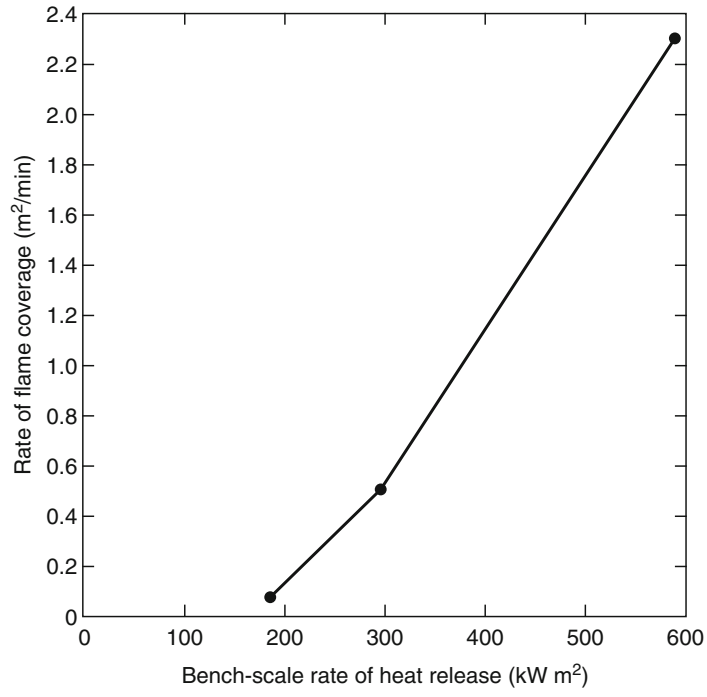

Fig. 26.44 Effect of bench-scale cable heat release rate on full-scale rate of flame coverage

Table 26.7 Heat release rates of typical cables in bench-scale tests

Specimen number	Cable sample	IEEE 383 test	$\dot{q}''_{bs}$ (kW m^{-2})
20	Teflon	Pass	98
21	Silicone, glass braid	Pass	128
10	PE, PP/Cl · S · PE	Pass	177
14	XPE/XPE	Pass	178
22	Silicone, glass braid asbestos	Pass	182
16	XPE/Cl · S · PE	Pass	204
18	PE, nylon/PVC, nylon	[a]	218
19	PE, nylon/PVC, nylon	[a]	231
15	FRXPE/Cl · S · PE	Pass	258
11	PE, PP/Cl · S · PE	Pass	271
8	PE, PP/Cl · S · PE	Pass	299
17	XPE/Neoprene	Pass	302
3	PE/PVC	[a]	312
12	PE, PP/Cl · S · PE	Pass	345
2	XPE/Neoprene	[a]	354
6	PE/PVC	[a]	359
4	PE/PVC	Fail	395
13	XPE/FRXPE	Pass	475
5	PE/PVC	Fail	589
1	LDPE	[a]	1071
20	Teflon	Pass	98

[a]Test not conducted

deep, with a total fuel load of 27.1 kg. Each bag of chips was approximately 200 mm wide by 100 mm (thick) by 360 mm high. Each bag weighed 33.8 g, of which chips accounted for 32.5 g and the plastic bag for the rest. The potato chip ingredients were listed by the manufacturer as: potatoes, sunflower oil and salt. Two replicate heat release rate experiments were conducted (Fig. 26.46). It is interesting to note that the NIST tests showed the same peak HRR (6 MW) as the SP test, albeit with a much shorter duration time due to the fact that the fuel load was 1/10 of SP amount.

Industrial Stored Commodities

Pallet loads of plastic-based commodities are commonly stored in factories, warehouses, and wholesale establishments. Most tests have involved multiple pallets being tested, and most of these have also involved some manner of water application being done during the test. But there have been a few tests reported where single pallet-loads were tested, without water. SP [112] tested single pallet-loads of four kinds:

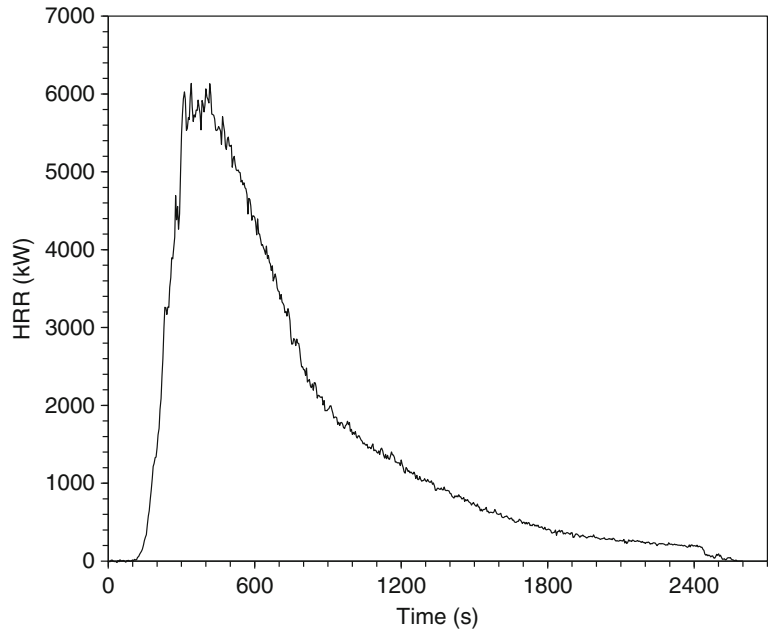

Fig. 26.45 HRR of potato chips and cheese nibbles set up in a shop display unit

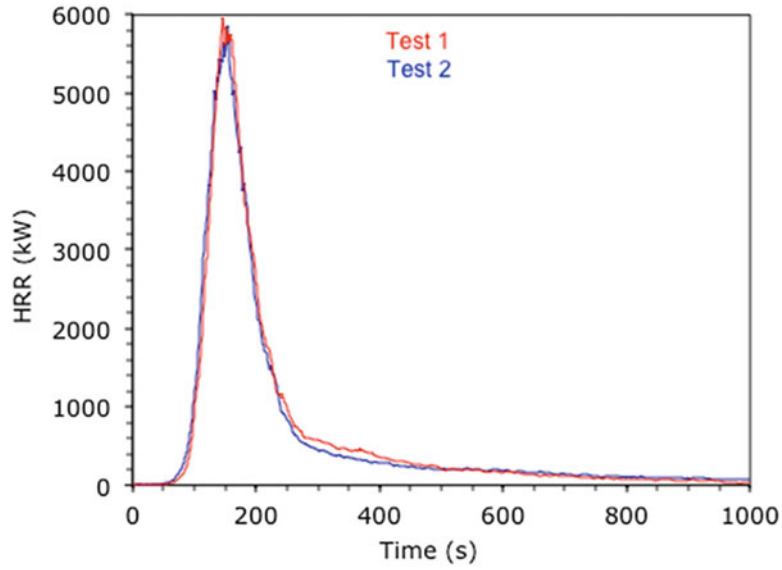

Fig. 26.46 Potato chip bags tested at NIST

- FM Group A plastic standard commodity (see Table 26.10)
- CEA standard commodity. Each corrugated-cardboard box is 450 × 550 × 370 mm and each (wood) pallet holds 12 boxes in a 2 × 2 × 3 array. Each box weighs 805 g and is filled with 340 g of polystyrene chips. The pallet-load is 800 × 1200 mm with a height of 1110 mm, excluding the pallet itself.
- SCEA standard commodity. This is a Swedish version of the CEA, with each box being 380 × 570 × 380 mm. Each box weighs 700 g and holds 420 g of chips. The pallet-load is 800 × 1200 mm with a height of 1140 mm, excluding the pallet itself.
- Large SCEA standard commodity. This is a variant where the box is 800 × 600 × 500 mm. Each box weighs 1470 g and contains 1220 g of chips. Each pallet holds a 1 × 2 × 2 array of boxes.

The HRR results for these tests are shown in Fig. 26.47.

Despite the intention being that Group A plastics represent a severe fire hazard, some plastic commodities produce significantly more HRR. In tests by Babrauskas [113], pellets of SBR (styrene-butadiene rubber) were packed in paper bags and loaded on a wooden pallet, with a total weight of 680 kg of pellets. The pallet was over-wrapped with clear plastic film and spillage did not occur during the test. The full-pallet test was ignited with a propane torch at the bottom. The half-pallet test was ignited with a propane torch at the top. The full-pallet test (Fig. 26.48) showed a HRR of close to 7 MW when conditions required that the commodity be extinguished; peak HRR conditions had not been reached.

Heskestad [114, 115] analyzed a large series of palletized[1] storage tests conducted at FM in 1975 by Dean [116]. These experiments pre-dated the availability of HRR calorimeters, so Heskestad obtained peak HRR values by using mass loss rate data and values of effective heat of combustion. The test arrangement was 2 × 2 × 3 pallets high, with a flue space running in only one direction. Heskestad also analyzed a later series of rack-storage tests by Yu and Kung [117, 118]. The test arrangement was 2 × 2, with heights being two, three, or four pallets, and with flue spaces running in both directions.

[1] 'Palletized' denotes a storage configuration where pallets are stored directly on top of each other, without use of shelving.

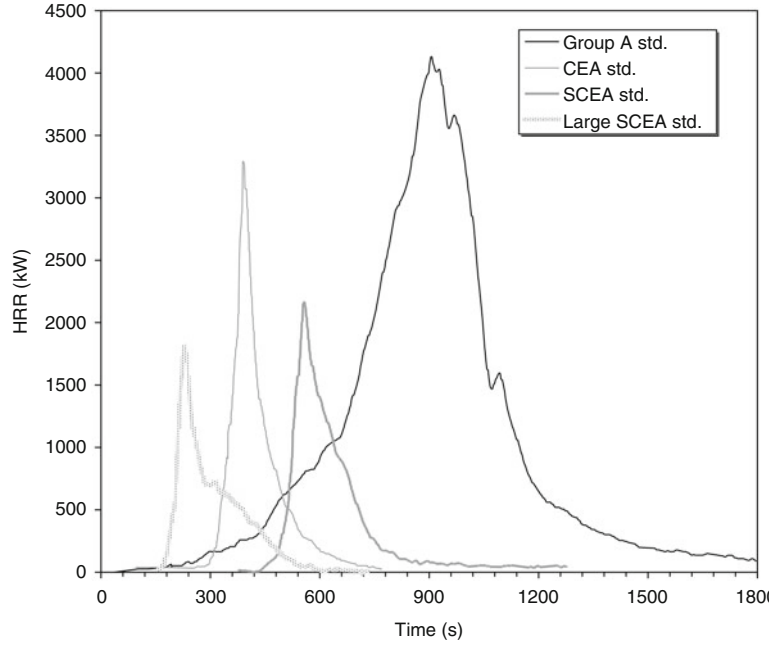

Fig. 26.47 HRR of single pallet-loads of various commodities tested at SP

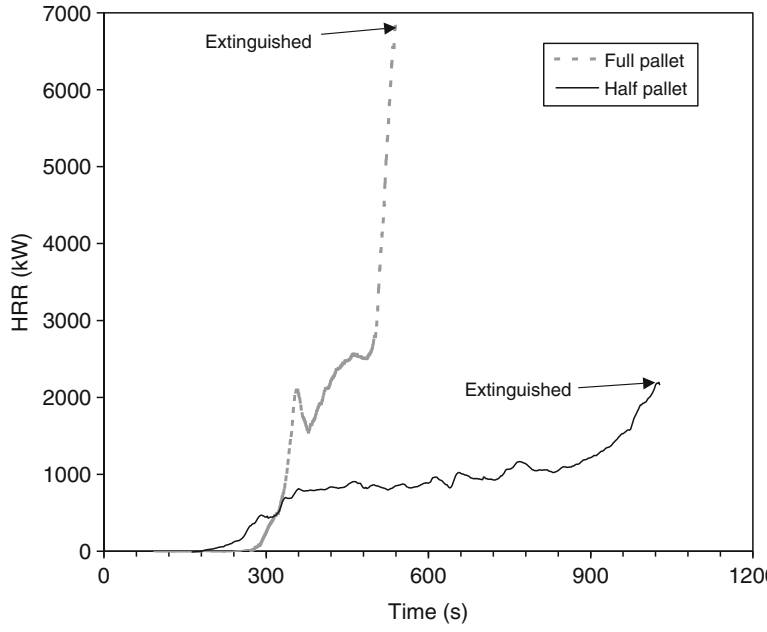

Fig. 26.48 HRR of pallets holding bags of SBR pellets

Heskestad's tabulated peak HRR values are given in Table 26.8. The peak HRR values were obtained by dividing the value in kilowatts by the floor area occupied by the commodity. The palletized test commodities occupied a floor area of 2.44 × 2.59 m, while the rack storage tests were 2.29 × 2.29 m. The cardboard cartons with metal liner are 'FM Standard Class II Commodity' (Table 26.10 [119, 122]) while the PS cups are 'FM Standard Plastic Commodity'

Table 26.8 HRR values of palletized and rack-storage commodities tested at FM

Test	Commodity	Storage ht. (m)	Peak HRR (kW m^{-2})	Time of peak (s)
SP-4	PS jars in compartmented CB cartons	4.11	16,600	439
SP-13	PS foam meat trays, wrapped in PVC film, in CB cartons	4.88	10,900	103
SP-23	PS foam meat trays, wrapped in paper, in CB cartons	4.90	11,700	113
SP-30A	PS toy parts in CB cartons	4.48	5,210	120
SP-35	PS foam insulation	4.21	26,000	373
SP-44	PS tubs in CB cartons	4.17	6,440	447
SP-15	PE bottles in compartmented CB cartons	4.20	5,330	434
SP-22	PE trash barrels in CB cartons	4.51	28,900	578
SP-43	PE bottles in CB cartons	4.41	4,810	190
SP-6	PVC bottles in compartmented CB cartons	4.63	8,510	488
SP-19	PP tubs in compartmented CB cartons	4.26	5,870	314
SP-34	PU rigid foam insulation	4.57	1,320	26
SP-41	Compartmented CB cartons, empty	4.51	2,470	144
RS-1	CB cartons, double tri-wall, metal liner	2.95	1,680	260
RS-2	〃 〃	2.95	1,490	89
RS-3	〃 〃	2.95	1,680	180
RS-4	〃 〃	4.47	2,520	120
RS-5	〃 〃	4.47	2,250	240
RS-6	〃 〃	5.99	3,260	210
RS-7	PS cups in compartmented CB cartons	2.90	4,420	95
RS-8	〃 〃	2.90	4,420	100
RS-9	〃 〃	2.90	4,420	120
RS-10	〃 〃	4.42	6,580	100
RS-11	〃 〃	5.94	8,030	148

CB cardboard, *PE* polyethylene, *PP* polypropylene, *PS* polystyrene, *PU* polyurethane

Table 26.9 Miscellaneous stored commodities tested by FM

Commodity	Storage ht. (m)	Peak HRR (kW m^{-2})
Fiberglass (polyester) shower stalls, in cartons	4.6	1,400
Mail bags, filled	1.52	400
PE letter trays, filled, stacked on cart	1.5	8,500
PE and PP film in rolls	4.1	6,200

(Group A Plastic). Note that there does not exist a scaling rule that would enable HRR values to be computed for stack/rack heights other than those tested. Thus, the reported values could conservatively be applied to shorter heights, but cannot be extrapolated to greater heights. Some older data [120] are listed in Table 26.9. These have not been re-analyzed by Heskestad.

The effect of storage height [121] on the HRR growth curve for Class II commodities is shown in Fig. 26.49. An initial period of limited fire growth has been removed from these curves. These results are from FM testing in the 1980s. Also shown is the HRR curve for a 2 × 2 × 2 array tested in 2005. For much of the time, the HRR exceeded the earlier results. This is because FM identified that the standard Class II commodity supplied in 2005 is somewhat different than that supplied earlier [125]. The early fire growth period [122] for Class I, III, and IV commodities is shown in Fig. 26.50. The early fire growth period for the FM Standard Plastic Commodity is shown in Fig. 26.51. These results are based on early FM studies [123, 124] which were

Table 26.10 FM Commodities and standard test commodities

Class	Products	Examples	Test commodity
Class I	Essentially noncombustible; may be in light cardboard cartons and may be on wood pallets	Glass, minerals, metals, ceramics	Single-wall corrugated cardboard carton measuring 21″ (0.533 m) on side, divided into five horizontal layers by corrugated cardboard sheets. Each layer was divided by interlocking cardboard partitions forming a total of 125 compartments. Each compartment occupied by one 16-oz (0.47 l) glass jar, without lid, open side facing down to prevent collection of water. A pallet load consists of one wood pallet and eight of the above-described cartons.
Class II	Class I products with more or heavier packaging and containers	Class I products in multiwall cartons, boxes, or barrels.	Double triwall (approx. 25 mm thick total) corrugated cardboard carton measuring 42" (1.07 m) on a side containing a 24 ga. (0.56 mm) sheet metal liner box measuring 38″ × 38″ × 36″ (1.07 × 1.07 × 1.02 m) high. A pallet load consisted of one wood pallet and one the above described cartons.
Class III	Combustible products in combustible wrapping or containers on wood pallets. May contain a limited amount of plastic.	Products of wood, paper, leather, and some foods	Single-wall corrugated cardboard carton measuring 21″ (0.533 m) on a side, divided into five horizontal layers by corrugated cardboard sheets. Each layer divided by interlocking corrugated cardboard partitions forming a total of 125 compartments. Each compartment occupied by one 16-oz (0.95 l) paper jar (wide mouth container/ cup), without lid, open side facing down to prevent the collection of water. A pallet load consists of one wood pallet and eight of the above described cartons.
Class IV	Class I, II, or III with considerable plastic content in product, packaging or pallets	Typewriters and cameras of metal and plastic parts	Single-wall corrugated cardboard carton measuring 21″ (0.533 m) on a side, divided into five horizontal layers by corrugated cardboard sheets. Each layer divided by interlocking corrugated cardboard partitions forming a total of 125 compartments. Each compartment occupied by forty 16-oz (0.95 l) polystyrene and eighty-five 16-oz (0.95 l) paper jars (wide mouth container/ cup), without lids, open side facing down to prevent the collection of water. A pallet load consists of one wood pallet and eight of the above described cartons.
Standard plastic (Group A Plastic)	Commodities containing a greater amount of plastic than would be permitted in Class IV commodities		Single-wall corrugated cardboard carton measuring 21″ (0.533 m) on a side, divided into five horizontal layers by corrugated cardboard sheets. Each layer divided by interlocking corrugated cardboard partitions forming a total of 125 compartments. Each compartment occupied by one 16-oz (0.95 l) polystyrene jar, without lids, open side facing down to prevent the collection of water. A pallet load consists of one wood pallet and eight of the above described cartons.

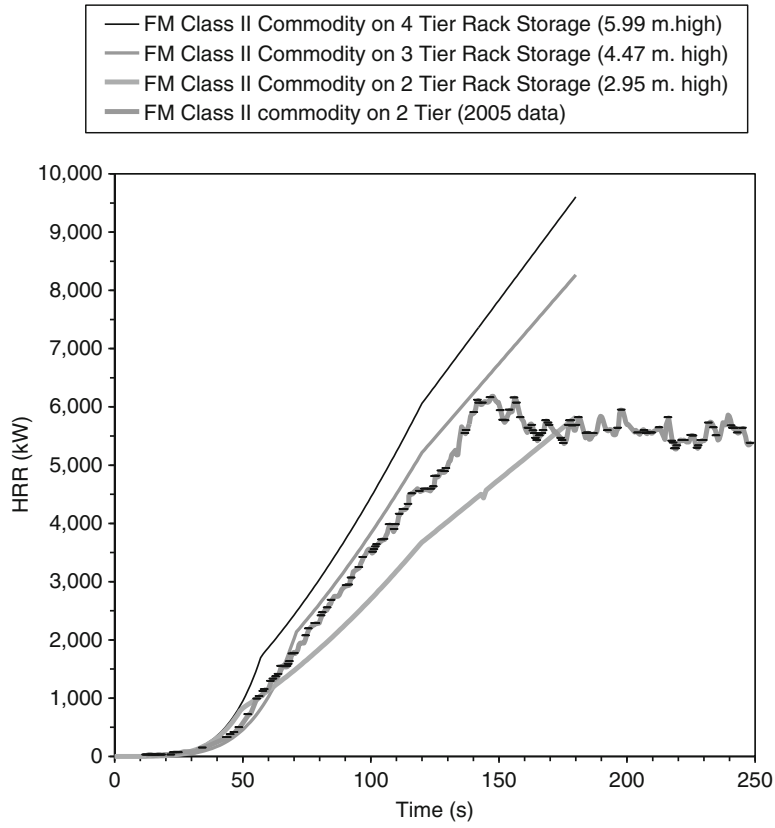

Fig. 26.49 Effect of storage height for Class II commodities

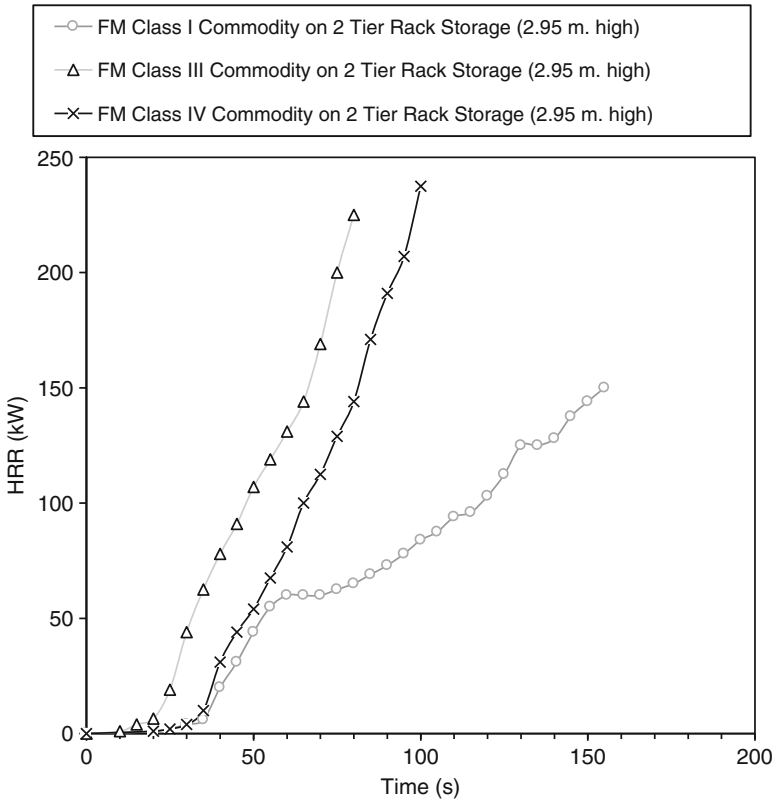

Fig. 26.50 The early fire-growth period for Class I, III, and IV commodities

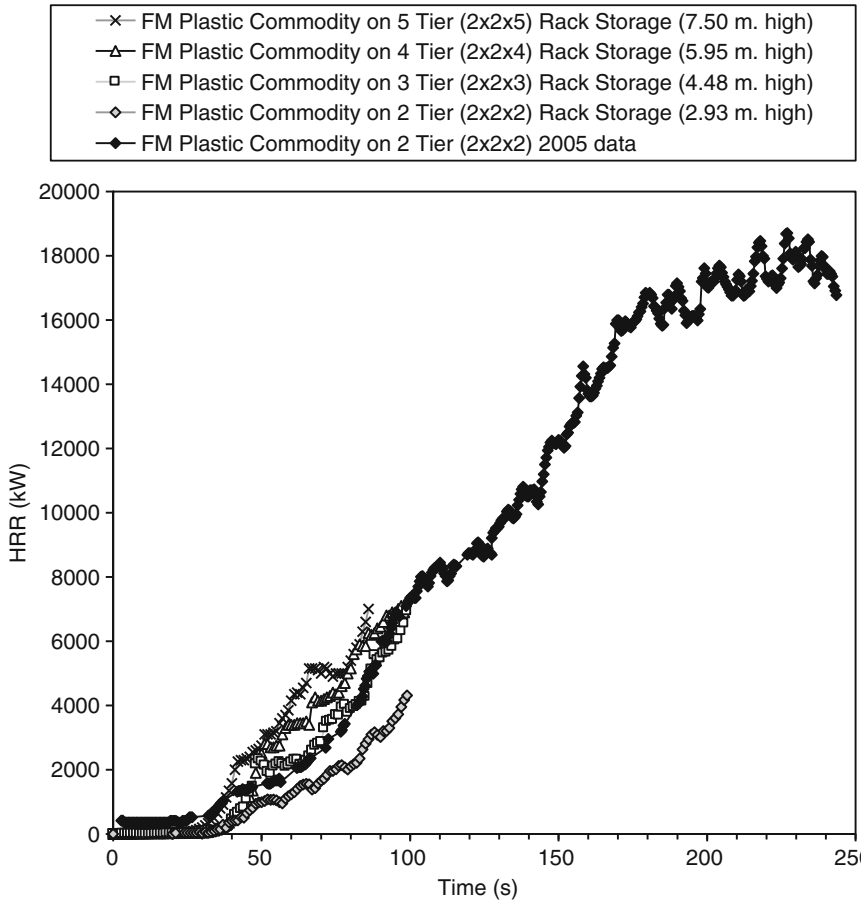

Fig. 26.51 The early fire-growth period for FM Standard Plastic commodity, as a function of storage height

conducted in their Norwood MA facility. Also shown are the results obtained in 2005 at their West Gloucester RI facility for the 2 × 2 × 2 configuration [125].

Additional FMRC data for different commodities loaded onto wooden pallets are shown in Fig. 26.52. The egg carton test [126] used foam-polystyrene egg cartons of 12-egg capacity. Polyethylene bags were used to hold 200–216 of these egg cartons, open and nested into each other. Each pallet held about 20.4 kg of egg cartons. Each pallet contained about 22.7 wood, and the load also contained about 0.4 kg polyethylene. In this test, a low density of water extinguishment was applied, but this did not appear to significantly reduce the HRR of the commodity. Only the convective portion of the HRR was measured. Polystyrene shows a very high radiant heat release fraction, thus, to account for the radiant fraction and for the diminution due to water spraying, the total HRR curve shown in Fig. 26.52 was estimated by multiplying the measured convective portion by a factor of 2. The polyurethane foam results [127] are for a three-tier (4.27 m high) stack of foam in cardboard boxes and used a PUR foam of high HRR; other results (not shown) were also obtained by FM for fire-retardant grades. The PET (polyethylene terephthalate) bottles test [128] used 46 bottles of a 2 L size packed into single-wall corrugated cardboard boxes. Each box contained 2.55 kg of plastic and 1.29 kg of cardboard. Total test arrangement comprised eight pallet loads arranged in a 2 × 2 × 2 arrangement. Each pallet contained eight cartons of the size 0.53 × 0.53 × 0.53 m. The

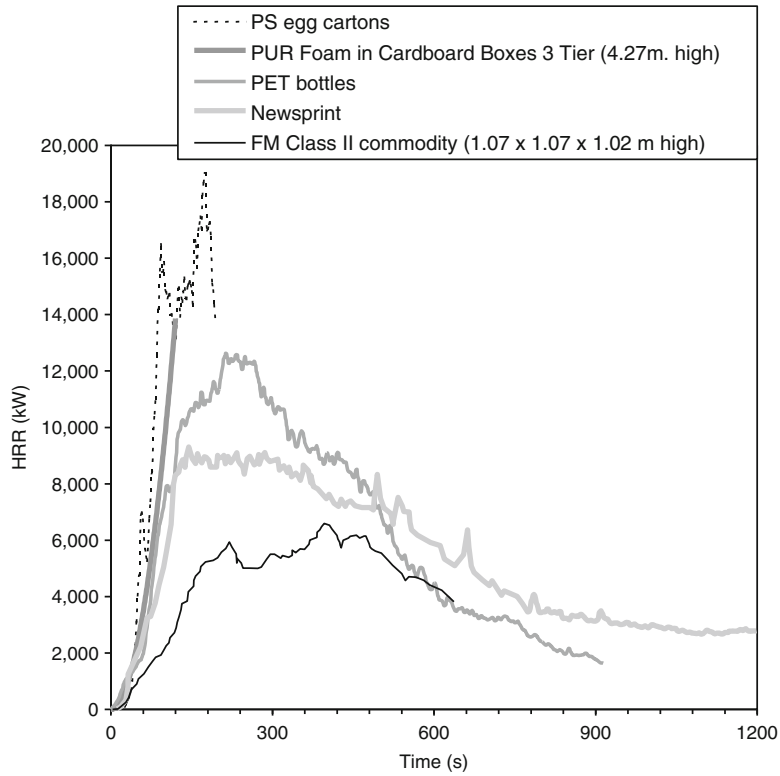

Fig. 26.52 FMRC HRR results for several additional commodities

Table 26.11 Boxed computer items tested by Hasegawa et al.

Code	Items	Peak HRR (kW)
P1	Boxed monitors, one pallet of 12	4700
P8	Boxed monitors, one pallet of 12, point-source ignition	5030
P5	Boxed monitors, one pallet of 12 (stabilized from collapse)	6400
P6	Boxed monitors, two pallets (side-by-side) of 12 each	17,300
P10	Boxed monitors, stack of two pallets high, 10 per pallet	14,100
P3	Boxed desktop computers, one pallet of 16	1400
P7	Boxed desktop computers, pallet of 16 + boxed accessory boxes on top	8190
P9	polystyrene foam in boxes	6730
P11	Monitor boxes, one pallet of 12	4600

newspaper test [129] comprised 8.2 kg of shredded newsprint placed in a $0.53 \times 0.53 \times 0.51$ m single-wall corrugated cardboard box of 2.73 kg. Eight cartons comprised one pallet load. The pallets were arranged in a $2 \times 2 \times 2$ arrangement. The newsprint test [130] used a $2 \times 2 \times 2$ arrangement of pallets, each load being $1.07 \times 1.07 \times 1.02$ m high. The Class II commodity results are from Khan [130].

Packaged computers and computer accessories were tested by Hasegawa et al. [131, 132]. They tested pallet-loads of packaged goods and also individual items, as packaged and boxed in individual cardboard boxes. The items were ignited using a line burner placed near the bottom edge of the package or stack. Ignition sources in the range of 50–200 kW were used. Table 26.11 identifies the specimens tested, while Figs. 26.53 through

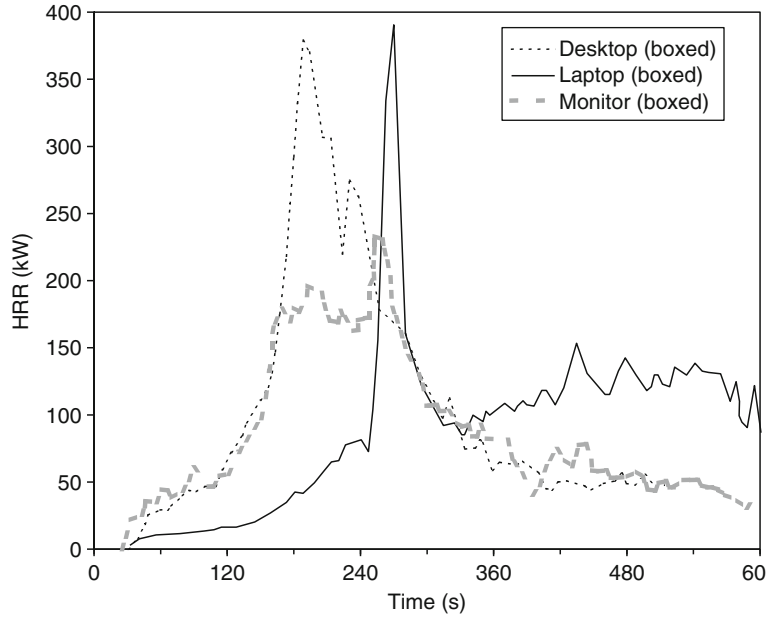

Fig. 26.53 HRR of single, packaged and boxed computers and monitors

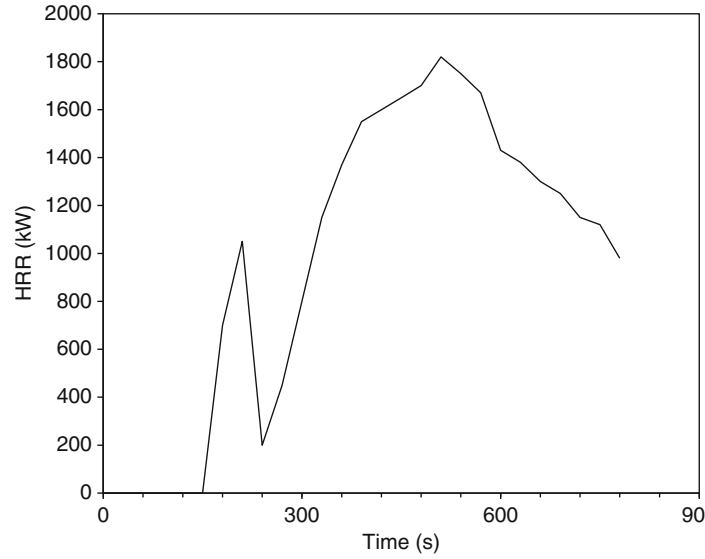

Fig. 26.54 HRR of a stack of polystyrene foam boards

26.57 show the results. The monitors were 16.8 kg each, while the desktop computers were 4.9 kg ea. The pallet load in test P1 collapsed during test and the full HRR was not registered, consequently, it was re-tested with supported sides.

A stack of expanded polystyrene boards was burned by Dahlberg at SP and results are reported by Särdqvist [97]. The total stack size was 1.2 × 1.2 × 1.2 m, with a mass of 1.4 kg. Ignition was with a 1 MW burner at the side of the stack. The HRR curve is shown in Fig. 26.54. Numerous other example data are tabulated by Särdqvist [97].

Dillon et al. [133] tested several commodities in a furniture calorimeter: acrylic yarns in boxes,

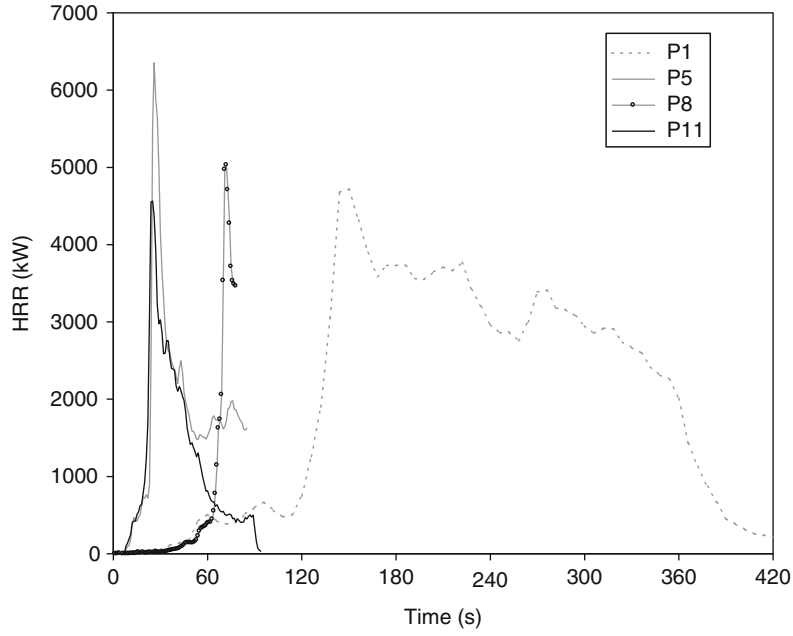

Fig. 26.55 HRR of pallets of packaged, boxed computer monitors

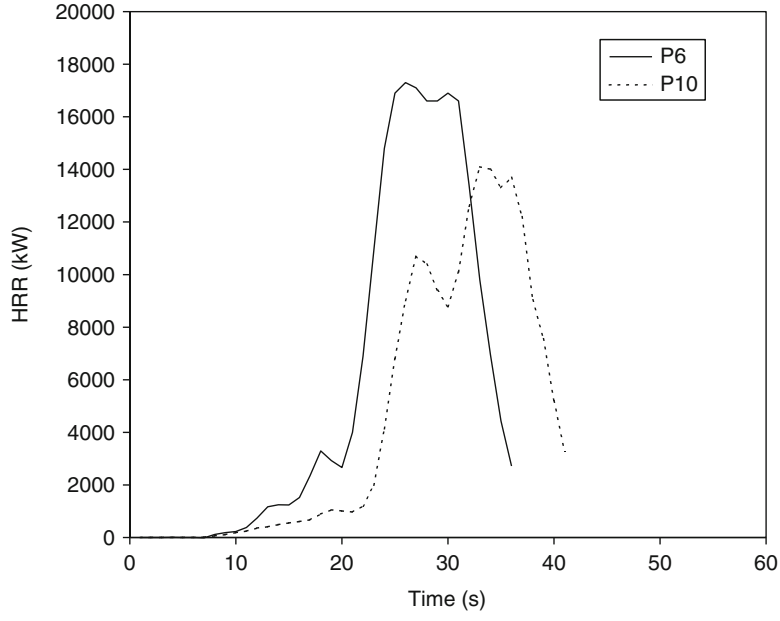

Fig. 26.56 HRR of pallets of packaged, larger arrays of computer monitors

computer monitors (US models, 430 mm [17″] screen) packed in shipping boxes, plastic coolers, and potato chip bags packed in cardboard boxes. The coolers with both insulated with polyurethane foam and had polyethylene outer shells; the #1 sample had a polystyrene liner while the #2 sample had a polypropylene liner. The computer monitors were padded with

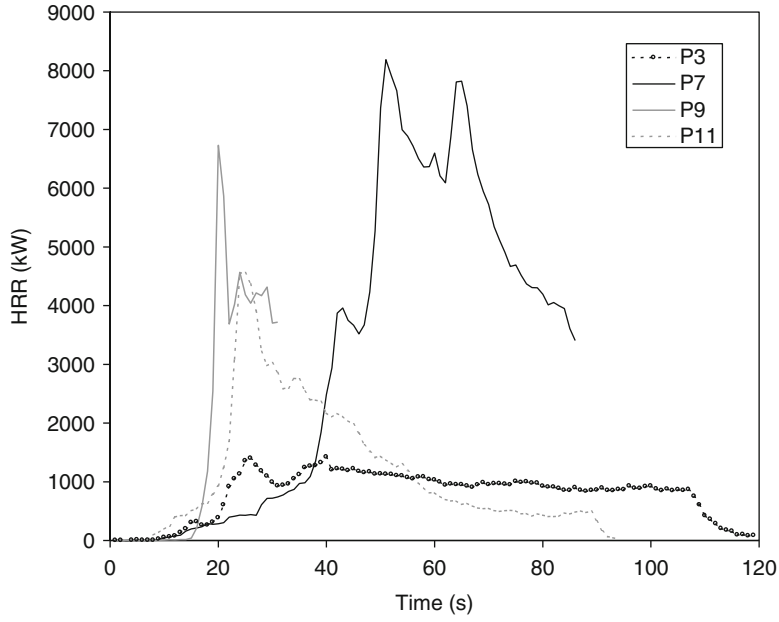

Fig. 26.57 HRR of pallets of miscellaneous computer items

Table 26.12 HRR of packaged household commodities tested by Dillon et al.

Commodity	Mass (kg)	Peak HRR (kW)	Time to peak (s)	Total HR (MJ)
Acrylic yarn skeins	8.7	263	210	127
Computer monitor	24.6	140	398	70
Cooler #1	6.4	400	648	147
Cooler #2	5.2	276	702	128
Potato chips	8.3	322	230	139

expanded polystyrene foam, as is customary for shipping. Their results are summarized in Table 26.12.

A study has been reported on burning pallet loads of organic peroxides [134]. Liquids were packaged in plastic containers within cardboard boxes, while solids were packaged in cardboard drums. The data are given only for a few packaging configurations with sufficient data not being available to generalize HRR predictions to other configurations.

For all rack storage tests, the times are very strongly affected by the ignition source location. Not enough data exist to make general correlations, but Fig. 26.58 illustrates the basic effect. The storeroom test [135] comprised a mocked-up small storeroom in a retail shop, with miscellaneous goods boxed in cardboard boxes, placed on shelving 2.4 m high. A small amount of additional shelving was provided across an aisle 1.4 m wide. The FMRC test involved pallets in a 2 × 2 × 2 arrangement. In the storeroom test, ignition was at the base of the face of the 'main' storage rack. The FMRC test [136] used the standard FMRC procedure whereby an igniter is also placed at the base, but is located internally, at the two-way intersection of flue spaces between piles. The data for the storeroom test are plotted as real time, while the FMRC test data were shifted 470 s to make the steep HRR rise portions coincide. From a comparison of this kind, one can roughly estimate that igniting a rack at the front face causes events to occur 470 s later than would happen if ignition were at the center of the flue spaces.

Kiosks

NIST have reported [137] some HRR results on full-scale tests of kiosks. These are the booths used in shopping malls, exhibitions, and other

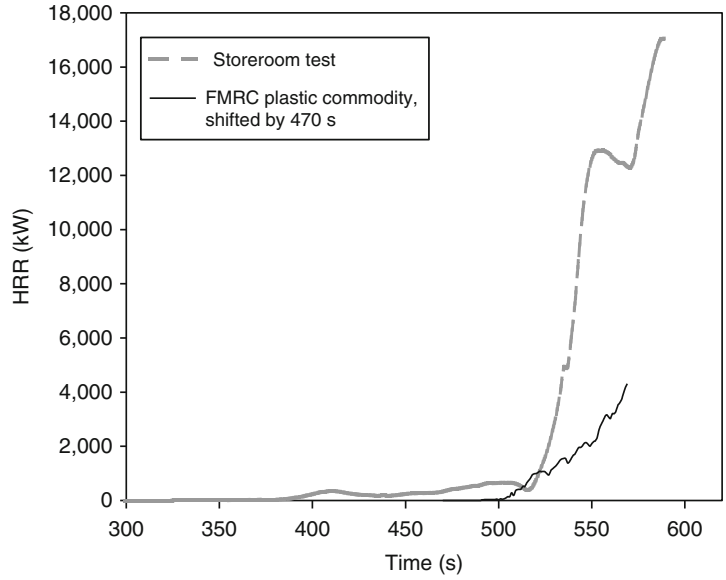

Fig. 26.58 Effect of ignition source location on fire development

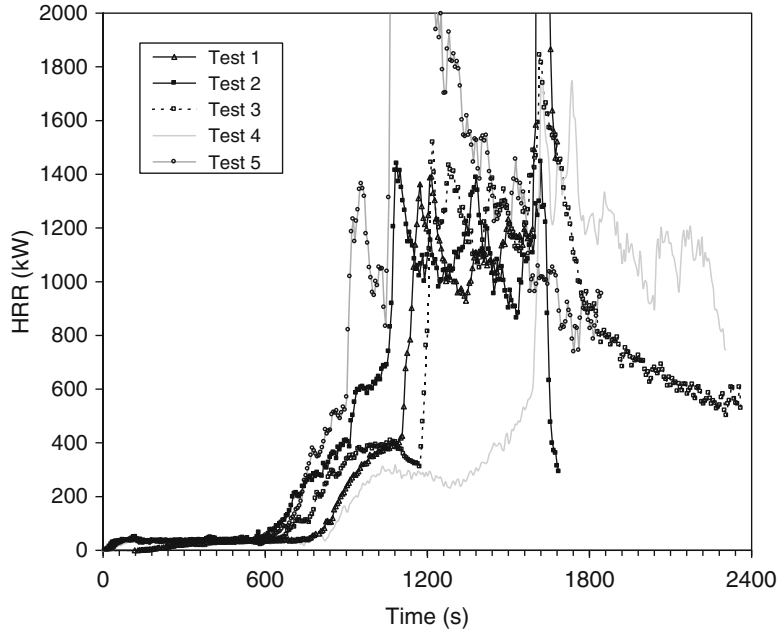

Fig. 26.59 HRR of display kiosks

places wherein a small amount of merchandise display or sales occur. Some HRR curves are illustrated in Fig. 26.59 for a kiosk, built largely of wood, which measured 1.2 m × 1.2 m × 2.1 m high. Tests 2–5 are all of the same sized kiosk, but refer to various configurations of the openable panels. Test 5 appears to have been more severe since all the panels were closed. Test 1 involved the same kiosk placed in a room, rather than in the furniture calorimeter.

Luggage

At the LSF Laboratories, Messa [138] tested the HRR of two suitcases filled with clothes. Ignition was with a square-ring burner applying approximately 5.5 kW. The test articles are described in Table 26.13 and the results are given in Fig. 26.60.

Magazine Racks

Chow et al. [139] conducted full-scale tests on several steel magazine racks, holding magazines, newspapers, and books. Ignition was with a small pool of gasoline. Test details are given in Table 26.14, while HRR results are shown in Fig. 26.61. The larger ignition source used Test 2 led to much greater HRR, despite the fact that the mass of paper goods was smaller than in Test 3. While all tests were conducted in an ISO 9705 room, the large HRR in Test 2 was evidently attributable to room-effect radiant heat flux reinforcement, which was of less significance for the other tests. Thus, for design purposes, only Tests 1 and 3 should be considered, unless the end-use environment is a relatively small room.

Table 26.13 Test description for suitcases tested at LSF

Condition	Soft suitcase	Hard suitcase
Mass empty (kg)	0.98	5.20
Mass filled (kg)	3.06	10.34
Burner HRR (kW)	5.5	5.5
Burner application time (s)	180	240
Total heat released (MJ)	33.4	139.0

Mattresses

Despite the relatively simple shape of mattresses, the prediction of mattress HRR from bench-scale data is difficult. Even the use of full-scale HRR data is problematic, due to a peculiarity of mattress fires. Most other combustibles interact only modestly with their environment, until large HRR values are reached or until room flashover is being approached. Liquid pools on the other hand, as discussed below, interact very strongly with a room, if either the room size or the available ventilation are not very large in comparison to the pool's HRR. The identical phenomenon is

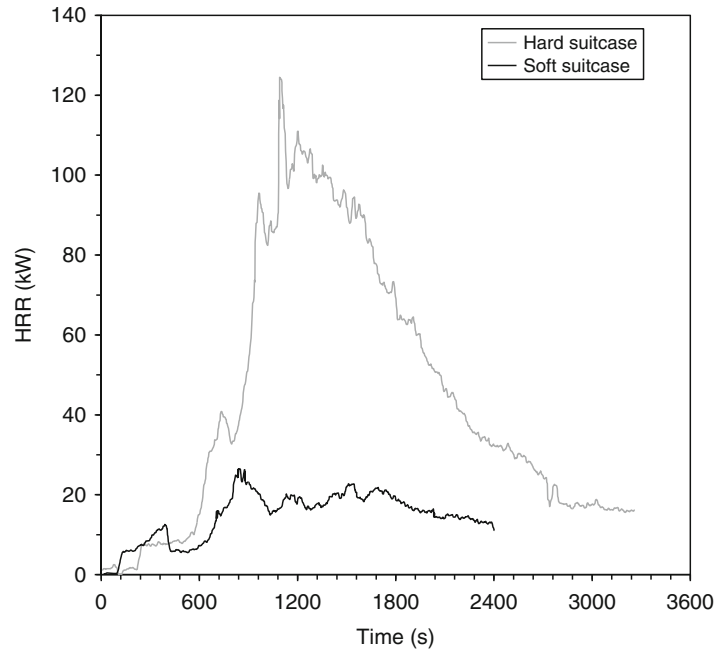

Fig. 26.60 HRR of suitcases

Table 26.14 Details of magazine rack tests

Test no.	Size of each rack (WxH), m	Location of racks in room	Mass of paper goods (kg)	Ignition source, quantity of gasoline (L)
1	1 × 2.2	Left, back	15	2
2	2 × 2.2	Back, right	60	15
3	2 × 2.2	Left, back, right	90[a]	3

[a]Of which 15 kg was placed on floor, in front of racks

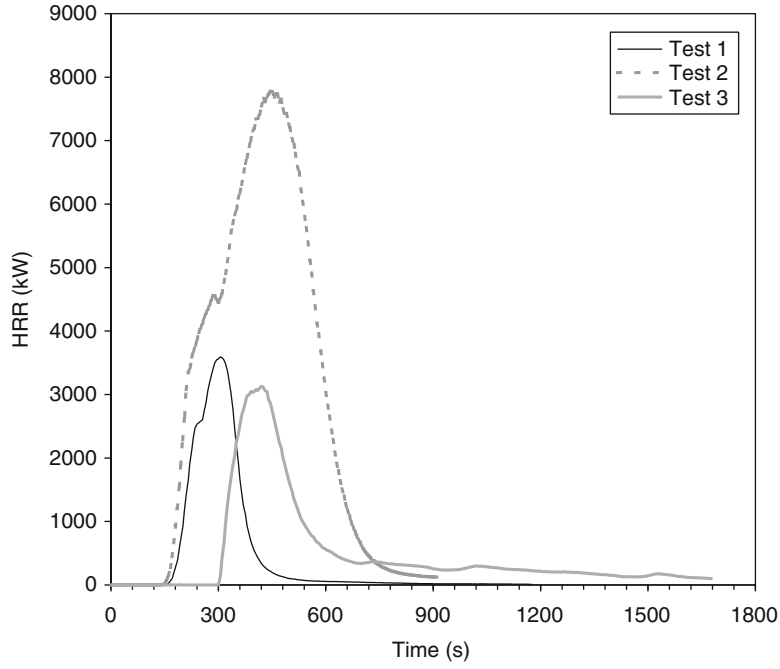

Fig. 26.61 HRR of magazine racks loaded with magazines, newspapers, and books

Table 26.15 Some mattress HRR data; full-scale data are for small or no room effect, bench-scale data are peak values, taken at 25 kW m^{-2} irradiance

Padding material	Ticking material	Combustible mass (kg)	Peak HRR, full-scale (kW)	Bench-scale HRR (kW m^{-2})
Latex foam	PVC	19	2720	479
Polyurethane foam	PVC	14	2630	399
Polyurethane foam	PVC	6	1620	138
Polyurethane foam	Rayon	6	1580	179
Polyurethane foam	Rayon	4	760	NA
Neoprene	FR cotton	18	70	89
Cotton/jute	FR cotton	13	40	43

observed with mattresses. Thus, there may not be a single value of the HRR of a mattress, the HRR having to be considered related to the room itself.

Some example data are compiled in Table 26.15 to illustrate the peak full-scale HRR values that are found for common material combinations [45]. The full-scale test protocol used a complete set of bedding; ignition was achieved with a wastebasket. Figure 26.62 illustrates the relation of bench-scale to full-scale

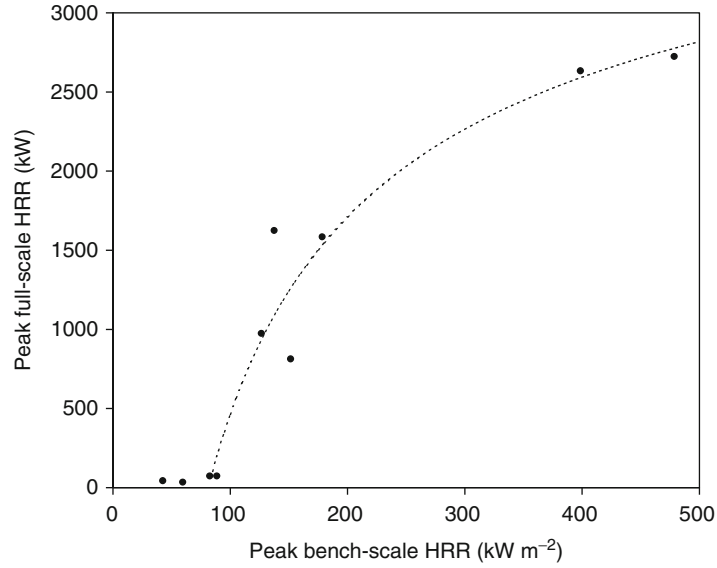

Fig. 26.62 HRR of mattresses predicted from bench-scale results. Full-scale tests under conditions of negligible room effect; bench-scale HRR measured at 25 kW m^{-2} irradiance

Table 26.16 Some mattress HRR data; full-scale data include room effect of small bedroom

Padding material	Ticking material	Combustible mass (kg)	Peak HRR, full-scale (kW)	180 s avg HRR, bench-scale (kW m^{-2})
Polyurethane foam	Unidentified fabric	8.9	1716	220
Melamine-type PUR/cotton batting/polyester fiber pad	Polyester/ polypropylene	NA	547	169
Polyurethane foam/cotton batting/ polyester fiber pad	Unidentified fabric	NA	380	172
Polyurethane foam/polyester fiber pad	PVC	NA	335	195
Melamine-type PUR	FR fabric	15.1	39	228
FR cotton batting	PVC	NA	17	36
FR cotton batting	Polyester	15.7	22	45
Neoprene	PVC	14.9	19	31

data from the same data set, where full-scale testing was done under conditions not leading to significant room fire effect. Not enough specimens were tested to develop a usable correlation, so the results should be taken only as indicative.

King-size mattresses dating from before the Federal HRR regulations can produce very high HRR values, even absent a room effect. NIST [140] tested a king-size bed assembly which contained box springs and an innerspring mattress consisting of polyurethane foam and felted cotton padding. Additional bedding included two pillows, pillowcases, two sheets, and a comforter. Two tests were run in an open calorimeter—in one test, an electric match was used to ignite the bed, while in the other test a newspaper-filled wastebasket was the ignition source. Unlike the typical findings in the case of upholstered furniture, here the ignition source type had a major effect, with the larger ignition source resulting in a peak HRR over 5000 kW, while the smaller only showed about 3500 kW and burner a longer

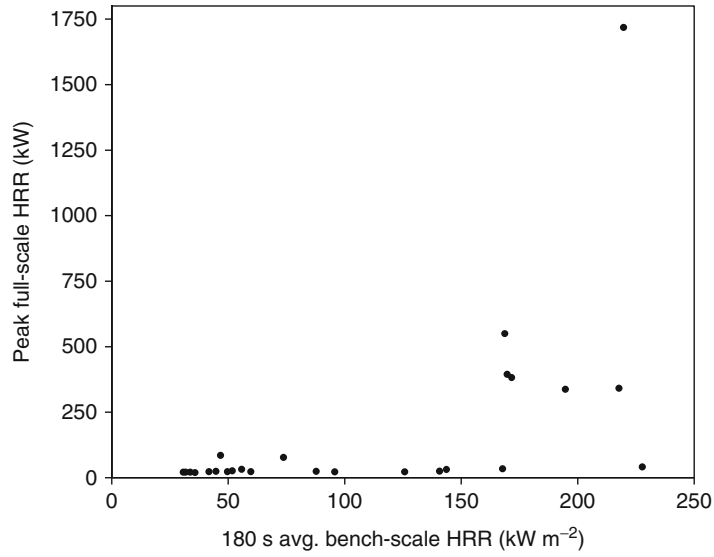

Fig. 26.63 HRR of mattresses predicted from bench-scale results. Full-scale tests under conditions of significant room effect; bench-scale HRR measured at 35 kW m^{-2} irradiance

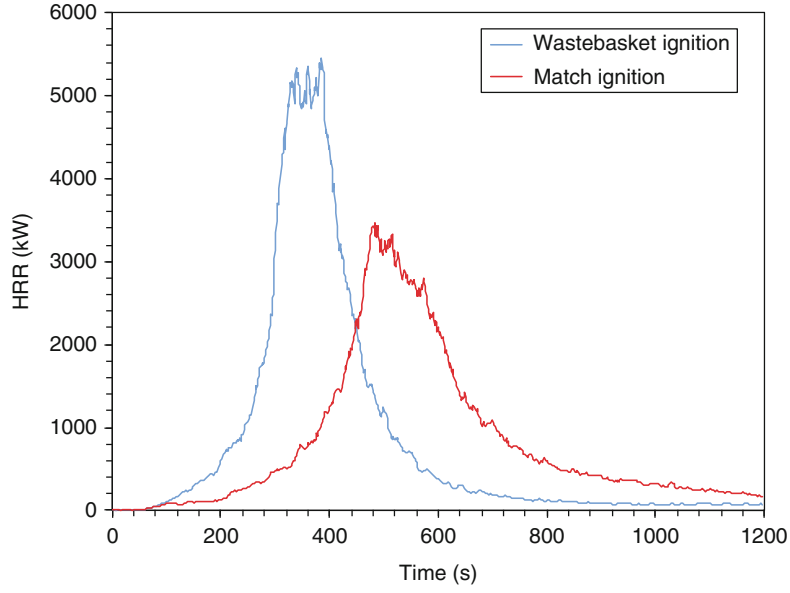

Fig. 26.64 Effect of ignition source on king-size bed assemblies

time at a slower rate (Fig. 26.64). In either case, however, the HRR values would suffice to cause flashover in a bedroom environment, especially in view of the fact that the HRR would be much higher due to room effect augmentation.

Some full-scale data obtained under conditions where a strong room interaction effect was seen are shown in Table 26.16 [141, 142]. The full-scale test setup was different for this data set, in that no bedding was used and ignition was with a burner flame at the edge of the mattress. Thus, some mattresses were able to show essentially zero HRR since bedding was not available to sustain burning, and the ignition source could be 'evaded' by receding specimens. A relation between full-scale and bench-scale

Table 26.17 Results on mattress from the CBUF study

Pk. HRR furn. calor. (kW)	Pk. HRR room (kW)	Springs	Thick. (mm)	Thick. factor	$\dot{q}''_{60}$	$\dot{q}''_{180}$	$\dot{q}''_{180} \times$ th. fac.	q''_{tot}	Prop. fire
26	42	Sofabed	22	0.44	162	135	59	50	N
31	45	N	50	1.00	136	82	82	21	N
47	61	Y	10	0.20	225	227	45	43	N
47	NA	Y	20	0.40	111	118	47	45	N
275	NA	N	90	1.00	111	118	118	45	Y
348	471	Y	20	0.40	327	159	64	30	Y
313	1700	N	100	1.00	256	191	191	62	Y
917	2550	N	140	1.00	232	198	198	37	Y

results from this study is shown in Fig. 26.63. The behavior in that study was found to be:

- Mattresses with a bench-scale HRR (180 s average value) of < 165 kW m^{-2} led to room fires of less than 100 kW.
- Mattresses with a bench-scale HRR (180 s average value) of > 165 kW m^{-2} generally led to room fires on the order of 1–2 MW.
- The transition between those extremes was very abrupt.

The sharp transition between trivial fires and room flashover conditions can be attributed to the details of the test room, but also to the use of an ignition source which specimens of intermediate characteristics could 'evade.'

Additional data on mattress HRR have been published by SP [143], Lund University [144], and in the CBUF project [10]. The CBUF study included full-scale room fire tests, open-burning furniture calorimeter tests, and Cone Calorimeter tests. The mattress results are given in Table 26.17. In both of the full-scale test environments, no bedding was used, but a square-head burner was applied to the top surface of the specimen, precluding complications from any receding-surface behavior. The bench-scale test data presented were obtained at a 35 kW m^{-2} irradiance. The results indicate that, when tested in the standard ISO 9705 room, a very drastic room effect occurs for open-air HRR values over about 300 kW.

The bench-scale data indicated that when widely varying mattress thicknesses exist, a simple relation of bench-scale to full-scale HRR cannot be sought, even if only predictions of open-burning (furniture calorimeter) results would be desired. As a first cut, it was concluded that mattresses can be grouped into two groups—those leading to propagating fires (the mattress being consumed in flaming combustion during a relatively short time), and those that do not. The former can be considered to be of the highest hazard, while the latter present only trivial hazard. Since, for practical reasons, all mattress composites must be tested in the Cone Calorimeter using a 50 mm thickness, to take into account effects due to thin mattresses, a thickness factor is defined:

$$Th.fac. = \min\left(\frac{thickness, mm}{50},\ 1.0\right)$$

For mattresses where the innersprings are used, the thickness is measured from the top of the mattress down to top of the metal springs; it is not the total thickness. To determine whether the mattress fire will propagate or not, the following rules were developed:

If $\dot{q}''_{180} \cdot (Th.fac.) < 100$ kW m^{-2}
and

$$\dot{q}''_{60} < 250 \text{ kW m}^{-2}$$

then,

$\dot{Q} < 80\ kW$ (non-propagating fire)

else,

$\dot{Q} > 80\ kW$ (propagating fire)

The HRR values over 80 kW in fact are flashover values of up to 2.5 MW, but the scheme does not assign a specific HRR number. Qualitatively, this scheme reflects the type of abrupt behavior change found in earlier studies

(Fig. 26.63), but here some more refined rules were developed that avoid non-predictions which would occur from simple correlation. During the same CBUF project, a more sophisticated mattress fire model has been developed by Baroudi et al.; this model is not easy to use, but details are available [10, 145].

In the US, mattresses made after July 1, 2007 have been required by law to conform to the 16 CFR 1633 standard of the Consumer Product Safety Commission. The latter augments the previous standard (16 CFR 1632) for smoldering by a flaming test procedure. The primary requirement for the new standard is that the peak HRR not exceed 200 kW; in addition the total heat release during the first 10 min of test must not exceed 15 MJ. NRCC [72] tested an example of one such mattress and did confirm a peak HRR < 200 kW. However, a room fire test run with this same model of mattress, an equally-conforming mattress foundation, and a set of bedding produced a peak HRR of 1812 kW. This would likely lead to flashover in a room of the ISO 9705 room size and doorway dimensions. Another test run by NRCC showed an extreme radiant feedback effect, since mattresses not made to the Federal standard typically showed HRR values in excess of 3000 kW even for small mattress sizes, while a bunk bed attained > 6000 kW in the room test.

Mining Equipment

Hansen and Ingason [146] tested two pieces of mining equipment, burning them in an underground mine facility. The first item was a Toro 501 DL diesel-powered wheel loader. The machine weighs 36,000 kg and stands 2.85 m tall. The structure is steel, but it also contains rubber tires, hydraulic oil, diesel fuel, and smaller components, including driver's seat, cables, etc., for an estimated fuel content of 76 GJ, the majority of this being the giant tires. The second item was a Rocket Boomer 322 drilling rig. This item weighs 18,400 kg and stands 2.95 m tall. Its fuel content was estimated at 46 GJ, with the fuel comprising hydraulic oil, hoses, tires, diesel fuel, cables, and

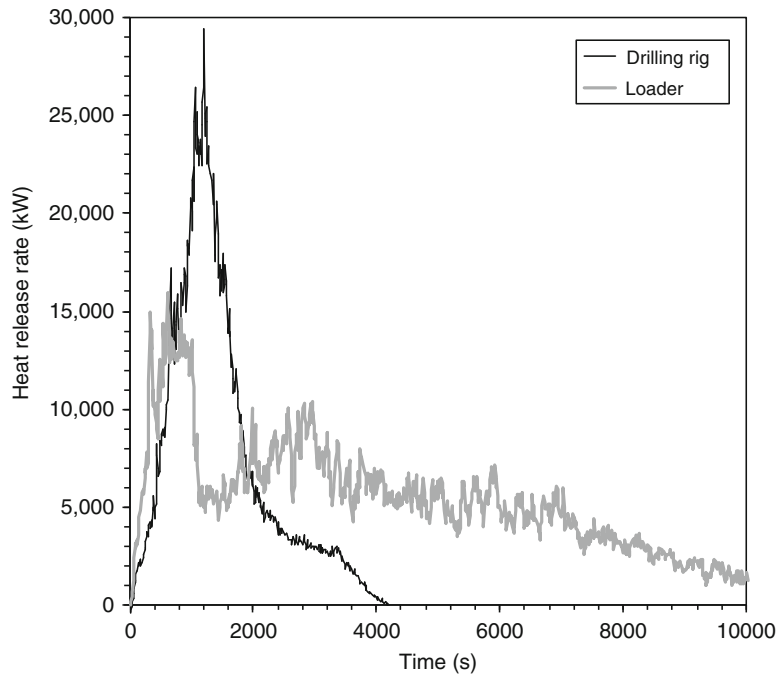

Fig. 26.65 HRR for two types of mining equipment

miscellaneous smaller items. With both items, the fuel tank was partly emptied and poured out to create a pool fire under the specimen, and this pool was ignited to start the fire. Figure 26.65 shows the HRR results, with loader achieving a peak value of 15.9 MW, while the drilling rig showing 29.4 MW.

Office Furniture

Office worker cubicles ('workstations') have been tested in several projects at NIST [147–149]. Figure 26.66 show that severe fire conditions can be generated by these arrangements. In some cases, fires of nearly 7 MW were recorded from the burning of a single person's workstation. The identification of the main conditions in these tests is given in Table 26.18. In one test series [147] replicates were tested in an open furniture calorimeter, then the configuration was tested again in a room test; this is illustrated in Fig. 26.67.

In 2004, NIST [150] reported results of some tests of modern office furniture, i.e., primarily plastics-based. Two full-scale tests were conducted, a single person cubicle, and a four-person cluster of cubicles. The one-person cubicle was tested in an open environment, while the four-person cluster was in a semi-open arrangement: three walls and a ceiling were present, but not the fourth wall. The results (Fig. 26.68) indicate both a radiant augmentation due to the ceiling and an augmentation due to multiple fuel

Table 26.18 Workstations tested by NIST in 1988 and 1992

Code	Combustible mass (kg)	Description	Number of sides w. acoustic panels	Ref.
A	291	Mostly old-style wood furniture	0	146
B	291	Semi-modern furniture	1	146
C	335	Modern furniture	2	148
D	NA	Modern furniture	3	148
E	291	Modern furniture	4	146
F	NA	Modern furniture	4	148

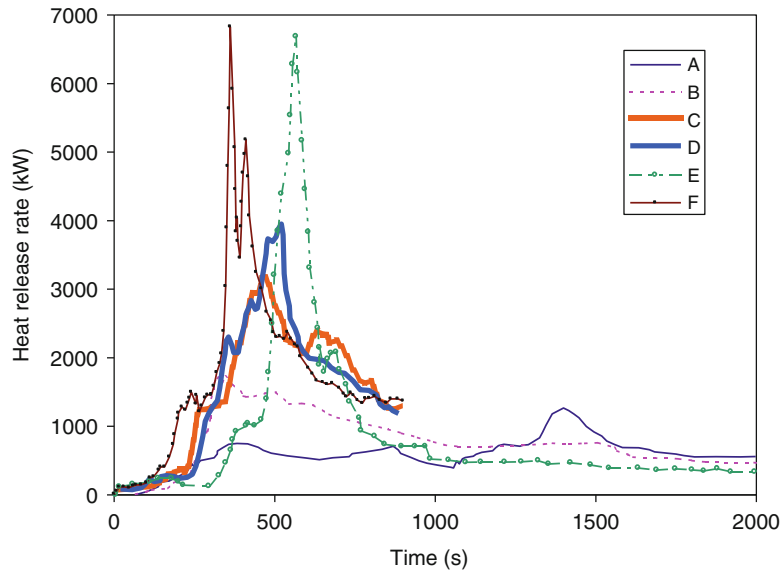

Fig. 26.66 HRR of office workstations tested by NIST in 1988 and 1992

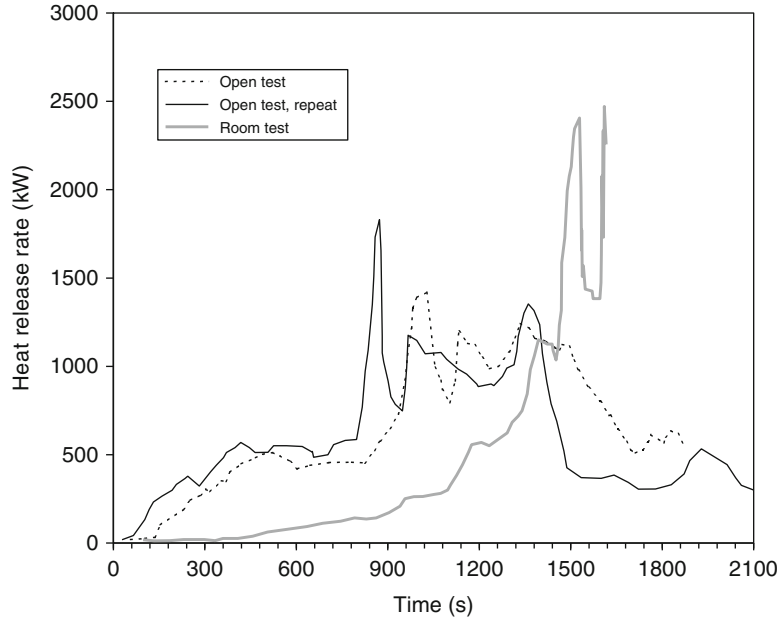

Fig. 26.67 NIST results for workstation tests of 1988 and 1992

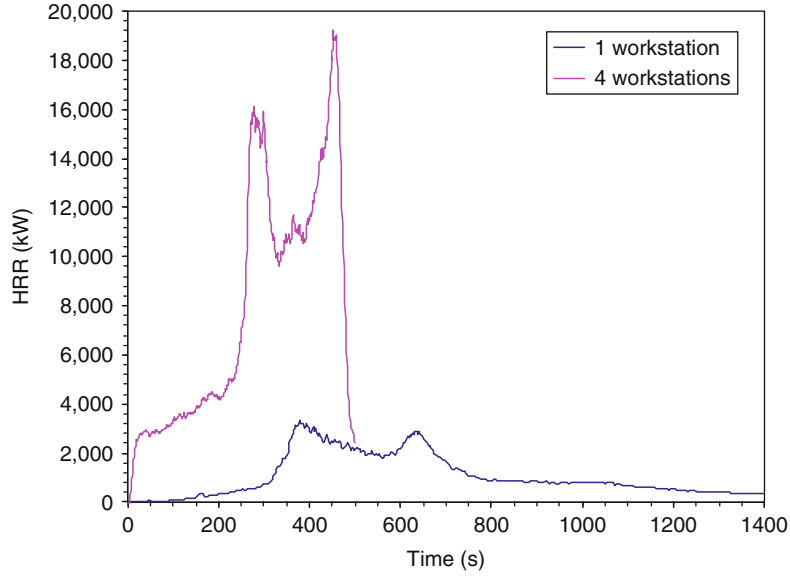

Fig. 26.68 NIST results for workstation tests of 2004

loads being present in direct proximity. In that same study, NIST also ran open calorimeter tests on two office chairs, a swivel chair and a chair with a fixed metal frame (Fig. 26.69). The gross mass for the chairs were 20.5 kg, and 11.8 kg, respectively, but the mass of the combustible portions was not evaluated, although the major fraction of the total mass was the mass of the steel components. The swivel chair had major components comprising hard-plastic shell material, and the fire involvement of these components was the cause of the second HRR peak.

Additional tests were conducted by Kakegawa et al. [151] at Japan's National Research Institute of Fire and Disaster. Each test was started by a

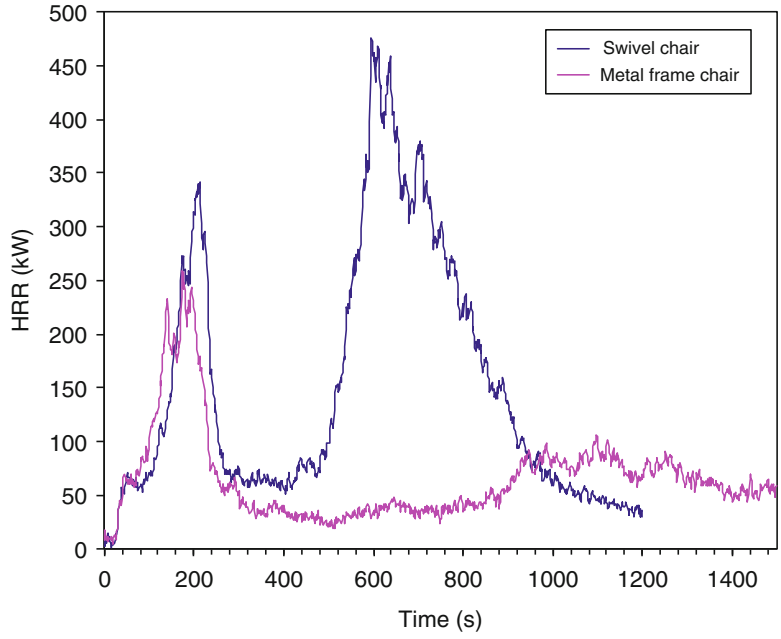

Fig. 26.69 HRR results for the two office chairs tested

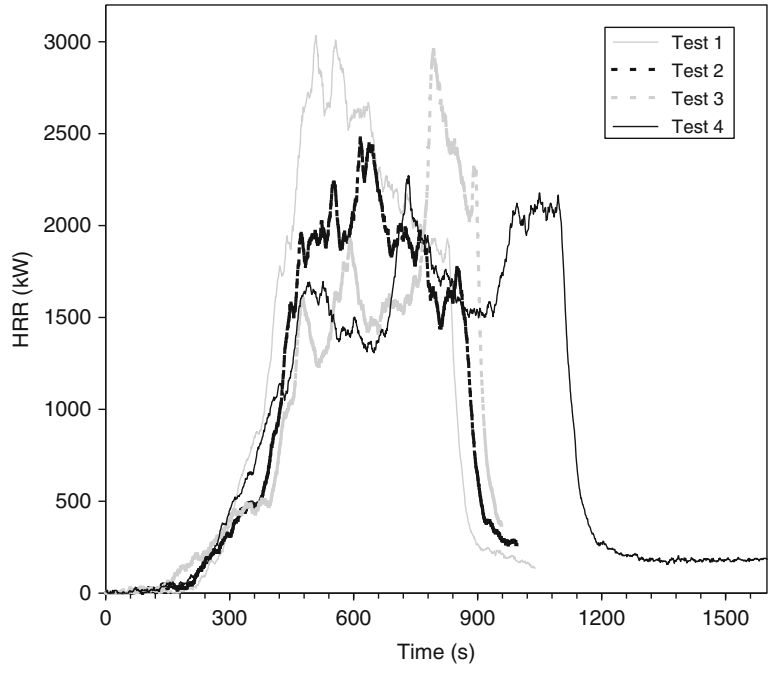

Fig. 26.70 HRR of four-unit workstations tested at NRIFD

polypropylene wastebasket filled with 0.2 kg of paper. The wastebasket, by itself, was found to show a peak HRR of 50–60 kW. The desks were of modern metal-frame construction, with plastic trim parts. In addition, the workstations contained small filing cabinets, telephones, chairs, computers, and a modest amount of office paper. The HRR results for the four-unit

Table 26.19 Workstations tested by NRIFD

Test	Combustible mass (kg)	Type of workstation	No. of desk units	Partition panels	Peak HRR (kW)	Time to peak (s)
1	570	Clerical	4	N	3035	508
2	597	Clerical	4	Y	2476	616
3	1054	Engineering	4	N	2957	793
4	1086	Engineering	4	Y	2271	732
11	272	Engineering	1	Y	1602	441
12	264	Engineering	1	N	1870	412
14	263	Engineering	1	N	1219	601

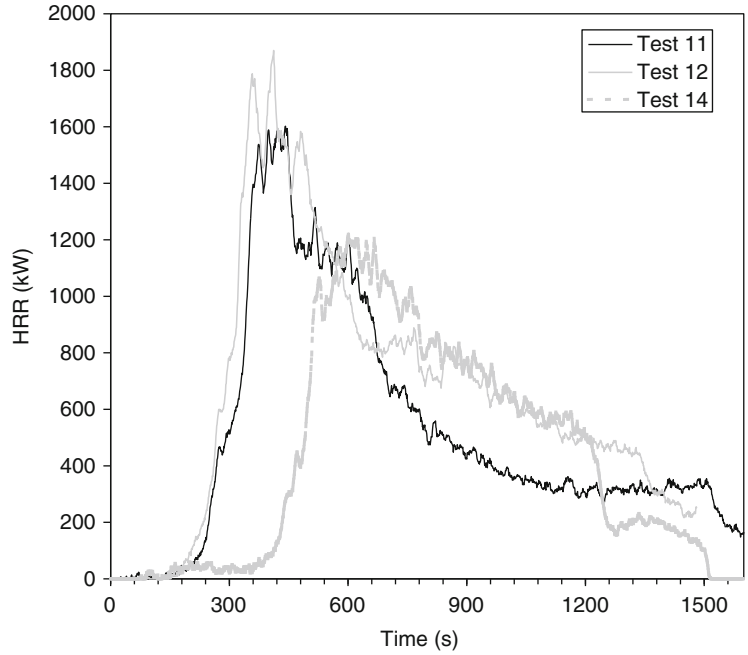

Fig. 26.71 HRR of one-unit workstations tested at NRIFD

workstations are shown in Fig. 26.70, while those for the one-workstation units are shown in Fig. 26.71. Even though the four-unit workstations had a very high fuel load, the HRR values were lower than the American units studied at NIST. This is presumably due to a more protected arrangement of the fuel, plus the fact that only short (0.45 m high) partition panels were used (Table 26.19).

Pallets

Conceptually, a wood pallet is a similar arrangement to a wood crib. The geometry, however, is different. Instead of being composed of identical rows of square-section sticks, pallets are made up of rectangular elements in a traditionally dimensioned configuration as shown in Fig. 26.72. The fire safety concern with pallets arises when they are idle and stacked many units high. Krasner [152] has reported on a number of tests where the burning rate of pallets was measured. A typical experimental heat release rate curve is shown in Fig. 26.73. This curve shows that, much like for a wood crib, a substantially constant plateau burning can be seen if the stack is reasonably high. The results for a standard pallet size of 1.22 × 1.22 m can be given as a general heat release rate expression

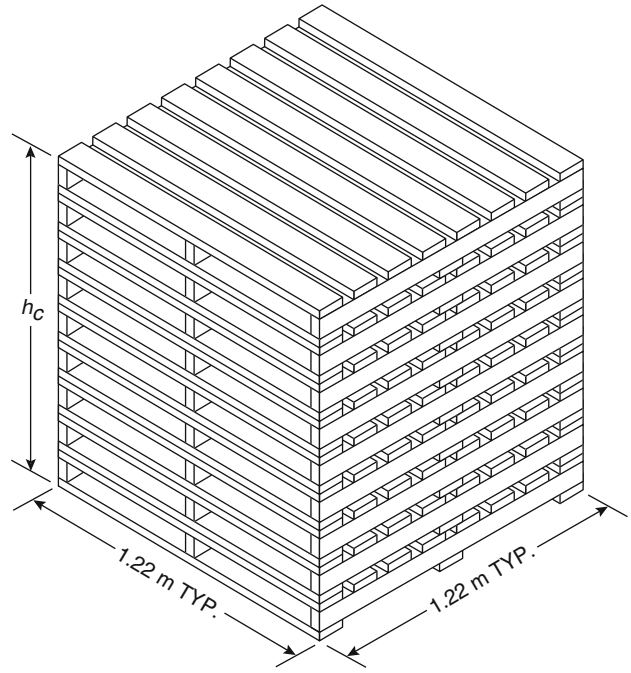

Fig. 26.72 The geometric arrangement of a stack of wood pallets

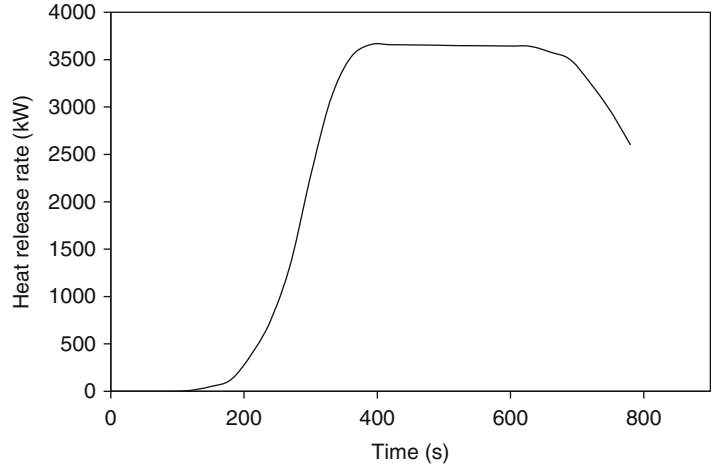

Fig. 26.73 HRR of a typical wood pallet stack (1.22 × 1.22 × 1.22 m high)

$$\dot{q} = 1368\left(1 + 2.14h_p\right)(1 - 0.03M) \qquad \dot{q}'' = 919\left(1 + 2.14h_p\right)(1 - 0.03M)$$

where h_p is stack height (m), M is moisture (%), and a net heat of combustion of 12×10^3 kJ kg^{-1} has been assumed. For convenience in applying to nonstandard pallet sizes, this can be expressed on a per-unit-pallet-floor-area basis as:

The agreement between the above equations and experimental data is seen to be good over a wide range of pallet heights (Fig. 26.74), but the expressions do somewhat overpredict the burning rates if applied to short stacks, with stack height $h_p < 0.5$ m.

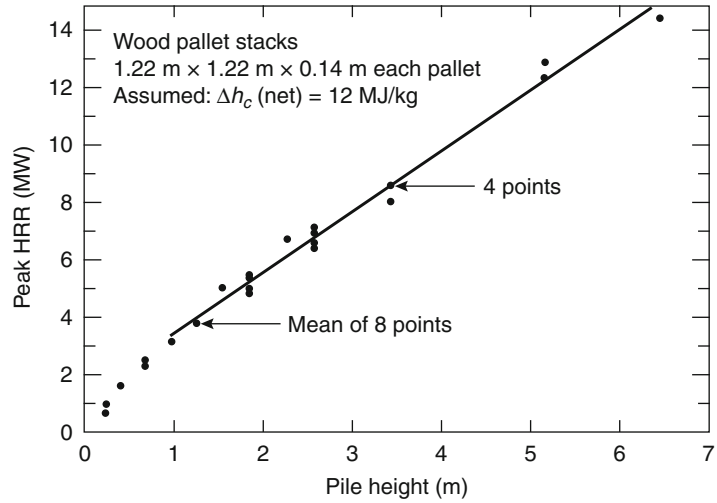

Fig. 26.74 Dependence of pallet HRR on stack height

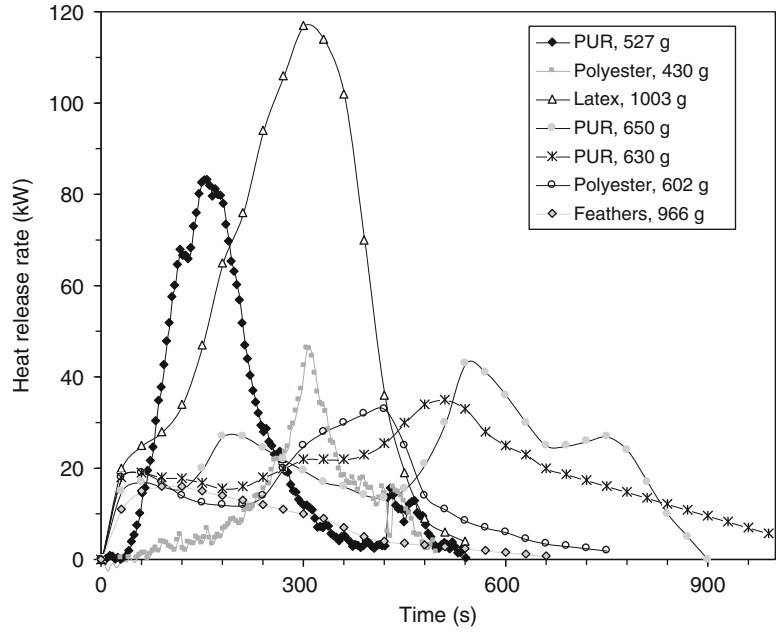

Fig. 26.75 HRR of pillows

Pillows

Pillow tests have been reported by NIST [153] and SP10. The results are given in Fig. 26.75.

Pipe Insulation

The available data are from the configuration where pipe insulation is used to entirely cover the ceiling of a test room. The test method used is a variant of ISO 9705 especially configured for pipe insulation testing [154]. Data on this configuration have been published by Wetterlund and Göransson [155] and by Babrauskas [156].

Plants and Vegetation

Trees, Natural

Some tests on Christmas trees were reported by VTT [157] and by Damant and Nurbakhsh [158].

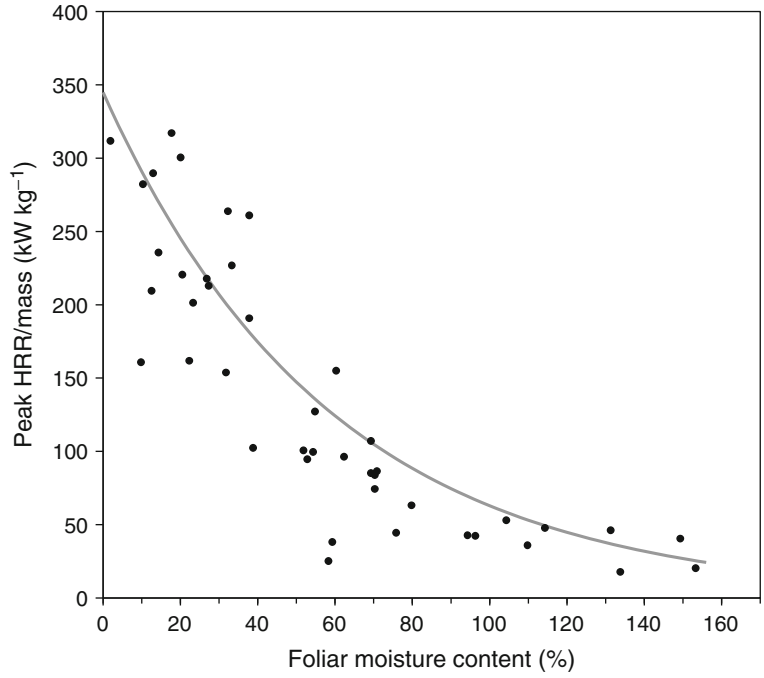

Fig. 26.76 The peak HRR for Douglas-fir Christmas trees, as a function of moisture and mass

Newer studies, however, indicated that these tests, which examined only a few trees, did not capture the full range of HRR values associated with Christmas trees. The main variables that govern the HRR of Christmas trees are the following:

- Moisture content of the needles
- Mass of the tree
- Species
- Ignition source used

Moisture is the dominant variable and this had not been studied previously. The results of an extensive series of fire tests [159] on Douglas-fir (*Pseudotsuga menziesii*) trees are shown in Fig. 26.76, while the HRR of a typical test is illustrated in Fig. 26.77. The trees were about 2.1 m tall, had an average mass of 11 kg. The trees were cut, placed in a watering stand, and watered according to various watering programs. The average tree was kept for 10 days prior to testing. The relation of the curve fit in Fig. 26.76 is:

$$\dot{q}/mass = \frac{400}{1 + 0.0538MC}$$

where MC = foliar moisture (%) and the units of $\dot{q}/mass$ are kW kg^{-1}. Moisture is measured on a dry basis, so values can readily exceed 100 %; also note that it is the needle (foliar) moisture that governs the burning behavior—trunk moisture is not a relevant variable. The mass of the tree used here is the entire mass; Evans et al. [160] suggested that if data are available only for the foliar mass, but not the mass of the entire tree, the approximation be used:

$$mass = 2 \times mass_{foliar}$$

To ignite trees with a small flame requires that the moisture content be below 50–60 %. Otherwise, ignition is still possible if using larger combustible objects. In the work reported, the trees which could not be ignited by a small flame were all ignited by first igniting wrapped gift packages placed under the tree. For design purposes, it should be adequate to assume that the heat release curve is a triangle. This requires knowing only the peak HRR and the total heat released. To estimate the latter, it was found in the tests that the Christmas trees showed an effective heat of combustion of 13.1 MJ kg^{-1}. Thus, from knowing the mass of the tree and the effective heat of combustion, the total heat

release may be estimated. The needle moisture may not be known for design purposes. It is governed both by the watering program and by the innate biology, e.g., the species, of the tree. No model is available at the present time that can predict the moisture. However, the research indicated that Douglas-firs are a notably short-lasting species. The data points shown in Fig. 26.76, with one exception, represent trees that had been on display for less than 16 days; some were watered carefully and regularly, while others were not. Other species of Christmas trees, such as Noble fir or Fraser fir are considered to be longer-lasting, but are less commonly bought.

A smaller test series on Scotch pine trees was tested at NIST by Stroup et al. [161]. They examined trees of 2.3–3.1 m height and mass between 9.5 and 20.0 kg; with one exception, the trees were of mass 12.7 kg or greater. Apart from one tree, which is not considered here since it was not successfully ignited, the trees were left without water for 3 weeks in a room at 50 % RH and 23 °C. Ignition was with an electric match to a lower branch of the tree. The Scotch pines were substantially taller and heavier than the Douglas-firs, so it is not surprising that higher peak HRR values were attained. The peak HRR values ranged from 1620 to 5170 kW. Normalized per mass, the average was 183 kW kg^{-1}, with the range being 103–259 kW kg^{-1}. The moisture of the branches was not recorded, but presumably was <20 % in all cases. Comparing to the above results, Douglas-firs showed about 160–330 kW kg^{-1}. This would suggest that there is a species effect and that Scotch pines show a HRR/mass ratio approximately 0.75 of that found for Douglas-firs. This conclusion is very tentative, however, since the test programs did not use the same test protocol. Part of the difference might also be attributed to a height effect, since this cannot separately be taken into account.

Madrzykowski [162] ran more recent tests at NIST on 2.05–2.54 m tall Fraser fir trees with a moisture content of 6–9 %. The peak HRR values ranged from 3231 to 4344 kW, while the mass of the specimens ranged from 10.97 to 13.81 kg, giving an average peak HRR/mass value of 286 kW kg^{-1}, with a range of 218–348 kW kg^{-1}. The author also ran one interesting test where a tree was burned lying on its side, instead of vertical. This gave a much lower peak HRR value of 1603 kW, indicating a major role of geometry.

Jackman et al. [163] tested Noble fir and Norway spruce specimens. For a relatively dry (26 % MC) Noble fir (16.3 kg, 3.07 m tall) they got a peak HRR of 2880 kW. A similar Norway spruce (20 % MC, 14.9 kg, 3.02 m high) showed only 1590 kW. Because very few tests were run, this should not be taken to indicate an intrinsic species effect.

Bushes, Natural

Stephens et al. [164] tested Tam juniper (*Juniperus savina tamariscifolia*) shrubs of various moisture contents, ignited by a medium gas flame. For MC < 50 %, rapid combustion resulted and samples showed 1800–2100 kW peak HRR. Specimens of 50–80 % MC typically showed 600–800 kW, while specimens of higher MC did not burn significantly. Unfortunately, neither the mass nor the size of the specimens were specified, except that they were denoted as "mature." Shrubs of this species in general reach about 0.45 m height and cover about 1 m of width.

Etlinger [165] conducted more extensive tests on a series of decorative-shrub species: Armstrong juniper (*Juniperus chinensis* 'Armstrongii'), hedge saltbush (*Rhagodia spinescens*), milkflower cotoneaster (*Cotoneaster lacteus*), mountain lilac (*Ceanothus ray* 'Hartman'), oleander (*Nerium oleander*), purple rockrose (*Cistus purpureus*), quail bush (*Atriplex lentiformis*), sageleaf rockrose (*Cistus salvifolius*), Santa Barbaras ceanothus (*Ceanothus impressus* 'Eleanor Taylor'), trailing rosemary (*Rosmarinus officinalis* 'Prostrata'), and vine hill manzanita (*Arctostaphylos densiflora* 'Howard McMinn'). The bushes were typically in the range of 0.5–1.0 m tall and weighed 1–3 kg. He ignited the bushes first with a 40 kW burner, which did not cause the specimens to show a significant HRR output, followed by an exposure to a 150 kW burner. Some typical results upon exposure to a 150 kW burner are shown in Fig. 26.78.

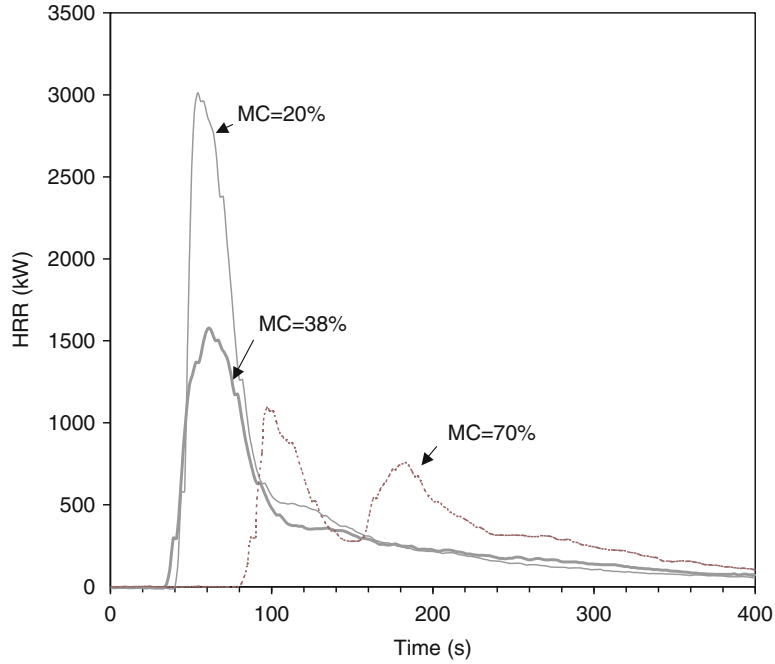

Fig. 26.77 Typical HRR curves of Douglas-fir Christmas trees

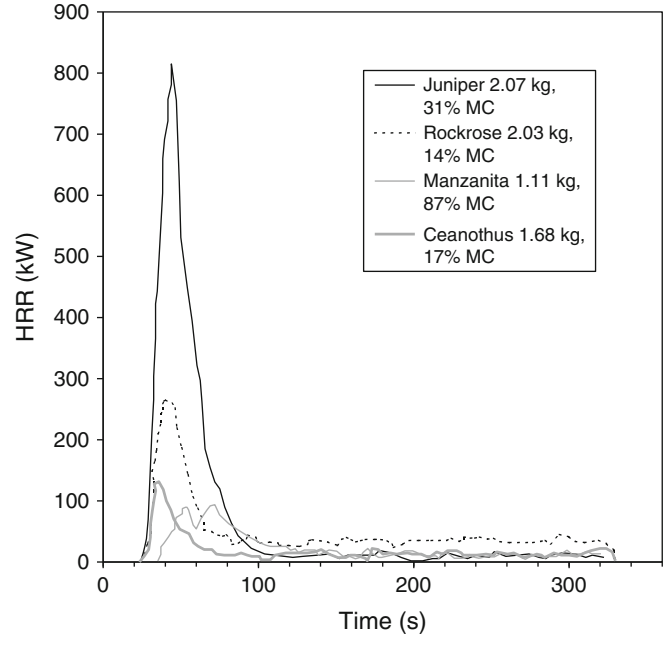

Fig. 26.78 Typical HRR for bushes obtained by Etlinger

A summary of Etlinger's peak HRR values is shown in Fig. 26.79. There is a significant amount of scatter, but the results for the bushes are not systematically different from those for trees, which are also shown on the same plot. Thus, a single expression for the peak HRR can be derived which is suitable for both trees and bushes:

$$\dot{q}/mass = \frac{700}{1 + 0.1295MC}$$

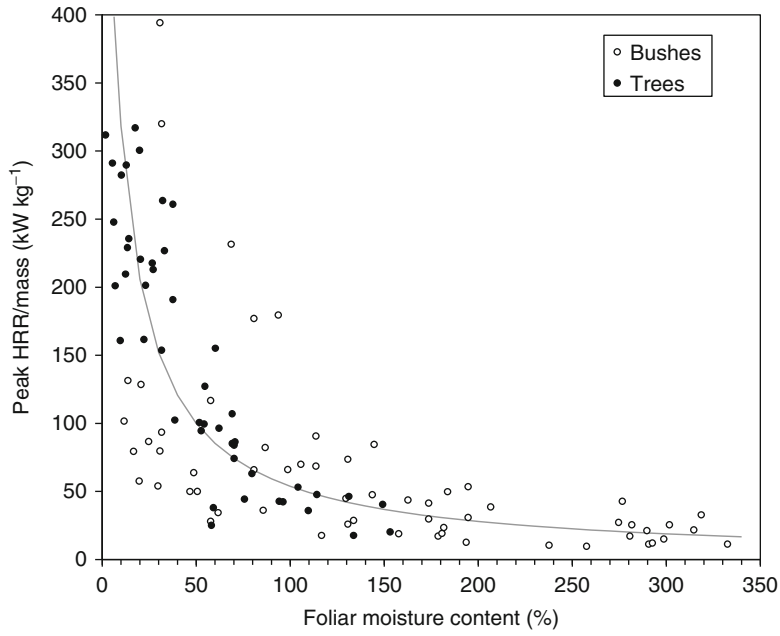

Fig. 26.79 HRR of bushes and trees, plotted on a unified basis

Trees, Plastic

UL had published a procedure for testing artificial Christmas trees. This was identified as Subject 411 [166]. It was eventually withdrawn due to lack of activity in this area, but the basic test procedure is sound. In the UL procedure, the ignition source comprises 454 g of shredded newspaper, conditioned at 35–40 % RH, and dispersed in a 610 mm diameter circle around the base of the tree. The newspaper is ignited at four points around the perimeter of the circle. This ignition source is realistic, since it represents the effect of burning gift packages or decorations at the base of the tree. Babrauskas [167] tested PVC trees of 4.2–4.7 kg mass and 1.96–2.01 m height.

Figure 26.80 shows the results for two replicates using the exact using the UL procedure and a third test where the newspaper was ignited at one point only. The specimens proved impossible to ignite with a small flame, but using the UL procedure they produced rapidly developing fires, with 500 kW being attained 11–20 s after ignition. The peak flame heights of the two specimens ignited in four places was 4.8–5.1 m. Using the Zukoski [168] or McCaffrey [169] flame height/HRR correlations, such flame heights imply peak HRR values of 2800–3100 kW. The values actually measured are systematically low due to two reasons: (1) mixing dilution effects due to use a large, room-sized calorimeter hood; and (2) inability of instrumentation to respond to a fast-growing fire.

Jackman et al. [162] tested three artificial trees (2.0–2.5 m height) and obtained peak HRR values of 100–400 kW. It is not clear whether these low values represent an intrinsically low HRR of these trees (of unspecified plastic) or whether it simply reflects the fact that an ignition source was used which is much less serious than the one in the UL procedure.

Bushes, Plastic

Some HRR data on plastic house plants are shown in Fig. 26.81 [170].

Pools, Liquid or Plastic

Possibly the simplest geometric arrangement of fuel is a liquid (or thermoplastic) pool. Over the last four decades, an enormous number of studies have been conducted where pool burning was

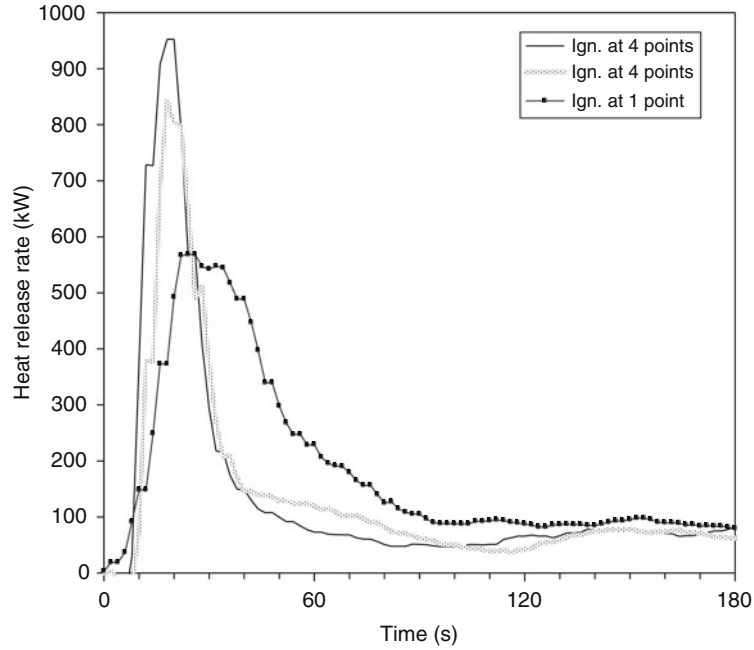

Fig. 26.80 Recorded HRR for PVC Christmas trees (actual HRR was greater, due to very fast rise time)

considered theoretically or measured empirically. The most systematic early study was by two Russian researchers, Blinov and Khudiakov [171]. Their results were analyzed by Hottel [172], who pointed out that conservation of energy can be applied to the pool:

$$\dot{q} = \dot{q}'' \times A = \left(\dot{q}_r'' + \dot{q}_c'' - \dot{q}_{rr}'' - \dot{q}_{loss}''\right) \times \left(\frac{\Delta h_c}{\Delta h_g}\right) \times A$$

where $\dot{q}$ is the heat release rate of the pool; double-prime denotes per unit area; A is the area of the pool (m^2); $\dot{q}_r''$ is the radiant heat flux absorbed by the pool; $\dot{q}_c''$ is the convective heat flux to the pool; $\dot{q}_{rr}''$ is the heat flux re-radiated from the surface of the pool; and into $\dot{q}_{loss}''$ are lumped wall conduction losses and non-steady terms. The heat of gasification is Δh_g (kJ kg^{-1}), while the (lower, or net) heat of combustion is Δh_c. Note that some authors use the symbol L for the heat of gasification. The heat of gasification is defined as the enthalpy required to bring a unit of mass of liquid-phase substance at 25 °C to the gaseous state at the temperature T_b, its boiling point. It should not be confused with the latent heat of evaporation Δh_v, which is the enthalpy required to change a unit mass of liquid to a gas at 25 °C. The relation between these two quantities is:

$$\Delta h_g = \Delta h_v + (T_b - 25) \times C_{pv}$$

where we have taken the simplification that C_{pv}, the heat capacity of the vapor (kJ kg^{-1} K^{-1}) is a constant. An extensive tabulation of these constants is provided by Babrauskas [173].

Table 26.20 The burning regimes for liquid pools

Diameter (m)	Burning mode
< 0.05	Convective, laminar
0.05–0.2	Convective, turbulent
0.2–1.0	Radiative, optically thin
> 1.0	Radiative, optically thick

Hottel's analysis of Blinov and Khudiakov's data showed two basic regimes are possible: radiatively dominated burning for large pool diameters, D, and convectively dominated burning for small D. Furthermore, in the convective regime the flow can be either laminar or turbulent (being always turbulent for radiatively driven pools), while in the radiative regime the flames

can be optically thin or thick. These distinctions can, in the simplest analysis, be made solely on the basis of pool diameter. Such a simple classification is possible if the pool is strictly circular, radiant heating is only from the pool's flames and not augmented by external sources, and there are no interferences to the flow streamlines which could trip the onset of turbulence. In such a simplified case, the regimes can be identified as in Table 26.20.

In the convective limit (small pools), one may make the following approximation:

$$\dot{q} = \dot{q}_c'' \times \left(\frac{\Delta h_c}{\Delta h_g}\right) \times A$$

however, the values of $\dot{q}_c''$ to be taken are not easily determined. Some additional details are given in [174]. For fire hazard analysis purposes, liquid pool fires will rarely be significantly dangerous if they are smaller than about 0.2 m in diameter. Thus, it will often only be necessary to treat pools burning in the radiative regime. In the radiative regime, it is found that data for most organic liquids can be well correlated by:

Table 26.21 Pool burning: thermochemical and empirical constants for a number of common organic fuels

Material	Density (kg m^{-3})	Δh_g (kJ kg^{-1})	Δh_c (MJ kg^{-1})	$\dot{m}_\infty''$ (kg m^{-2} s^{-1})	$k\beta$ (m^{-1})
Cryogenics					
Liquid H_2	70	442	120.0	0.017 (±0.001)	6.1 (±0.4)
LNG (most CH_4)	415	619	50.0	0.078 (±0.018)	1.1 (±0.8)
LPG (mostly C_3H_8)	585	426	46.0	0.099 (±0.009)	1.4 (±0.5)
Alcohols					
Methanol (CH_3OH)	796	1195	20.0	[a]	[a]
Ethanol (C_2H_5OH)	794	891	26.8	[a]	[a]
Simple organic fuels					
Butane (C_4H_{10})	573	362	45.7	0.078 (±0.003)	2.7 (±0.3)
Benzene (C_6H_6)	874	484	40.1	0.085 (±0.002)	2.7 (±0.3)
Hexane (C_6H_{14})	650	433	44.7	0.074 (±0.005)	1.9 (±0.4)
Heptane (C_7H_{16})	675	448	44.6	0.101 (±0.009)	1.1 (±0.3)
Xylenes (C_8H_{10})	870	543	40.8	0.090 (±0.007)	1.4 (±0.3)
Acetone (C_3H_6O)	791	668	25.8	0.041 (±0.003)	1.9 (±0.3)
Dioxane ($C_4H_8O_2$)	1035	552	26.2	0.018	5.4
Diethyl ether ($C_4H_{10}O$)	714	382	34.2	0.085 (±0.018)	0.7 (±0.3)
Petroleum products					
Benzine	740	–	44.7	0.048 (±0.002)	3.6 (±0.4)
Gasoline	740	330	43.7	0.055 (±0.002)	2.1 (±0.3)
Kerosene	820	670	43.2	0.039 (±0.003)	3.5 (±0.8)
JP-4	760	–	43.5	0.051 (±0.002)	3.6 (±0.1)
JP-5	810	700	43.0	0.054 (±0.002)	1.6 (±0.3)
Transformer oil, hydrocarbon	760	–	46.4	0.039	0.7
Fuel oil, heavy	940–1000	–	39.7	0.035 (±0.003)	1.7 (±0.6)
Crude oil	830–880	–	42.5–42.7	0.060	0.62
Solids					
Polymethylmethacrylate	1184	1611	24.9	0.020 (±0.002)	3.3 (±0.8)
Polyoxymethylene $(CH_2O)_n$	1425	2430	15.7		
Polypropylene $(C_3H_6)_n$	905	2030	43.2		
polystyrene $(C_8H_8)_n$	1050	1720	39.7		

[a]See text

$$\dot{q} = \Delta h_c \dot{m}''_\infty \left(1 - e^{-k\beta D}\right) \times A$$

This requires determining two empirical constants: $\dot{m}''_\infty$ and the term $(k\beta)$; the first of these is the asymptotic mass loss rate per unit area as the pool diameter increases towards infinity; the second is the product of the extinction-absorption coefficient k and the beam-length corrector β. These constants are given in Table 26.21 for a number of common fuels.

The net heat of combustion, Δh_c, is also listed in the table. In principle, a slightly lower value, the *effective heat of combustion*, should be used instead of the net heat of combustion that is determined with oxygen bomb calorimetry. Some bench-scale values of a combustion efficiency factor to convert oxygen bomb values into experimentally-measured values are given in Chap. 36, "Combustion Characteristics of Materials and Generation of Fire Products." For most liquids, however, the bench-scale values are not greatly below unity and realistic large-scale measurements are not available, thus the improvement in accuracy by extrapolating from bench-scale results may be nil.

Alcohol fuels show minimal radiative flux, in comparison to other fuel types. Thus, the best recommendation previously had been to use constant values of $\dot{m}''$, independent of diameter. Based on some newer test results [175], it is clear that a diameter effect does exist, although it cannot be expressed in standard form. Thus, it is recommended that for methanol or ethanol the values be used: $\dot{m}'' = 0.015$ (D < 0.6 m); $\dot{m}'' = 0.022$ ($0.6 <$ D < 3.0 m); and $\dot{m}'' = 0.029$ (D > 3.0 m).

The above discussion implicitly assumed that the pool depth is at least several millimeters. If liquids are spilled on a horizontal surface that has no low spots and no diking, then a liquid layer will form that is less than 1 mm thick. *Thin-layer pools* of this nature (which can occur in arson cases) show a lower HRR than do pools of greater depths. Putorti et al. [176] studied gasoline spills on wood parquet, vinyl floor tiles and carpeting. When a specified volume of liquid is spilled, the problem to be solved can be separated into two components: (1) determining the area of the spill, or, equivalently, the spill thickness; and (2) determining the HRR per unit area.

For wood floors, Putorti found the $A = 1.5\ V$, where A = area (m^2) and V = volume (L). For vinyl tile, a similar relation was also found, but the constant being 1.8. Converted into layer thicknesses, the thickness for wood was 0.67 mm

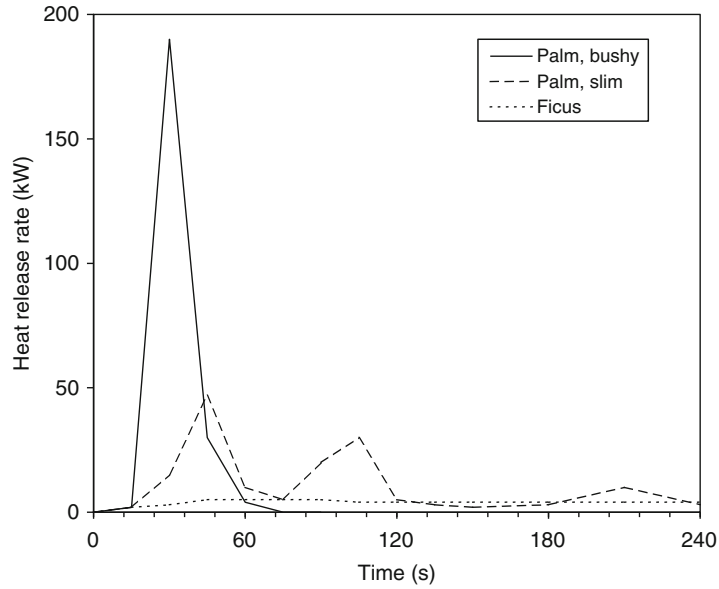

Fig. 26.81 HRR of plastic house plants

and for vinyl tile it was 0.56 mm. Earlier work has indicated that a relation of this kind should only be applied to smooth floor surfaces. For rough, absorptive surfaces a constant thickness is not obtained, and larger spill volumes produce, effectively, greater layer thicknesses [177].

Putorti's study with carpets both indicated large differences between carpet types and also showed that the data could not be represented as a constant layer thickness. The HRR per unit area values are shown in Fig. 26.82. For the solid surface pours, the spill areas were in the range 0.4–1.8 m^2. As presented above, pools of large depths in this size range would show HRR values of 1900–2400 kW m^{-2}. Thus, the carpet-surface values are about 70–80 % of values that would have been computed using the normal pool fire formulas. The smooth-surface values, however, are only about 1/5 of the values that would be found for pools of sizable depths.

A similar study by Gottuk et al. [178] also describes HRR values for spills on hard surfaces that are, very roughly, about 1/5 of those for 'normal' pools. The relationships found by Putorti can only be expected to hold on dead-flat surfaces. If surfaces are crooked, then ponding at low spots will occur and uniform spill depths should never be anticipated.

DeHaan [179] conducted two tests using 1.9 L of Coleman camping fuel. This is a straight-run petroleum distillate containing normal and iso-alkanes ranging from hexane to undecane. When poured on an unpadded carpet, a HRR peak of 1150 was found, with a burning time of roughly 3 min. When poured upon a carpet that had an pad underneath it, a lower HRR peak (890 kW) was found, the peak was slightly delayed (85 s, versus 65 s) and there was a long tail to the HRR curve.

The discussion above pertains only to open-burning fires. Thus, the literature-derived burning rates can be used only in the case of a very large, well-ventilated room (compared to the size of the fire). If calculations show that the 'free-burning' pool would cause a temperature rise of more than, say, 100 °C, then it is clear that radiative feedback will start being important and such an approximation cannot be made. No simple formulas exist for computing the enhanced burning rates when a pool receives significant room radiation. If computations under these conditions are necessary, the theoretical study of Babrauskas and Wickström [11] should be consulted. The computer program COMPF2 [180] can also be used to treat this case.

The problem of pool burning is interesting from a combustion science point of view, and over the years there has been a very large number of studies which attempted to go beyond empirical predictions [181–184]. In addition, work is occurring to provide more detailed experimental measurements for specific fuels [185, 186].

Table 26.22 HRR of European refrigerators

Specimen	R1	R2	R3
Initial mass (kg)	70.0	67.2	43.7
Mass loss (kg)	18.0	14.3	18
Peak HRR (kW)	2125	1816	852
Extinguishment time (s)	925	722	–
Total heat (MJ)	537	404	432

Refrigerators

VTT tested [105] two European refrigerators using a propane burner of 1 kW (designated R1, R2), while EFRA tested a single refrigerator (R3), ignited with a needle-flame burner. The specimens are described in Table 26.22, while test results are shown in Fig. 26.83. The VTT specimens were extinguished before the ultimate peak burning would have occurred, while the EFRA specimen was not. These results must not be applied to appliances used in North America, since European appliance styles are different from North American ones and also because local standards are such as to permit appliances of greater flammability in Europe.

Shop Displays

Chow [187] tested shop displays of three types: clothing display, compact disc (CD) display, and

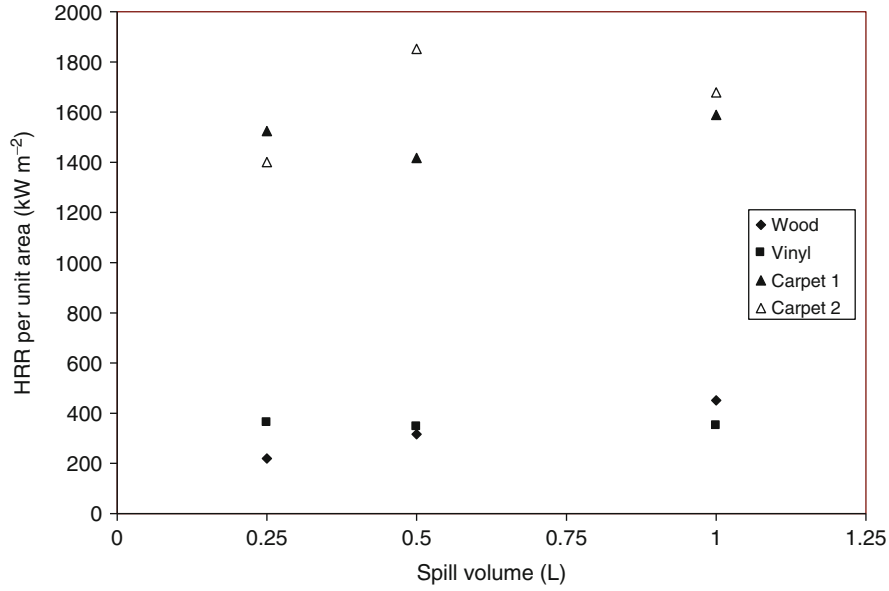

Fig. 26.82 HRR of thin pools of gasoline over various surfaces

Table 26.23 Shop-display commodities tested by Chow

Display type	Combustible mass (kg)	Size (m)	Ignition source (kW)	Peak HRR (kW)
Clothing			470	2400
Compact discs		2 ea, 1.5 m wide × 1.6 m high	1100	
Newsstand	15	2 ea, 1 m wide × 2.2 m high	400	3600

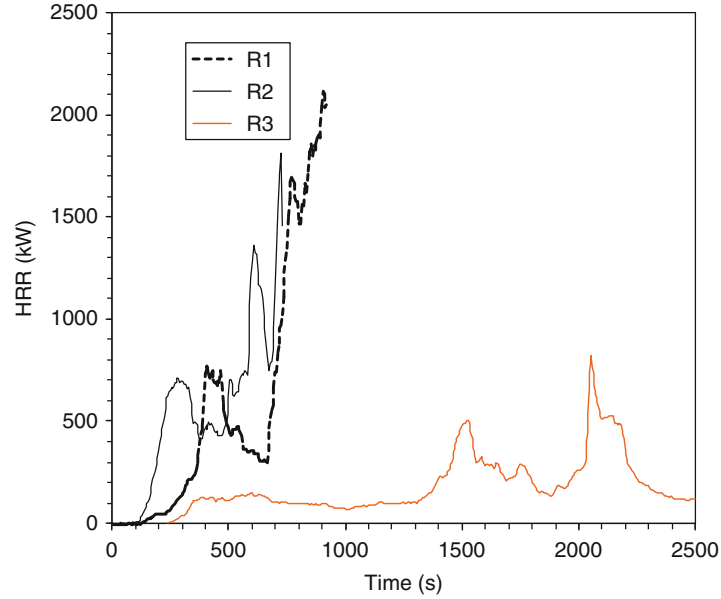

Fig. 26.83 HRR of European refrigerators tested by VTT and EFRA

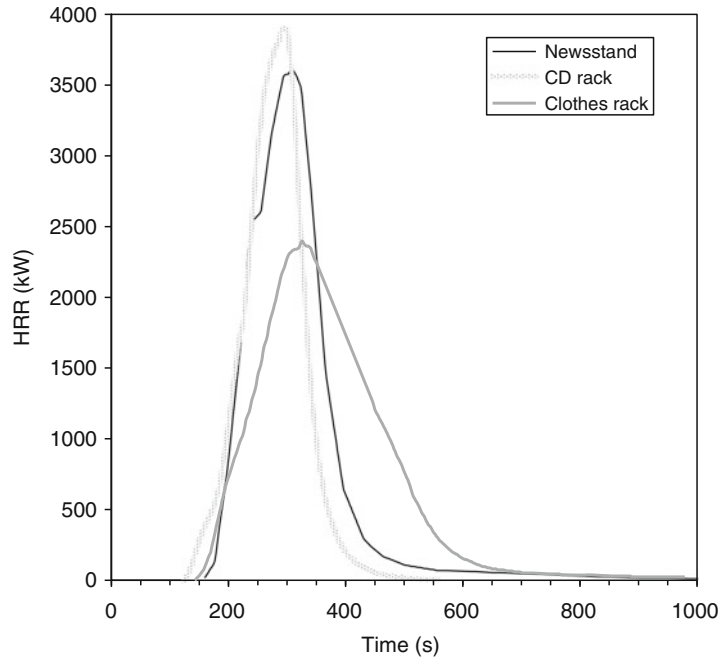

Fig. 26.84 HRR of various shop-display commodities tested by Chow

newsstand. The clothing display comprised all-cotton T-shirts arranged on four small display racks. The CD display contained a total of 240 discs. The ignition source in each case was a small pool of gasoline, to represent an arson fire. The results are shown in Table 26.23 and Fig. 26.84.

Television Sets

The burning characteristics of TV sets depend greatly on whether they have been made for the North American market, following the requirements of UL, or not. In countries where UL standards do not apply, plastic TV cabinets are generally highly flammable, commonly being made of plastics that only have an HB rating according to the UL 94 [30] procedures. These are readily ignitable from small-flame ignition sources and burn vigorously when ignited [44, 188]. By contrast, sets made for the North American market have to obtain a V-0 classification under UL 94 and will resist ignition from small flame sources.

Babrauskas et al. [88] tested at NIST small polystyrene television cabinets of two types, fire-retarded and not. Since the circuit components contribute negligible HRR in comparison to the outer shell, only the cabinets were tested. Two very small ("personal size") units were tested side-by-side in each test. This can represent either two appliances or simply the mass of one larger set.

SP tested two television sets [29], a US-market set with housing having a V-0 rating, and a Swedish set with a housing having an HB rating. The US set was a 690 mm (27 in.) model, while the Swedish one was 710 mm (28 in.). The US set had a total combustible mass of 6.5 kg, with 2.9 kg comprising the enclosure, while the Swedish set had 6.0 and 2.7 kg, respectively. The Swedish set was successfully ignited and burned with a small flame the size of a match flame. The US set resisted ignition from this source and was then subjected to a 10 kW burner. With this challenge, the set burned, but showed little HRR beyond the 10 kW of the source. Finally, the test protocol chosen was a 30 kW burner. The burner HRR was subtracted out from the data shown in Fig. 26.85.

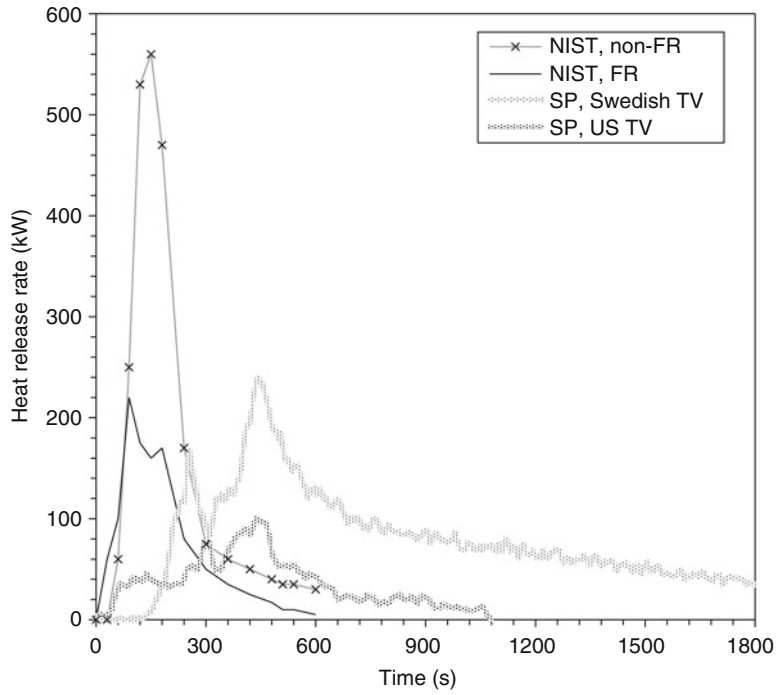

Fig. 26.85 HRR of various television sets tested by NIST and SP

Table 26.24 European televisions tested by VTT

Specimen	TW1	TW3	TP1	TP2	TP3
Type	Wood	Wood	Plastic	Plastic	Plastic
Size (inches)	24	26	28	25	28
Initial mass (kg)	32.7	39.8	31.8	24.4	30.5
Mass loss (kg)	10.2	10.2	5.2	4.6	5.3
Peak HRR (kW)	230	290	274	239	211
Total heat (MJ)	146	150	140	116	137

VTT conducted two projects where TV sets were tested. In the first study [156], they tested two old, 1960s vintage (black-and-white) televisions with large wood cabinets; these were ignited with a small cup of alcohol. In a newer study [105], they tested modern plastic-cabinet televisions using a propane burner of 1 kW. The specimens are described in Table 26.22, while test results are shown in Fig. 26.86. Nam et al. [189] tested a modern TV set (plastic cabinet) together with a wood stand for it. They obtained peak HRR values of 200–300 kW, although the peak took 20–40 min to reach.

The most recent results come from Hoffmann et al. [190] who tested TV sets in a wooden entertainment center. The ignition source was a small amount of alcohol for HB-rated cabinets. For the V-0 rated cabinets, some small consumer goods, HB rated, were first ignited and these were then used to ignite the test TV sets (Tables 26.24 and 26.25). After the initial peak (Fig. 26.87), the burning involved the wood entertainment center, thus the latter portion of these HRR curves is not germane to TV sets per se.

Transport Vehicles and Components

Passenger car HRR was measured at the Fire Research Station [191] and VTT [192]. The FRS laboratory examined a 1982 Austin Maestro and a 1986 Citroën BX, while VTT examined a Ford Taunus, a Datsun 160, and a Datsun 180. The dates of manufacture were only stated as late 1970s. These results are shown in Fig. 26.88. Additional tests were reported by MFPA [193] and SP [194]. MFPA tested a Citroën, a Trabant, and a Renault Espace, while SP tested a Fiat 127 of unspecified vintage. These results are shown in Fig. 26.89. The peak values range

Table 26.25 Characteristics of TV sets tested by Hoffmann et al.

	TV					
Test No.	Screen Size	Rating	Other HB Devices	Ignition Source	Peak HRR (kW)	Time to Peak (s)
1A	510 mm (20 in.)	V0	1 cordless Phone, 1 small radio	5 mL IPA	363	273
2A	510 mm (20 in.)	V0	1 telephone	5 mL IPA adjacent to phone	199	594
3A	480 mm (19 in.)	HB	None	5 mL IPA	>1450	615
1B	510 mm (20 in.)	V0	1 cordless phone, 1 small radio	5 mL IPA	>1000	216
2B	510 mm (20 in.)	V0	1 telephone	5 mL IPA adjacent to phone	299	975

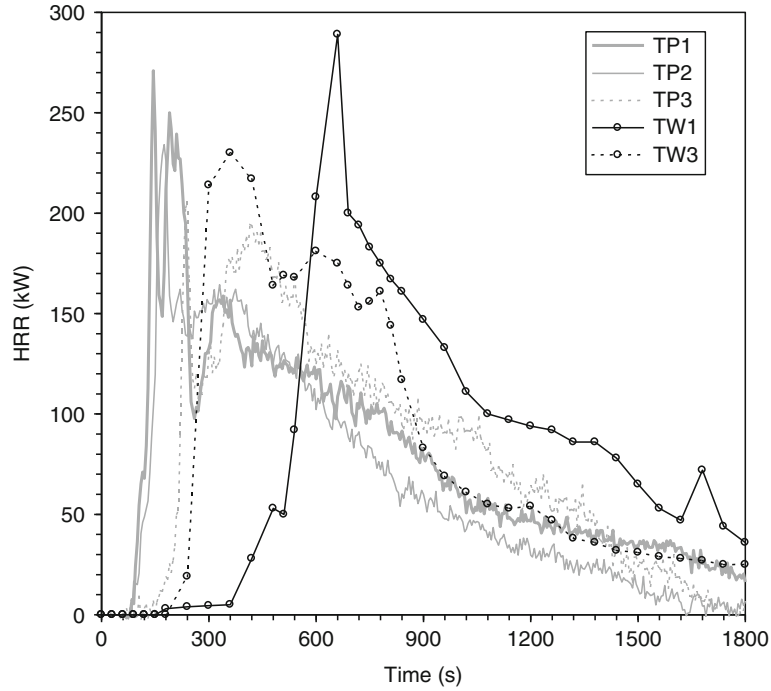

Fig. 26.86 HRR of European television sets tested by VTT

from 1.5 to 8.5 MW. These numbers are rather widely disparate and it is not fully clear why, except that this is not due to the fraction of polymer content onboard.

Some very extensive testing was conducted at CTICM, as shown in Fig. 26.90. Test 2 was a Renault 18 (951 kg), Test 3 a Renault 5 (757 kg), Test 4 another Renault 18 (955 kg), while the specimens for the remaining tests were only identified as a "Large car, 1303 kg" (Test 7), and "Small car, 830 kg" (Test 8). Additional tests were run in a two-car configuration, involving one small car (790 kg) side-by-side to a large car (1306 kg). These results are shown in Fig. 26.91, but test details were not published. The mass loss values are shown in Table 26.26.

Okamoto et al. [195] ran a series of experiments where they tested replicates of the same vehicle (Toyota Cressida, also known as Mark2 GX81) but varied the test conditions (Table 26.27). Figure 26.92 shows the HRR results; spikes judged to be spurious were

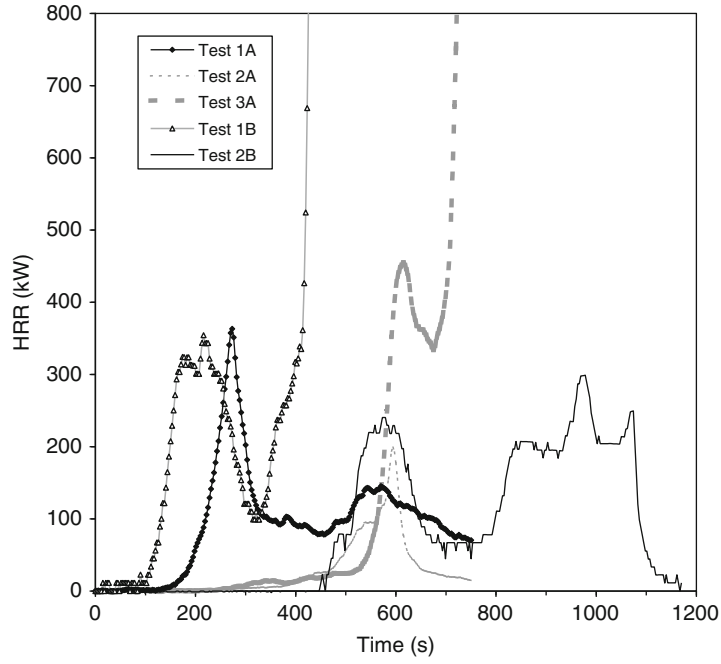

Fig. 26.87 HRR of TV sets tested by Hoffmann et al.

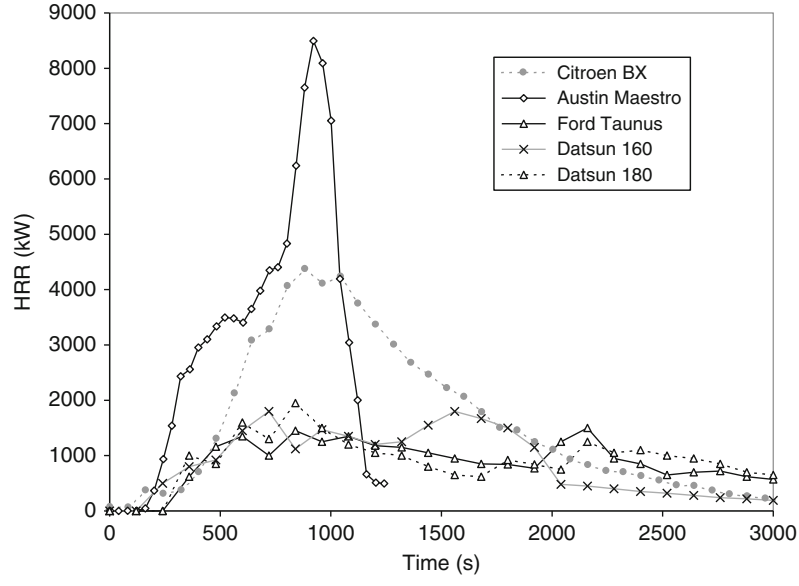

Fig. 26.88 HRR of cars tested at FRS and VTT

removed from these data. In Test B, an explosion occurred at 1517 s, when pyrolysates accumulated in the passenger compartment suddenly ignited. Explosions did not occur with the other tests. The tests are especially valuable since, in their paper, the authors documented many details of fire development in these experiments. The results suggest that small differences in test conditions can affect the time scale of fire development in an automobile quite notably, also that windows should be open if maximum HRR conditions are to be elicited. It

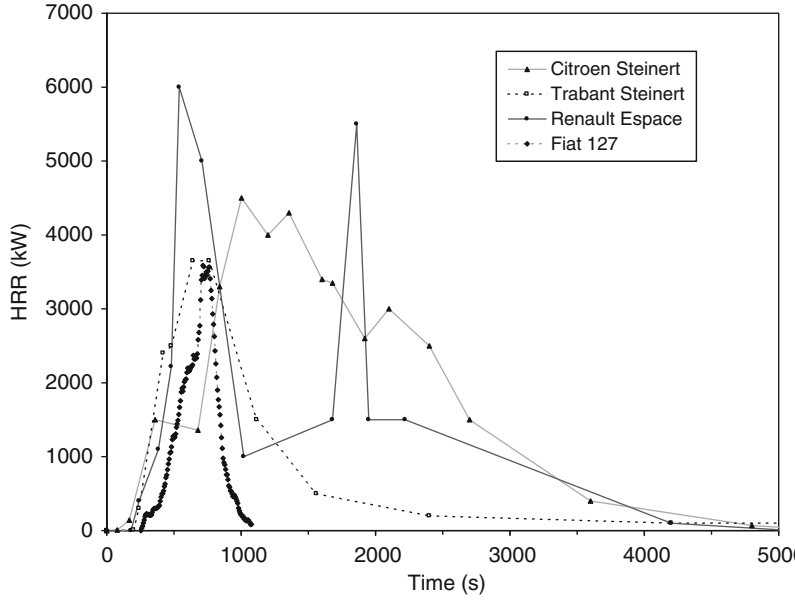

Fig. 26.89 HRR of cars tested at MFPA and SP

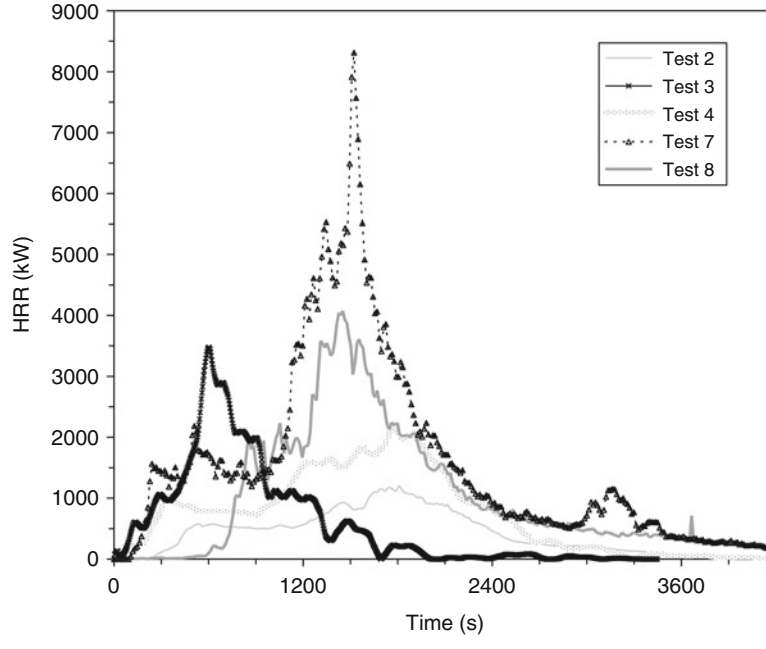

Fig. 26.90 HRR results of CTICM one-car tests

Table 26.26 Results of CTICM car tests

Test	Peak HRR (kW)	Total heat released (MJ)	Mass loss of car #1 (kg)	Mass loss of car #2 (kg)
2	1208	1758	185	–
3	3476	2100	138	–
4	2159	3080	145	–
7	8310	6670	278	–
8	4073	4090	184	–
9	7500	8890	124	172
10	8230	8380	175	166

Table 26.27 Test conditions for sedan vehicles tested by Okamoto et al.

Test	Windows	Amount of fuel in tank (L)	Ignition point	Peak HRR (kW)	Total HR (MJ)
A	Open	10	Rear wheel splashguard	3512	4950
B	Closed	10	″	3034	4860
C	Closed	20	″	1856	4930
D	Closed, exc. part of left-front window	10	Left front seat	2395	5040

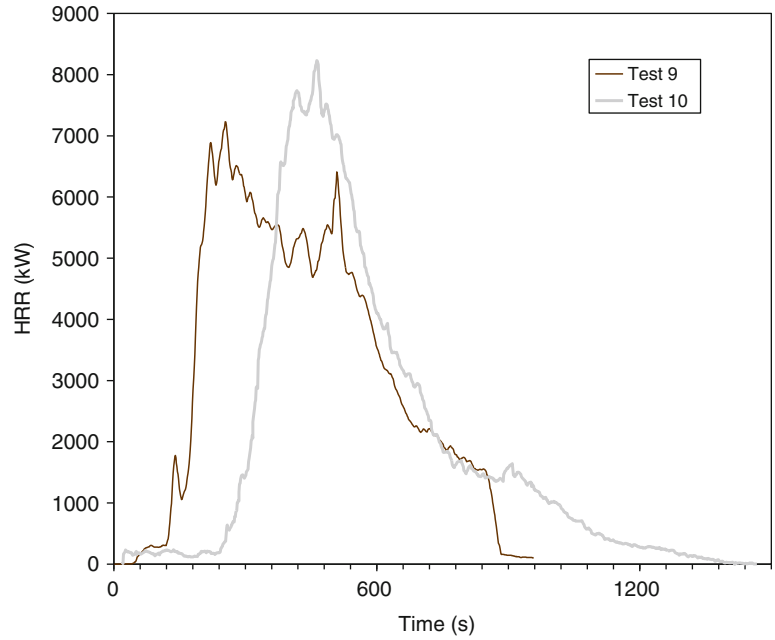

Fig. 26.91 HRR results of CTICM two-car tests

Table 26.28 Test conditions for minivan vehicles tested by Okamoto et al.

Test	Windows	Amount of fuel in tank (L)	Ignition point	Peak HRR (kW)	Total HR (MJ)
A	Closed	10	Rear wheel splashguard	3603	5367
B	Closed	10	Right front bumper	3144	5006
C	Closed	10	Center of the second row seat	–	–
D	Closed, exc. part of left-front window	10	Center of the third row seat	4094	5153

is also noteworthy that the total HR values were nearly identical for all tests.

Okamoto et al. [196] later ran tests on minivan type vehicles, using only one model of vehicle (Nissan Serena), but four different test conditions (Table 26.28). The vehicle weighed 1440 kg and had a 2.0 L gasoline-powered engine. Same as for the sedan vehicles, the HRR development was ragged and not approximately triangular or constant (Fig. 26.93). In Test C, the fire self-extinguished due to dropping oxygen levels since no windows broke.

Ohlemiller and Shields [197] tested a number of individual components from a passenger vehicle (a minivan). The components that has a mass of around 2 kg or less all showed small HRR

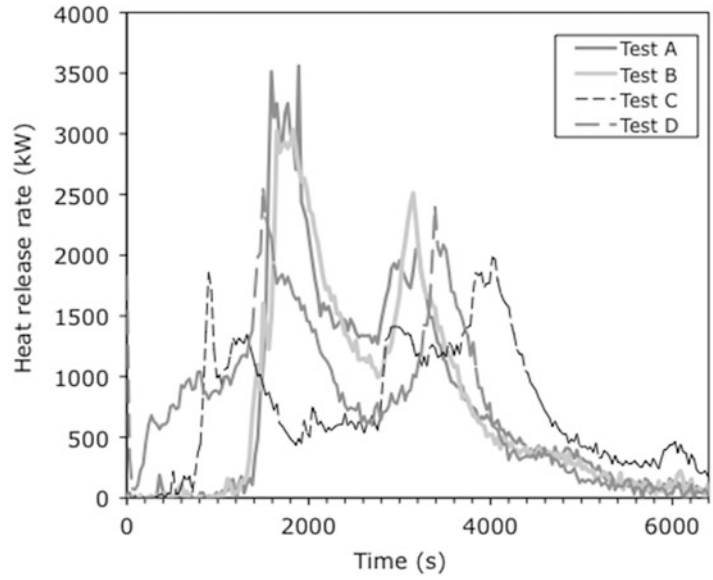

Fig. 26.92 HRR results for automobiles tested by Okamoto et al.

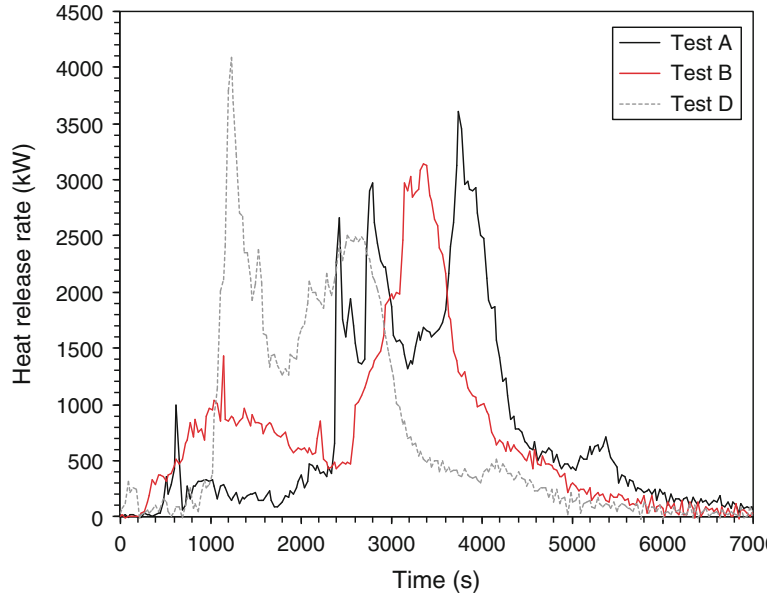

Fig. 26.93 HRR results for minivans tested by Okamoto et al.

values, typically less than 80 kW. Three components, however, showed substantial HRR values—an empty plastic fuel tank (8.5 kg), a passenger seat (8 kg), and an instrument panel (10.6 kg). The HRR curves for these items are shown in Fig. 26.94. In a separate study, Ohlemiller [198] tested one production version of an automotive HVAC unit, along with two experimental versions containing fire-retardant agents. The non-FR version showed HRR in excess of 200 kW, while the FR versions developed only about 5 kW.

Railway car results were reported by SP [197] and by Steinert [198]. Figure 26.95 shows a passenger railway car (European type IC train) reported by SP and an ICE train car by Steinert, who also published the data labeled as "two halves." The latter comprised two half cars, one being aluminum

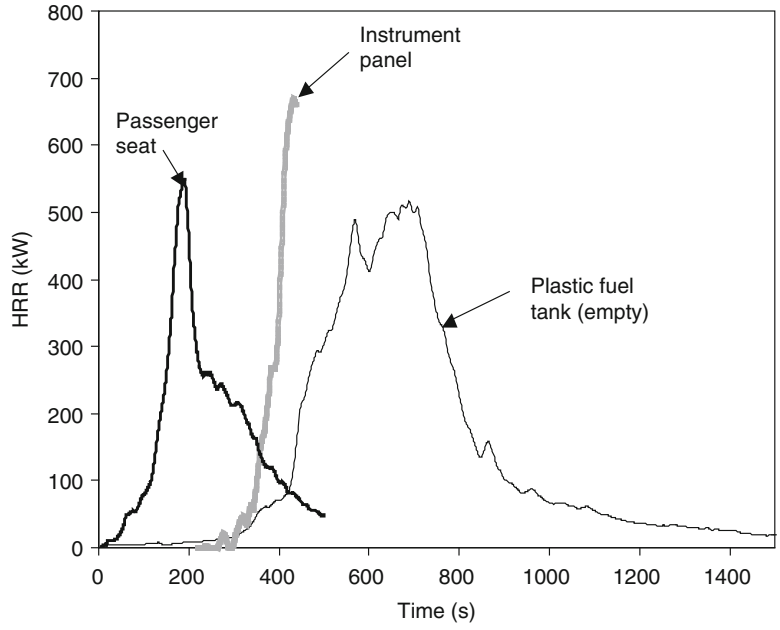

Fig. 26.94 HRR of some larger components from a passenger vehicle

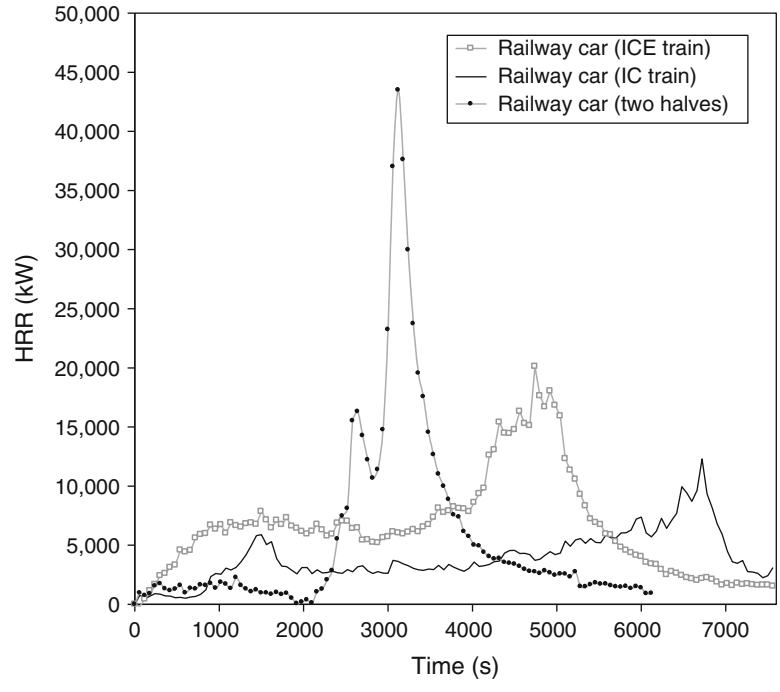

Fig. 26.95 HRR of railway cars

and the other steel. These were abutted to form one test specimen. A fire was ignited in the aluminum car, but did not become rapid until windows failed at around 40 min. SP also reported results on two subway cars [205] and half a tram car [169]; these results are shown in Fig. 26.96. Data on school buses from SP [199] and Steinert [200] are shown in Fig. 26.97.

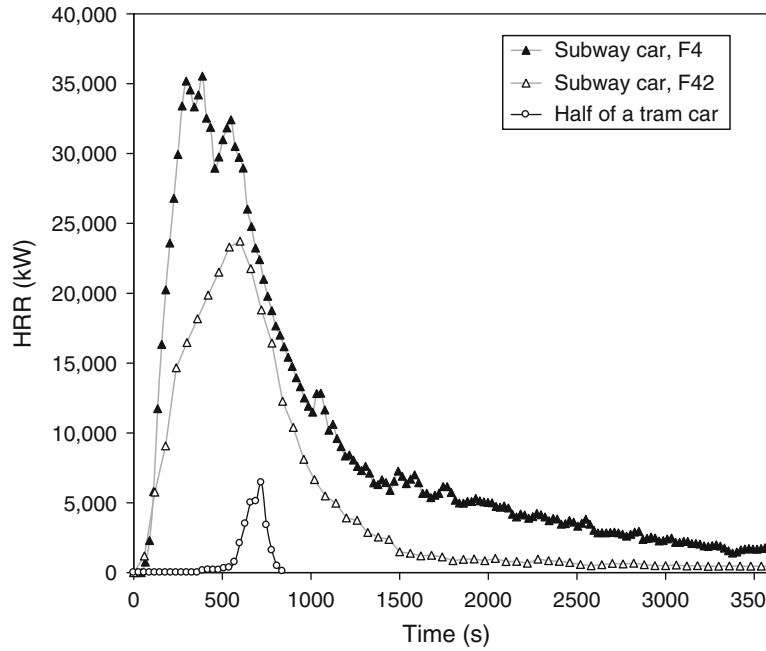

Fig. 26.96 HRR of subway cars and half a tram car

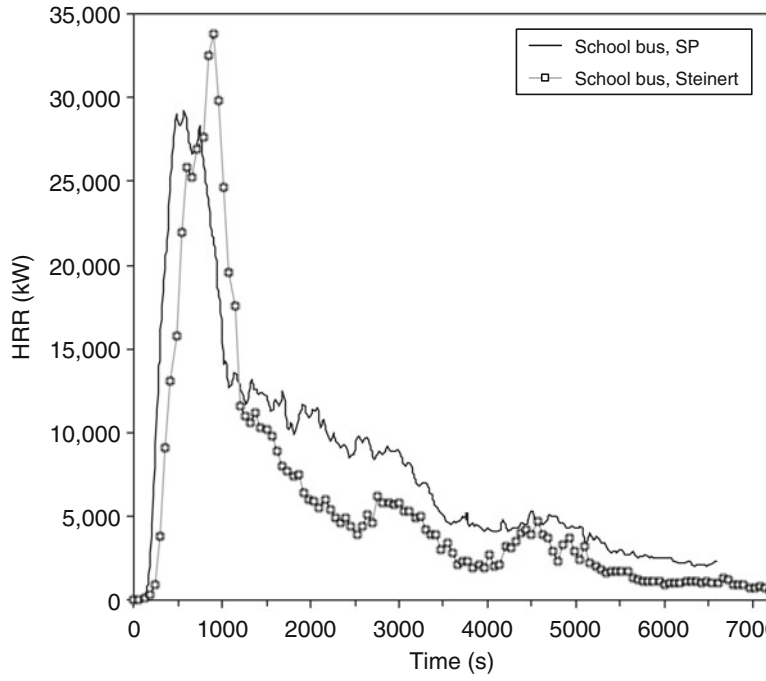

Fig. 26.97 HRR of school buses

A number of researchers have tested portions of various heavy vehicles. Tests on transport seating were done at SP [201]. They measured an array of four double bus seats and a similar arrangement of train seats. The foam was HR polyurethane, while the cover was a viscose/wool/polyester/polyamide blend for the bus seats and 100 % wool fabric for the train seats. These HRR results are shown in Fig. 26.98.

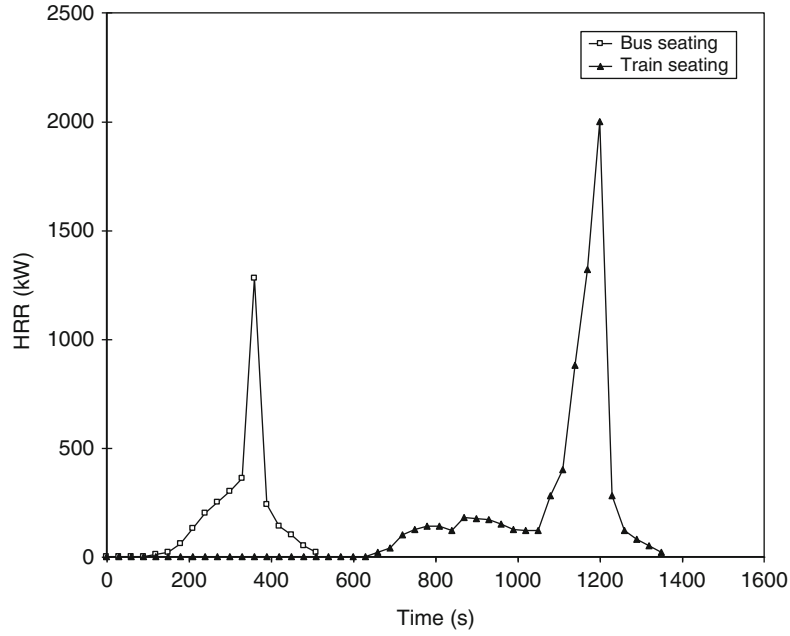

Fig. 26.98 HRR of seating components of heavy vehicles

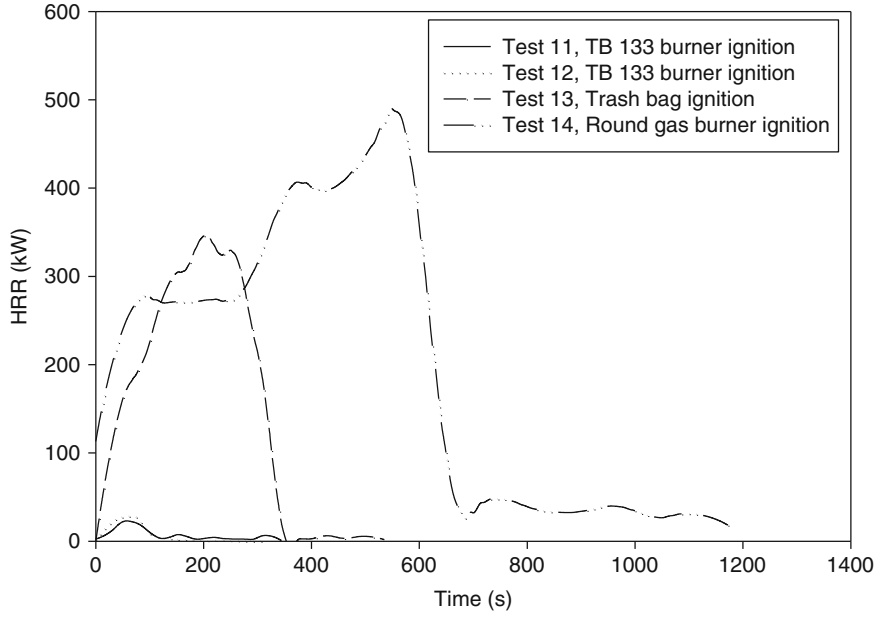

Fig. 26.99 HRR of Amtrak seats (pair), as tested by NIST, exposed to various ignition sources

NIST conducted tests [202] on a pair of Amtrak seats, presented with various ignition sources; these results are shown in Fig. 26.99. In the same research study, NIST also tested sleeping Amtrak berths; these results are shown in Fig. 26.100. Quite high HRR values were seen from Amtrak wall/soffit carpeting tested in the same study (Fig. 26.101). These test specimens were only 1.0 m wide by 1.5 m high for wall carpeting, while the test that also added soffit carpeting had an 0.5 m deep carpeted soffit. Additional test results were obtained for Amtrak

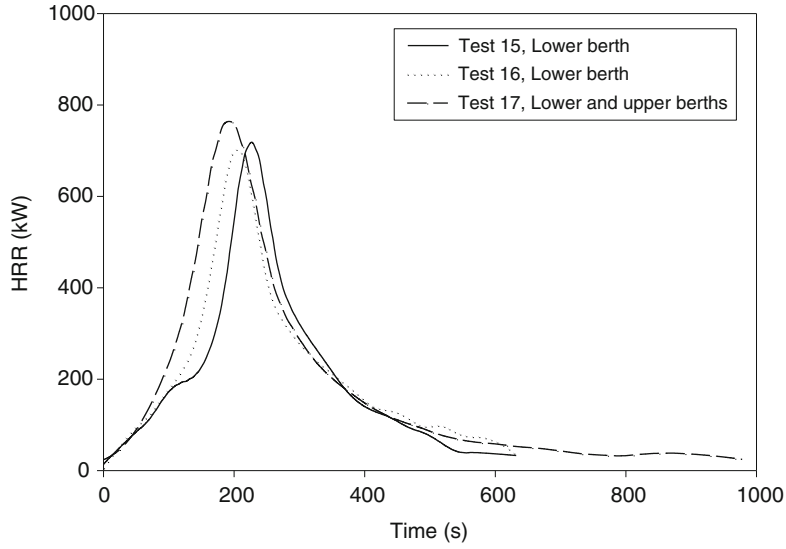

Fig. 26.100 HRR of Amtrak sleeping berths

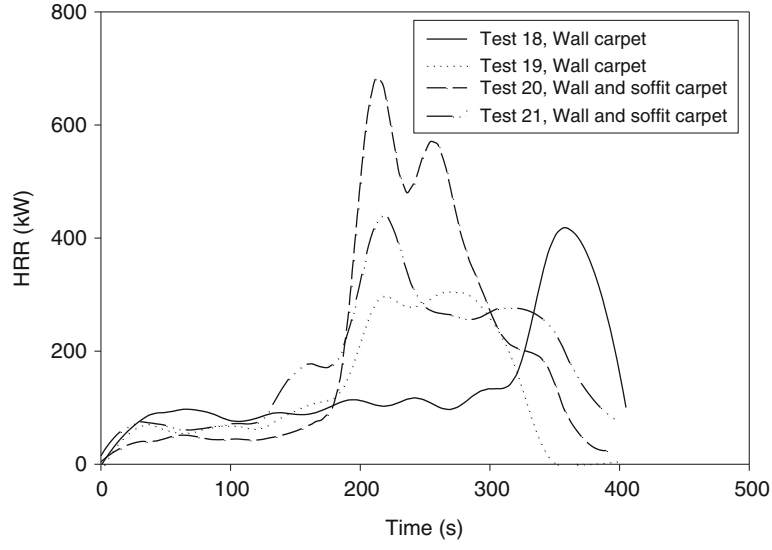

Fig. 26.101 HRR of Amtrak wall carpet and wall/soffit carpet specimens

window drapes (Fig. 26.102) and compartment door privacy curtains (Fig. 26.103). Amtrak window assemblies are made from polycarbonate glazing material and also have polymeric gasketing and trim; these show substantial HRR (Fig. 26.104).

Vehicle tires can ignite from an overheated axle and can release a substantial amount of heat if they burn. There is one study in the literature which documents such a fire. Hansen [203] burned a pair of 285/80 R22.5 truck tires mounted on a tandem wheel arrangement. The HRR curve is given in Fig. 26.105.

Vehicle tires are also prone to be ignited and to burn in tire dumps. The HRR will depend directly on the geometry and on the amount of tires involved. Some quantitative HRR experiments have been reported [204] on experiments done at the Fire Research Station. These experiments were for flaming tires, but most recent tire dump problems have been associated with a smoldering condition and no

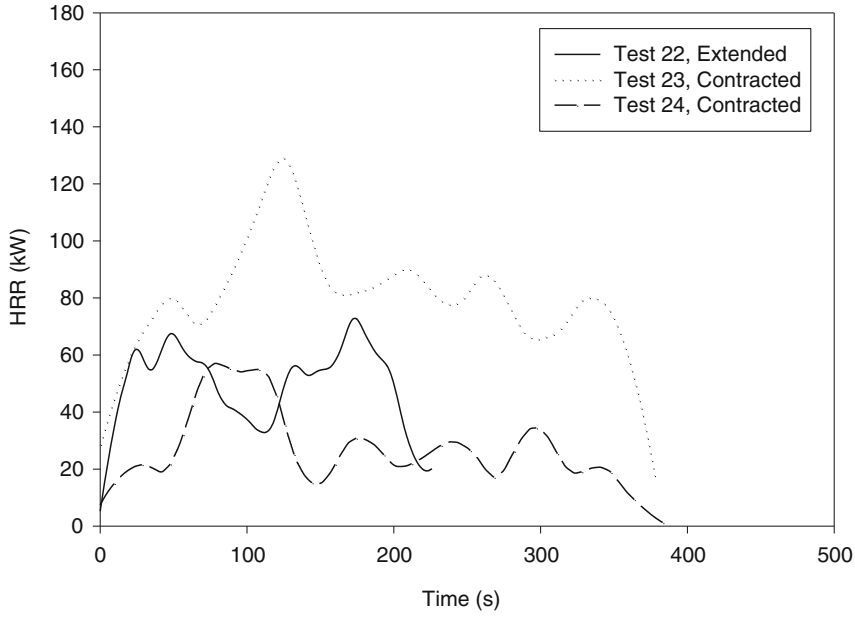

Fig. 26.102 HRR of Amtrak window drapes

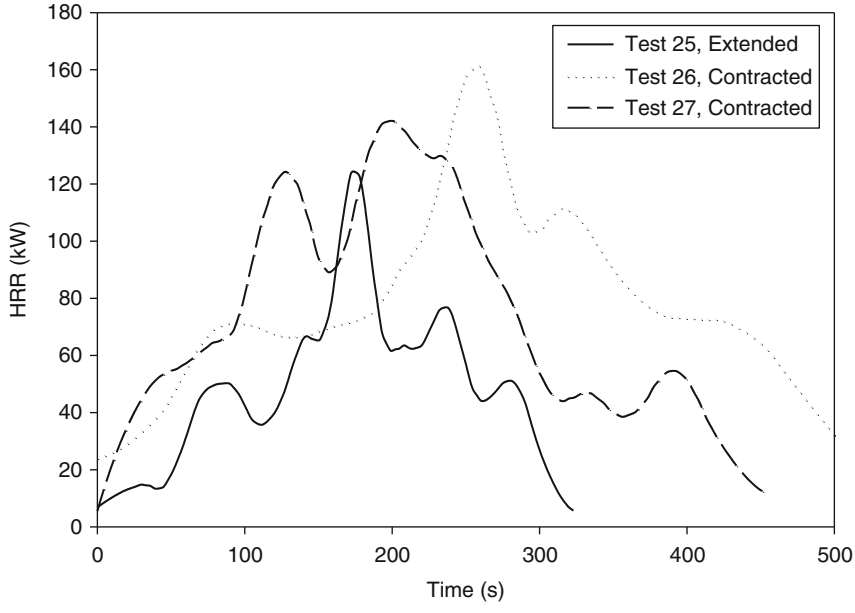

Fig. 26.103 HRR of Amtrak privacy curtains

HRR quantification under these conditions has been reported.

Tests were also reported on two plastic mud guards [205], as used on large tanker trucks. One specimen failed to get ignited from a 100 kW burner, while the HRR for the second specimen is shown in Fig. 26.105. The ignition source was a 100 kW burner, and its HRR has not been subtracted from the results shown.

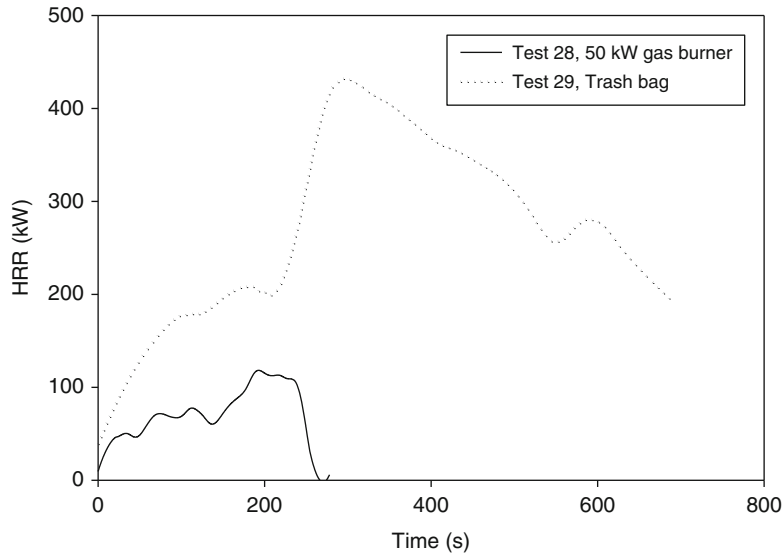

Fig. 26.104 HRR of Amtrak coach window assembly

Table 26.29 Characteristics of the SP Runehamer Tunnel tests

Test	Load	Total mass (kg)	Peak HRR (MW)	Time to peak (s)	Total heat release (MJ)	Fire growth rate during linear-growth period (MW s^{-1})
T1	380 wood pallets, 74 polyethylene pallets	11,010	201.9	1110	242,000	0.335
T2	216 wood pallets, 240 PUR foam mattresses	6,930	156.6	846	141,000	0.438
T3	Mixed goods, comprising plastic and wood furniture, fixtures, and toys; also 10 large tires	8,550	118.6	600	131,000	0.273
T4	600 cardboard cartons with 18,000 polystyrene cups, 40 wood pallets	2,850	66.4	444	57,000	0.282

For heavy-goods vehicles, the heat content of the combustibles being hauled is likely to greatly exceed the heat content of the vehicle itself. Thus, a recent research program at SP conducted by Ingason and Lönnermark [206] ("Runehamer Tunnel tests") characterized the HRR of some typical commodities of this type. Four large-scale tests were conducted (Table 26.29), with the results shown in Fig. 26.106. The commodities were arranged as volume 10.45 m long, 2.9 m wide, and 4.5 m high, but were not enclosed by a trailer body. In many cases, the trailer body is aluminum or tarpaulin, thus nearly-free burning may be expected in such worst-case situations.

For all except T4, the goods themselves were wrapped with polyethylene film. The authors especially noted that the primary period of fire growth in each case, up to ca. 100 MW (66 MW in the case of test T4), was linear and not of a t^2 type. These linear-growth rates are given in Table 26.29. These results are especially noteworthy since they represent the highest HRR fires, of realistic products thus far studied. An earlier European research program [207–209] estimated the HRR of a truck loaded with 2,000 kg of modern upholstered furniture; however, these estimated HRR values, as derived by several investigators, varied widely.

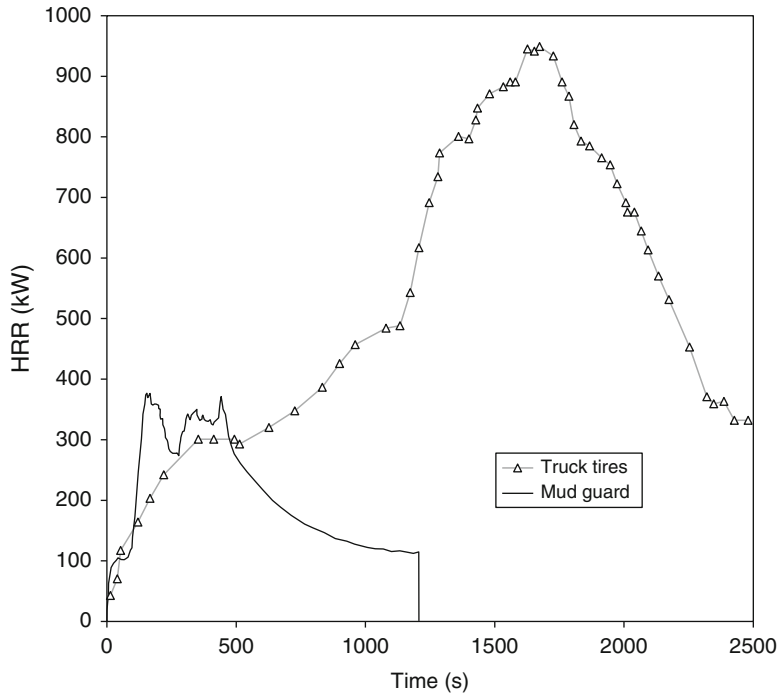

Fig. 26.105 HRR for truck tires and mud guard

Table 26.30 Some data obtained at VTT on 14 L polyethylene wastebaskets showing effect of packing density and basket construction

Basket sides	Basket mass (kg)	Filling type	Filling mass (kg)	Filling density (kg m^{-3})	Peak HRR (kW)	Total heat released (MJ)
Solid	0.63	Shredded paper	0.20	14	4	0.7
Netted	0.63	Milk cartons	0.41	29	13	3.0
Solid	0.53	Shredded paper	0.20	14	18	7.3
Netted	0.53	Milk cartons	0.41	29	15	5.8

Trash Bags and Containers

Bench-scale measurements of trash are not readily feasible, due to the naturally irregular arrangement of these combustibles. There are full-scale test results available, however, that can suggest appropriate values to be used in different circumstances. A small "bathroom size" (6.6 L) plastic wastebasket stuffed with 12 milk cartons used at NIST as an ignition source in early HRR testing [45] was found to show a HRR of about 50 kW, sustained for about 200 s.

This value evidently represents a worst-case condition, since most researchers have measured significantly lower HRR rates. For example, Mehaffey et al. [210] tested a similar wastebasket filled with mixed paper/plastic fuel load and obtain a HRR curve which can be approximated as being 30 kW for 60 s. NIST [140] tested slightly larger, 8.5 L "office style" round polypropylene wastebaskets, filled with sheets of newspaper, totaling about 300 g of newspaper in a 315 g container. These gave peak HRR values of 28–35 kW and an active burning time of ca. 800 s. Table 26.30 shows some additional data [156], where, over a certain range, increasing packing density is seen to increase the heat release rate. Some typical trash-bag fires are shown in Fig. 26.107 [109].

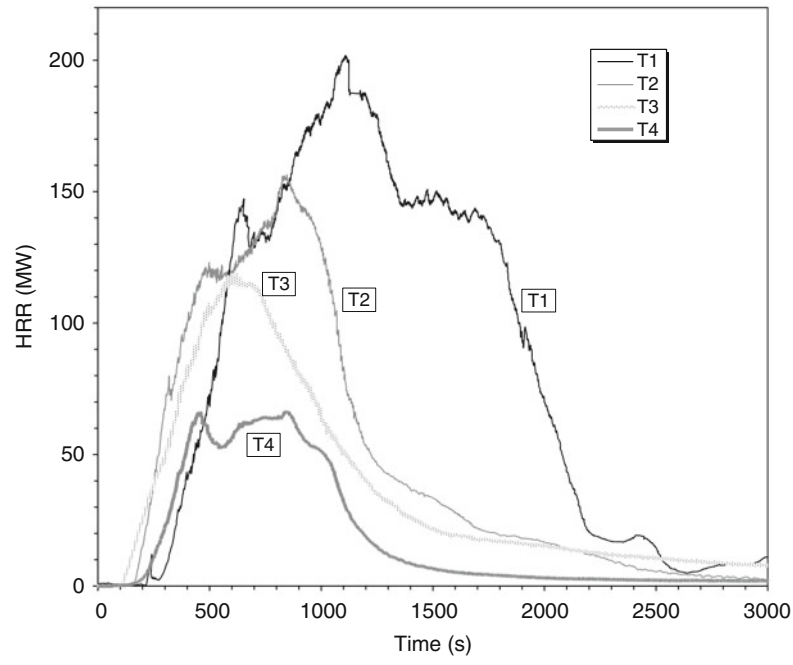

Fig. 26.106 HRR of representative heavy-goods vehicle cargo, as determined in SP's Runehamer Tunnel tests

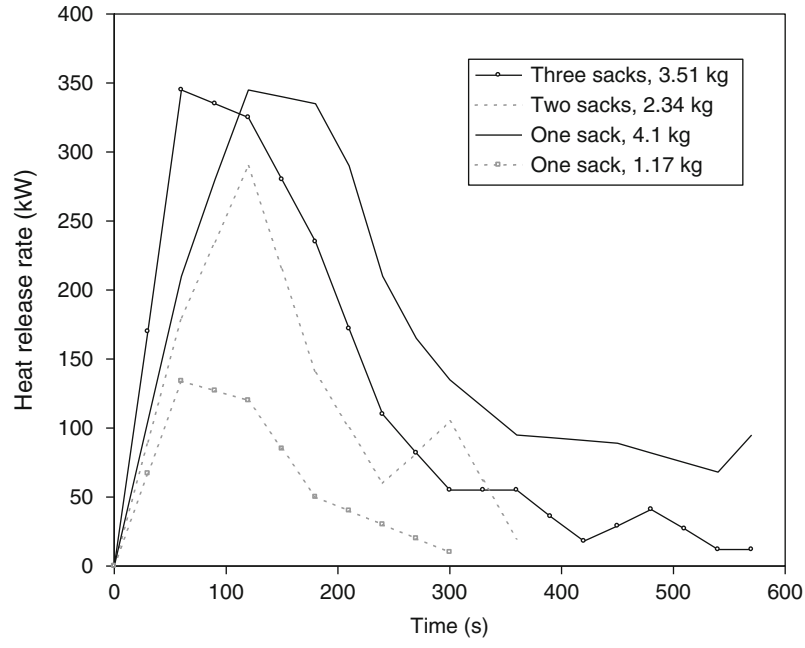

Fig. 26.107 HRR of trash bags

Lee has correlated the peak heat release values according to the effective base diameter and packing density [109]. Figure 26.108 shows that the total burning rate (kW) increases with effective base diameter, but decreases with the tighter packing densities. Figure 26.109, conversely, illustrates that when the results are normalized per unit base area, a downward trend is seen. The correlations according to packing density should only be considered rough observations, and not firm guidelines. For design purposes, the range of 50–300 kW appears to cover the bulk of the expected fires

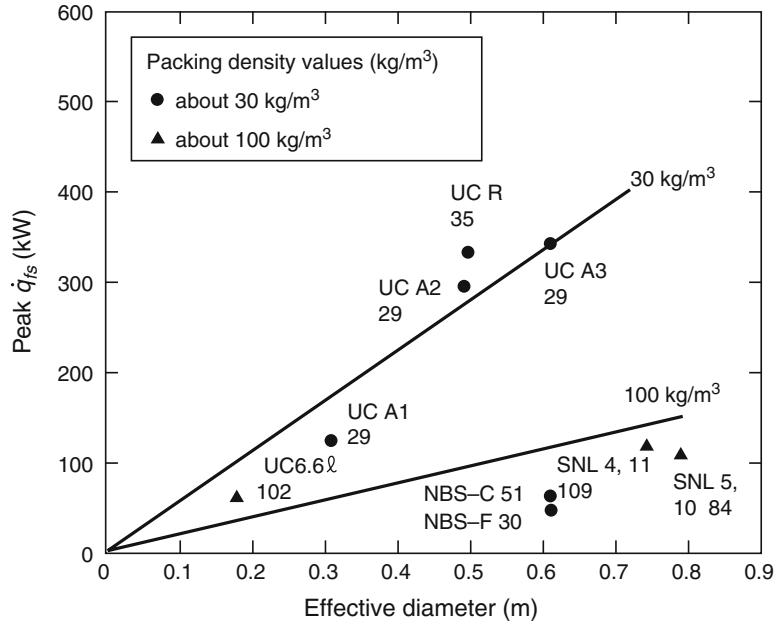

Fig. 26.108 Peak HRR of trash fires

Table 26.31 Peak HRR of small wastebaskets

	Fuel load	
Wastebasket material	PS	paper
Steel	12	8
Polyethylene	50	30
Polypropylene	50	40
Polystyrene	37	22

from normal residential, office, airplane, or similar occupancy trash bags and trash baskets.

Yamada et al. [102] measured the HRR of 6.5–11.8 L wastebaskets made of steel and plastic and filled with paper and polystyrene foam trash. The peak HRR values found are shown in Table 26.31. The authors concluded that the HRR characteristics could be reasonably well represented by one of two paradigms: (1) 30 kW for 600 s; or (2) 50 kW for 300 s.

NIST conducted tests [200] on trash bags collected from Amtrak overnight trains. The bags were about 450 mm diameter and 800 mm high and were ignited with a 25 kW burner. Test results are shown in Fig. 26.110. Based on these results, NIST researchers endeavored to create a 'standard' trash bag by filling the bag with 110 sheets (2.7 kg) of crumpled newspaper; these results are shown in Fig. 26.111.

NIST also tested [211] 30-gal size (136 L) plastic trash containers made from high-density polyethylene (HDPE) and filled with construction-site debris. The debris included cut pieces of lumber, sawdust, cardboard, paper, cups, food wrappers and pager bags. The containers were 515 mm diameter, 700 mm tall and had a mass of 3.6 kg. The debris totaled 10 kg for each test. Figure 26.112 shows the results for two test replicates.

Tests have been reported on some very large (364 L, 96 gal) polyolefin garbage cans (wheeled, household type) [212]. These were tested empty, and they were ignited with the wood crib specified in UL 1975 [213]. That particular crib weighs 340 g and is ignited with 20 g of excelsior. Three tests were conducted; two gave fairly similar peak HRR values (2383 and 1942 kW), while the third one was much lower at 977 kW (Fig. 26.113). Such variability is typical of polyolefin products, when they are tested in an arrangement where the product can melt and recede from the ignition source.

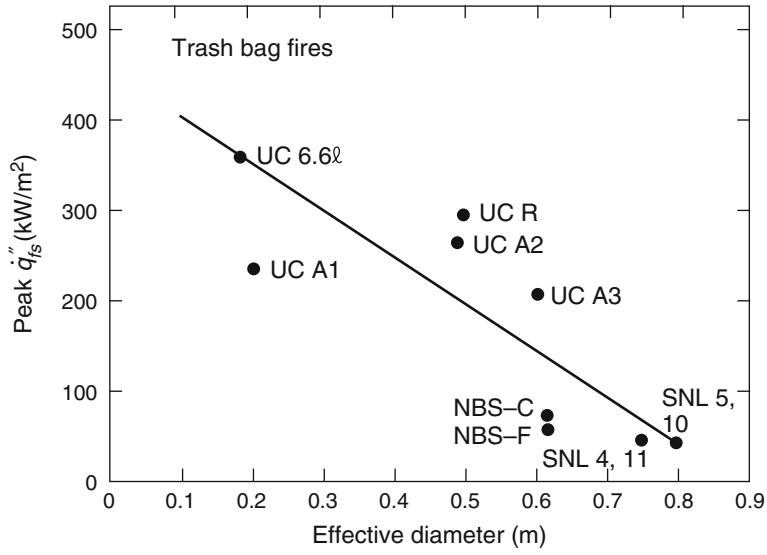

Fig. 26.109 Trash heat release rates, normalized per unit base area

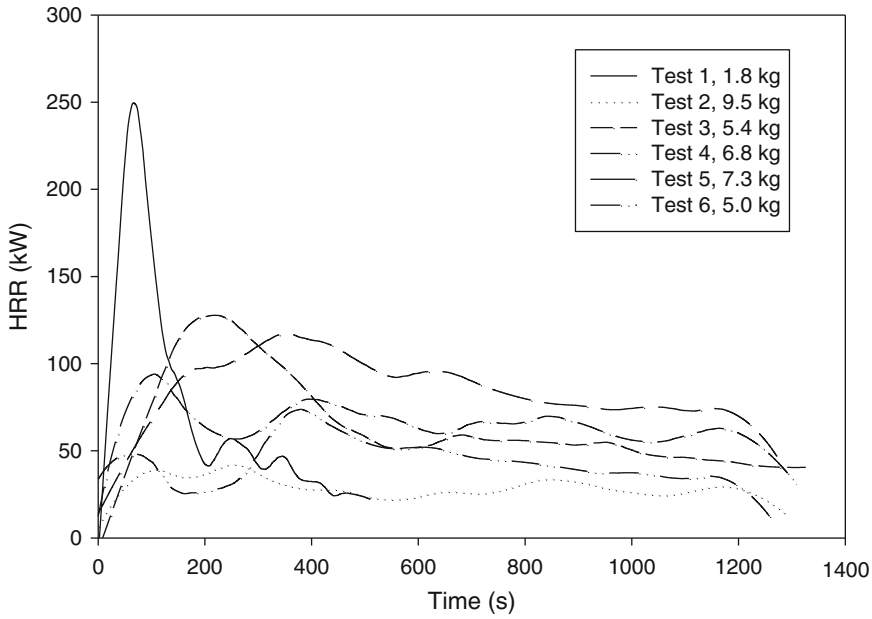

Fig. 26.110 HRR of Amtrak trash bags in NIST tests

Upholstered Furniture

The HRR of upholstered furniture can be determined in three different ways: (1) by room fire testing; (2) by testing in the furniture calorimeter; (3) by conducting bench-scale tests in the Cone Calorimeter and then using a mathematical method to predict the full-scale HRR. Of all the occupant goods that can be found in a normal residence, upholstered furniture normally has the highest HRR, thus knowledge of its performance is essential for many applications.

Until the 1970s, upholstered furniture used to be made from 'traditional' materials. Thus,

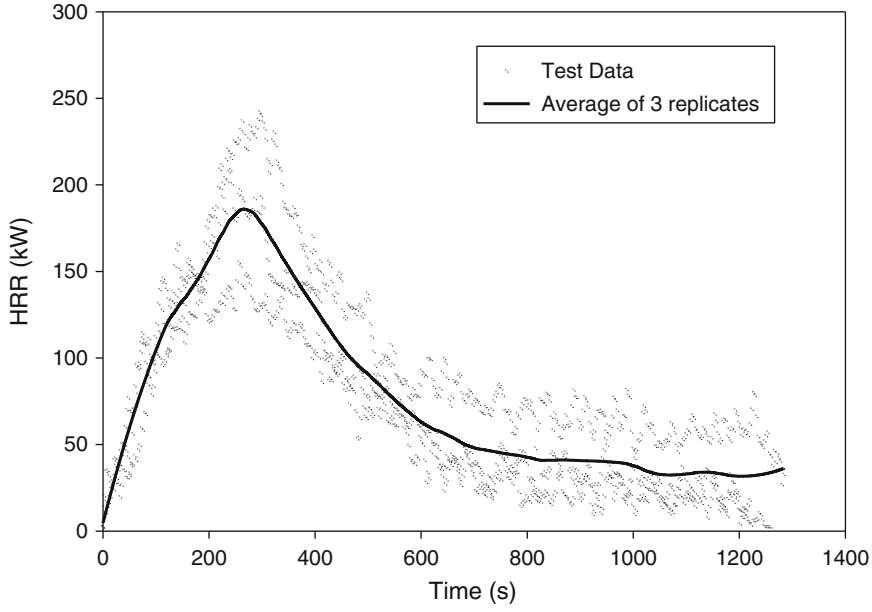

Fig. 26.111 HRR of 'standard' Amtrak trash bag, based on crumpled newspaper

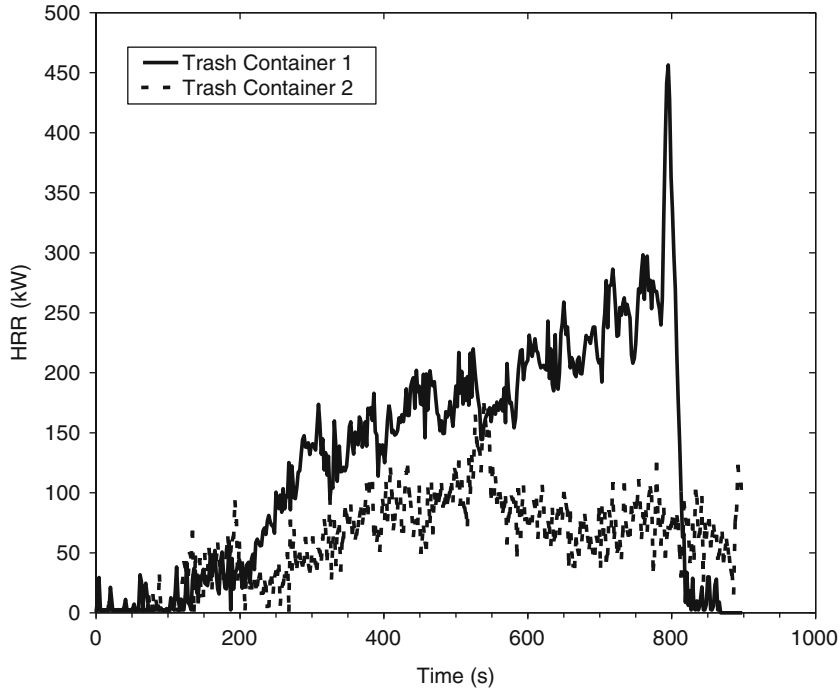

Fig. 26.112 HRR of 136-L HDPE trash containers filled with construction-site debris

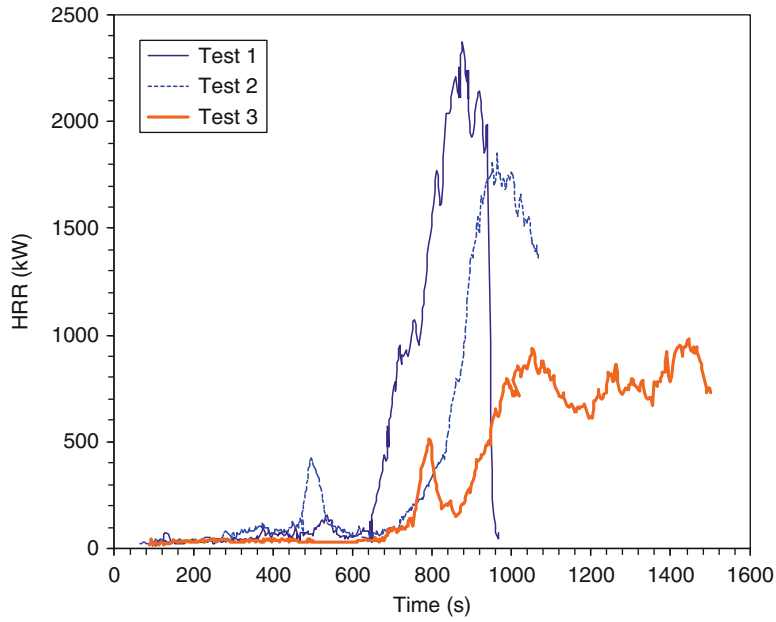

Fig. 26.113 HRR of 364 L (96 gal) PE garbage cans

during the 1950s and 60s, in the US furniture commonly had a wood frame, steel springs, cotton batting padding, and an upholstery fabric which was commonly a natural fiber such as wool, silk, or cotton. A fraction of the furniture used latex foam padding instead of cotton batting. In earlier-yet times, furniture was commonly stuffed with rubberized horse hair. By the 1970s, however, the predominant padding material became polyurethane foam, and fabric selection became very wide, including both thermoplastic synthetics and natural fibers. The HRR of the modern furniture were found to be many times that of traditional types [214], apart from the special case of latex foam. The latter shows HRR values distinctly higher than for polyurethane foam, but the material has a finite life and few specimens would survive to this day.

Figure 26.114 illustrates several furniture items tested at NIST [2]. Chair F21 used polyurethane foam complying with the 1975 California TB 117 standard [215] and polyolefin fabric. A specimen using ordinary polyurethane foam gave essentially identical results. This level of performance represents a very common, but unfortunately worst-performance furniture item widely bought by consumers. Specimen F32 is a sofa made from the same materials. Chair F24 illustrates the large improvement in HRR when cotton fabric is substituted for polyolefin fabric. The peak HRR decreases by about 2/3, from 2 MW to 700 kW. Further improvements, at present, are not readily available on the retail market. Contract furniture can be procured to advanced specifications, however, notably California TB 133 [213]. The latter limits the peak HRR to values less than 80 kW, which will present negligible fire hazard in almost any circumstance.

In the case of the tests discussed above, ignition was from the flame of a 50 kW burner placed at the side of the specimen, representing the burning of a small trash can. Such an ignition source provides the minimum time between ignition and peak HRR. The effect of ignition source on the HRR curve has been found to be almost exclusively that of time shifting—use of smaller flames, non-flaming sources, or placing of ignition sources in less vulnerable locations results in an increase of time to peak HRR (Fig. 26.115), but otherwise does not have a statistically significant effect on the HRR curve [216–218].

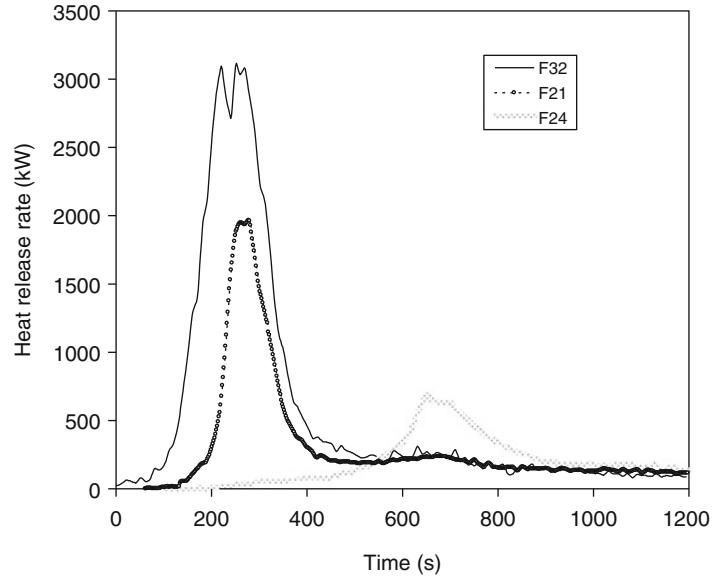

Fig. 26.114 HRR of several upholstered furniture items tested at NIST

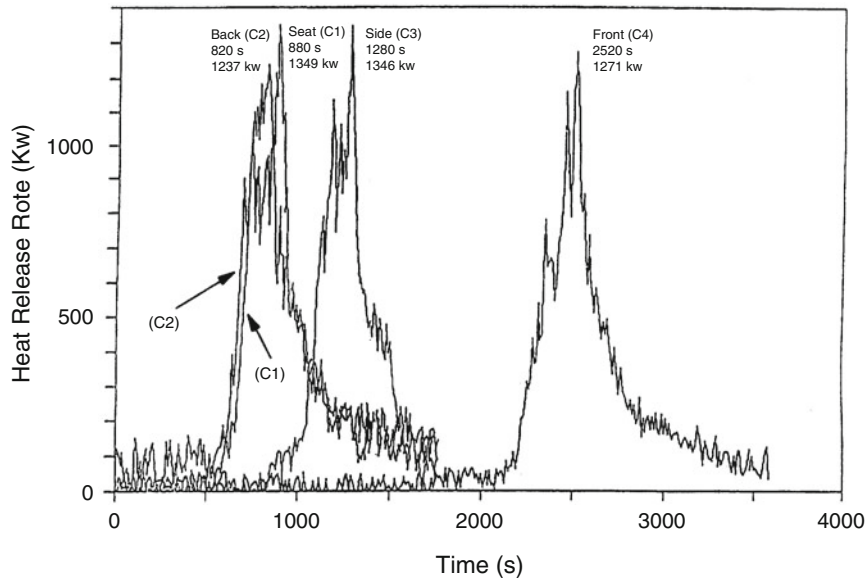

Fig. 26.115 Effect of ignition source location on the HRR curve of upholstered chairs [214]

Foams with fire retardant chemical additives (FR) improve the fire performance only if large loadings are used. Furniture made for the State of California had been required to use FR foams since 1975, but the loading of FR chemicals used was very small (3–5 %). For furniture with a HRR high enough to be a room fire hazard, such minimal FR levels have no effect on HRR [219]. A recent study with a very small ignition source compared the performance of furniture with non-FR foams and with TB117 foams using cotton upholstery [220]. Using specially constructed, non-commercial furniture for testing, no effect was found for three-seater sofas, and an effect was only seen for single-seat chairs. But the latter were of a design where even the

non-FR version showed HRR values so low (approx. 400 kW) as to not comprise a room fire hazard.

Interestingly, the same study reported test results for a large number of commercial chairs and sofas burned for comparison. With few exceptions, the latter showed peak HRR values in the range of 900–2500 kW (Fig. 26.115), indicating that the custom-made furniture was not representative of the retail residential furniture market. Furniture made to the 1975 TB117 standard was actually not intended to have lower HRR values but, rather, to resist small-flame ignitions. However, studies also showed that it was ineffective for that purpose [221]. During recent years, concerns have emerged that the 1975 TB117 standard, while ineffective from a fire safety point of view, resulted in use of noxious chemicals which have been found to have environmental toxicology problems [222]. Consequently, in 2012 the State of California replaced the 1975 TB117 regulation with TB117-2012. The latter is a cigarette-ignition (smolder resistance) test and will not require use of toxic FR chemicals to meet test requirements.

A Cone Calorimeter-based prediction method was proposed by Babrauskas and Walton, based on data obtained in 1982 [223]. This was the earliest effort, and was based on a data set comprising materials primarily from the 1970s. Since that time, the materials in use by the furniture makers changed substantially and, especially, some highly improved materials became available to the contract furniture market. In addition, predictive techniques readily available in the early 1980s were less sophisticated than those developed more recently. Thus, during the course of the European fire research program CBUF, two new predictive models were developed [10, 145]. 'Model I' is a relatively simple model and is described below briefly. A more advanced model was also developed and its details are provided in the above references.

To use the CBUF Model I, Cone Calorimeter data must first be obtained at an irradiance of 35 kW m^{-2}. A well-controlled specimen preparation method is needed, and this is provided in ASTM E 1474 [224]. Then, one determines if the furniture item is likely to sustain a propagating fire, or whether a moderate external flame source will simply result in limited burning and no propagation. This is determined from the 180 s average of Cone Calorimeter HRR results. If $\dot{q}''_{180} < 65$ kW m^{-2}, then no propagation is assumed to occur; otherwise further calculations are made to estimate the peak HRR. The scheme is as follows:

If

$$(x_1 > 115) \; or \; \left(\dot{q}''_{35-tot} > 70 \; and \; x_1 > 40\right) \; or \; (style = \{3,4\} \; \text{and} \; x_1 > 70)$$

then $\dot{q}_{fs} = x_2$

Else,

If $x_1 < 56$

then $\dot{q}_{fs} = 14.4\, x_1$

Else, $\dot{q}_{fs} = 600 + 3.77 x_1$

where $x_1 = (m_{soft})^{1.25}$ (style factor A) $\left(\dot{q}''_{35-pk} + \dot{q}''_{35-300}\right)^{0.7} (15 + t_{ig-35})^{-0.7}$

and the subscript *35* denotes that the Cone Calorimeter HRR tests run at a 35 kW m^{-2} irradiance. The m_{soft} is the mass of the 'soft' = combustible parts of the item (kg); it includes fabric, foam, interliner, dust cover, etc., but does not include the frame nor any rigid support pieces.

And, $x_2 = 880 + 500(m_{soft})^{0.7}$(style factor A) $\left(\frac{\Delta h_{c,eff}}{\dot{q}''_{35-tot}}\right)^{1.4}$

Here, $\Delta h_{c,eff}$ is the test-average effective heat of combustion in the Cone Calorimeter (MJ kg^{-1}), and $\dot{q}''_{35-tot}$ is the total heat released

Table 26.32 Style factors used in the CBUF model for predicting upholstered furniture heat release rates

Type of furniture	Style factor A	Style factor B
Armchair, fully upholstered, average amount of padding	1.0	1.0
Sofa, 2-seat	1.0	0.8
Sofa, 3-seat	0.8	0.8
Armchair, fully upholstered, highly padded	0.9	0.9
Armchair, small amount of padding	1.2	0.8
Wingback chair	1.0	2.5
Sofa-bed (convertible)	0.6	0.75
Armchair, fully upholstered, metal frame	1.0	0.8
Armless chair, seat and back cushions only	1.0	0.75
Two-seater, armless, seat and back cushions only	1.0	1.0

at a flux of 35 kW m^{-2}. Another correlation predicts the total heat release:

$$q_{tot} = 0.9\, m_{soft} \times \Delta h_{c,eff} + 2.1\left(m_{comb,\,tot} - m_{soft}\right)^{1.5}$$

where $m_{\mathrm{comb,tot}}$ denotes the total combustible mass of the item (kg), that is, everything except metal parts.

Finally, the time to peak, t_{pk} (s) for the full-scale item is estimated as:

$$t_{pk} = 30 + 4900(\text{style factor B})\left(m_{soft}\right)^{0.3}\left(\dot{q}''_{pk\#2}\right)^{-0.5}\left(\dot{q}''_{trough}\right)^{-0.5}\left(t_{pk\#\,1} + 200\right)^{0.2}$$

where the 'peak' and 'trough' notations refer to the fact that, in the general case, the Cone Calorimeter HRR of furniture composites shows two main peaks and one trough in between them. The style factors are obtained from Table 26.32.

With these values computed, a triangular HRR curve can then be constructed. The peak HRR and the time to peak are given directly, while the base width of the triangle is determined from the calculated total heat release of the furniture item.

Video Games

Edenburn [225] tested the joystick controller from video game console having a plastic enclosure made from ABS (UL 94 V-2 rated). When ignited with a needle flame, the unit showed a peak HRR of 6.7 kW and a total heat release of 2.52 MJ. HRR results for the main portion (console) were not provided.

Wall/Ceiling Lining Materials

Combustible interior finish materials are substantially more difficult to treat than free-standing combustibles. They cannot be measured in a device such as the furniture calorimeter, and require any full-scale study to be a room fire. The materials cover a large area, but the area of active flame involvement is generally not predictable, except after flashover, when in many cases it can be assumed that all surfaces are involved. In the early 1980s, a series of wall materials was studied by Lee at NIST [15] in full-scale room fires, and also in bench-scale, with the Cone Calorimeter. This work comprised the first attempted correlation between bench scale and full scale for wall lining materials. For several materials in the test series, which included both cellulosics and plastics, it was found that, after flashover, the per-unit-area full-scale heat release rates, were approximately

the same as the values obtained from the Cone Calorimeter. Lee's work did not yet lead to a predictive method, since no technique for estimating the flame-covered area, A(t) was found.

At about the same time, Babrauskas found that full-scale fire development on wall/ceiling linings could be approximated [226] by the expression $\dot{q}''_{bs-pk}/t_{ig}$, where the HRR value and the ignition time were obtained from the Cone Calorimeter. The $1/t_{ig}$ factor effectively represented the growth of A(t), but such a scheme was only semi-quantitative.

The first successful quantitative method came with the work of Wickström and Göransson in 1987 [227]. The model was based on the premise that the full-scale scenario involves the combustible materials located on the walls and ceiling of the ISO 9705 room. Note that the same material is expected to be placed on both walls and ceiling. The model uses the principle of area convolution and elaborates on Babrauskas' assumption that $1/t_{ig}$ controls the growth of the burning area. The model was later extended and extensively validated in the European research program EUREFIC, EUropean REaction to FIre Classification [228]. The primary assumptions in the model are:

1. The burning area growth rate and the HRR are decoupled.
2. The burning area growth rate is proportional to the ease of ignition, i.e. the inverse of the time to ignition in small scale.
3. The history of $\dot{q}''$ at each location in the full scale is to be the same as in the Cone Calorimeter test.

The model pays mind to the observation that burning patterns on wall/ceilings can be very different and, especially, that some products stop spreading fire under certain conditions, while others continue. The basic area growth regimes are illustrated in Fig. 26.117, where the regimes are marked in Roman numerals. The fire spread may follow three different routes. At points 'A' and 'B' fire spread may or may not continue, based on whether a calculated fictitious surface temperature is higher than a critical value. The calculation is based on data from the Cone Calorimeter. Within the different flame spread regimes, the burning area growth rate depends on ignitability, i.e. time to ignition in the Cone Calorimeter. Once the flame spread rate

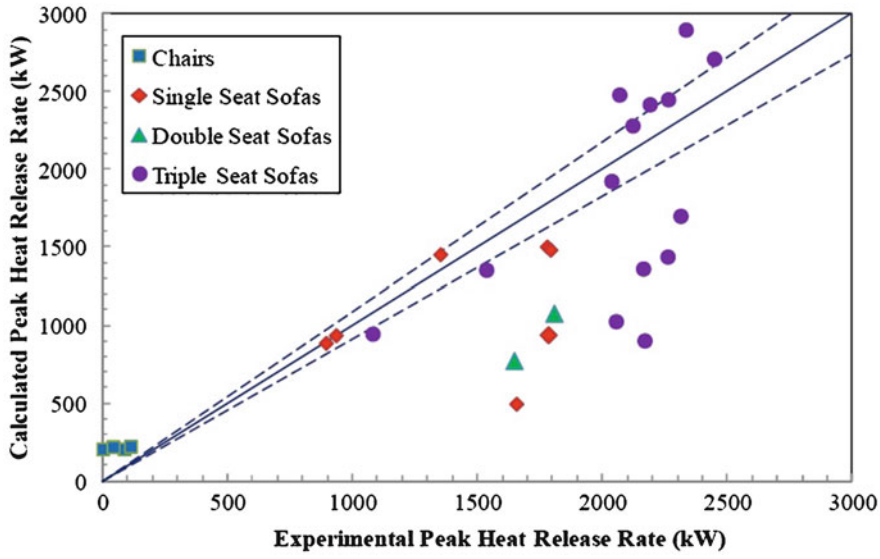

Fig. 26.116 SwRI test results on commercial residential furniture showing that peak HRR values are primarily in the range of 900–2500 kW

is determined, the HRR is calculated assuming that $\dot{q}''$ is the same in small and large scale. This is understood to be a simplification. The HRR depends on the actual heat flux level received by the product as a function of time. Experience showed, however, that the errors average out and can be included in empirical constants. The method is only of moderate difficulty to apply, but the description is somewhat lengthy. Details are available [23]. This reference also contains graphs illustrating the kind of agreement that is obtained between predictions and experiments.

While highly successful for its intended purpose, the EUREFIC model does have notable limitations. It:

- Can only treat the standard ISO 9705 room, with the standard doorway for ventilation
- Only predicts the ISO 9705 100/300 kW burner
- Requires that the material be on both walls and ceiling
- Cannot deal with products that do not ignite in the Cone Calorimeter at a 25 kW m^{-2} irradiance.

It must be remembered that the primary purpose for developing this model was to predict product performance categories to be obtained in the ISO 9705 test, while only using bench-scale Cone Calorimeter data. For its intended purpose, it has been an unquestionable success.

The above limitations indicate that the EUREFIC model, while a major breakthrough, was certainly not the final answer to modeling needs for wall/ceiling products. Two extensions have been proposed to generalize the applicability of this model. Göransson, one of the developers of the EUREFIC model, proposed an extension [229] to encompass a 'huge-scale' room. Such a test room was constructed at VTT. Its dimensions were 6.75 m by 9.0 m, with a ceiling height of 4.9 m. The door opening, 0.8 by 2.0 m high, however, was the same as for the ISO 9705 room. The burner operation was at the 100 kW level for 10 min, then at 300 kW for another 10 min, finally at 900 kW for 10 more minutes. An extended model was created for this situation by introducing a new set of regimes to correspond to the 900 kW burner level. In addition, it was found that the constant had to be modified for the 100 and 300 kW time periods. The agreement between model and prediction was very good, but only five tests were available for validation at the huge scale.

A second extension was developed by Sumathipala and coworkers [230, 231]. This model extends the applicability to the case of the room fire test studied by Lee [15]. The dimensions of that room are almost identical to the ISO room. The differences arise because (a) the two burner regimes are 40 and 160 kW, (b) the burner face size is different, and (c) the product is normally mounted on walls only, rather than walls and ceiling. The authors, however, in their development work, included tests of both rooms in both mounting configurations. The success of these extension confirms that the basic ideas behind the EUREFIC model are sound and can potentially have flexibility. On the other hand, it must be borne in mind that even the extensions are 'hard-wired' configurations and do not yet approach a technique which could be applicable towards user-selected room sizes, burner levels, and product configurations.

Perhaps the most ambitious model so far for wall/ceiling products has been one developed by Karlsson and coworkers [232–234]. Karlsson's model incorporates much more of current concepts of plumes, flame length calculations, ceiling jets, and similar constructs than does the EUREFIC model. The model has the same 'hard-wired' limitations that the EUREFIC model has in terms of ignition sources, product configuration, and room size being fixed. Another wall/ceiling model was developed by Quintiere and Cleary [235–237] and extended by Janssens and coworkers [238].

Wardrobes

Information on the HRR of wardrobes is available from a NIST study [239]. The test wardrobes are illustrated in Fig. 26.118; data

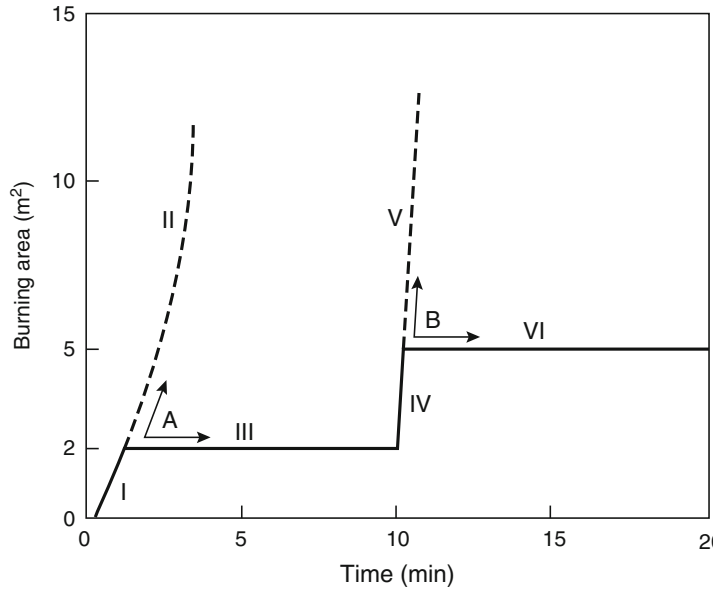

Fig. 26.117 EUREFIC fire spread regimes

Table 26.33 The HRR properties of wardrobes

Test No.	Construction	Wardrobe combustible mass (kg)	Clothing and paper (kg)	Peak HRR (kW)	Total heat released (MJ)	Avg. heat of combustion (MJ kg^{-1})
21	Steel	0	1.93	270	52	18.8
43	Plywood, 12.7 mm thick	68.3	1.93	3100	1068	14.9
41	Plywood, 3.2 mm thick, unpainted	36.0	1.93	6400	590	16.9
42	Plywood, 3.2 mm thick, 1 coat FR paint	37.3	1.93	5300	486	15.9
44	Plywood, 3.2 mm thick, 2 coats FR paint	37.3	1.93	2900	408	14.2
61	Particleboard, 19 mm thick	120.3	0.81	1900	1349	17.5

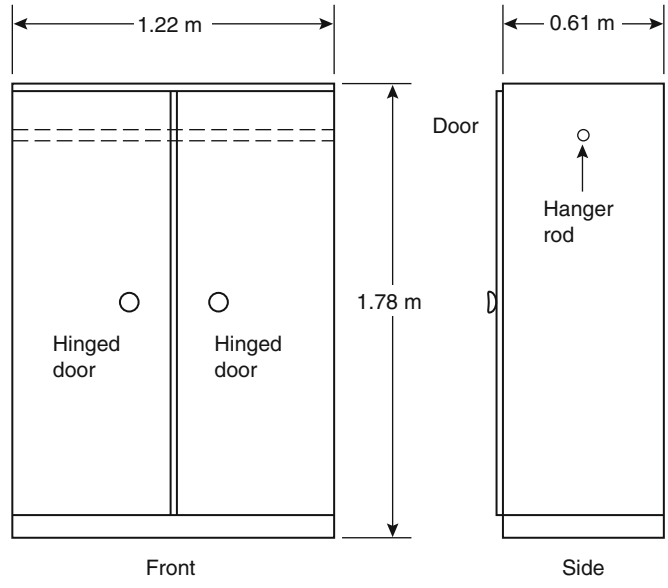

Fig. 26.118 Configuration of the tested wardrobes

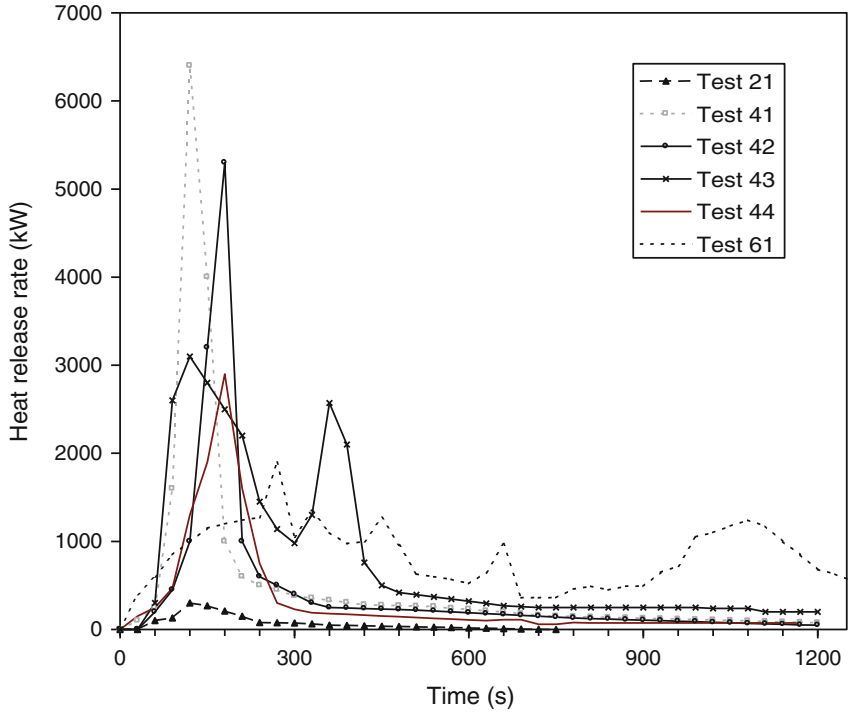

Fig. 26.119 HRR of various wardrobes

Table 26.34 European washing machines tested by VTT

Specimen	W1	W2	W3
Ignition source (kW)	1	1	300–550
Initial mass (kg)	69.3	69.9	63.3
Mass loss (kg)	10.1	10.4	12.3
Peak HRR (kW)	345	431	221
Total heat (MJ)	259	245	383

are given in Table 26.33 and Fig. 26.119. The wardrobes were outfitted with a small amount of clothing, or simulated clothing, and some paper. Tests were not run on the clothes items by themselves. However, since in the case of the steel wardrobe, the only other combustible present was the paint on the metal, it is reasonable to assign a value of about 270 kW peak for the 1.93 kg clothes load. The most important conclusion, however, was that, for combustible constructions, the peak HRR is inversely dependent on wardrobe panel thickness (and, by contrast, no simple connection to combustible specimen mass is seen). Thus, while the total heat content of the 19 mm particleboard specimen is high (see Table 26.33), its peak HRR is quite low, since flame spread and fire involvement proceed more slowly over a thick material (Fig. 26.120).

Washing Machines

VTT tested [105] European washing machines. The specimens are described in Table 26.34, while test results are shown in Fig. 26.120. The specimens were extinguished before the ultimate peak burning would have occurred. These results must not be applied to appliances used in North America, since European appliance styles are different from North American ones and also because local standards are such as to permit appliances of greater flammability in Europe (Fig. 26.120). HRR data on North American washing machines are not available.

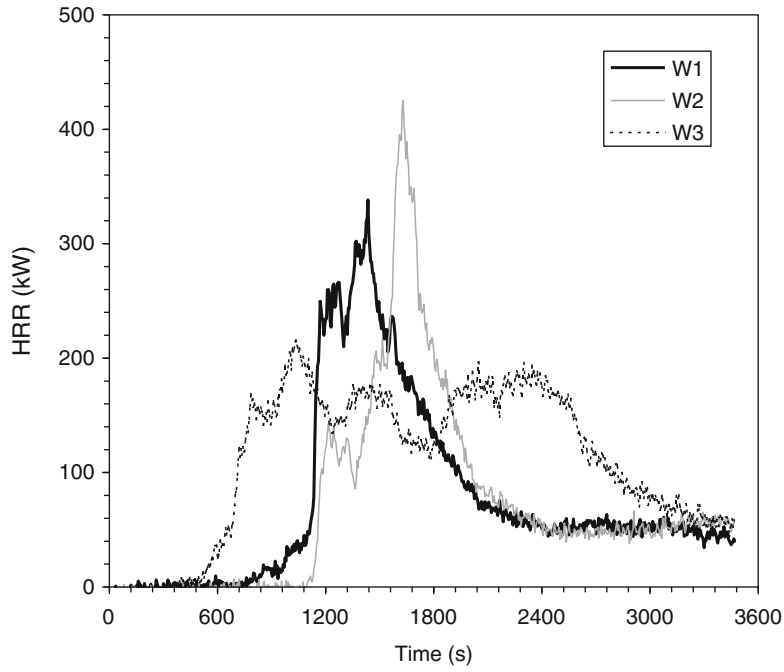

Fig. 26.120 HRR of European washing machines tested by VTT

Windows, Plastic

In applications where vandal resistance is needed, polycarbonate windows are sometimes used. This material is combustible, and limited testing was reported by Peacock et al. [240]. The tests indicated that it is hard to derive an 'innate' HRR value. The windows do not burn unless a sustained flame or heat source is applied. In that case, the HRR of the product increases with increasing severity of the ignition source. For a 50 kW exposure source, a test window showed an additional 50 kW HRR, with a burning time of ca. 80 s. For a 200 kW exposure source, the window peak HRR was about an additional 250 kW, but with a longer duration of about 200 s, at progressively diminishing HRR values.

Estimating the HRR for General Combustibles

The previous edition of the Handbook suggested a hypothetical method for estimating the HRR for general combustibles. This was based on some very simplified assumptions, especially that flame spread could, in the first approximation, be ignored. Further experience gained with additional classes of combustibles, as discussed above, suggests that such a condition will only very rarely hold. Furthermore, the user has no way of knowing when it might hold. Thus, prudent design practice should now demand that first recourse be made to the specific sections above which may address the modeler's needs. If they do not, then testing is indicated. For the modeler wishing to start up a major research activity, the schemata outlined for upholstered furniture, mattresses, and wall/ceiling lining should serve as illustrations of appropriate starting points in theory and practice. It must be pointed out, however, that such research programs have proven to be complex and that quick or inexpensive results cannot be expected.

Uncertainty of HRR Measurements

As in any engineering measurement, uncertainty in HRR measurements can be subdivided into:
1. Bias,

Table 26.35 The 95 % confidence limits for HRR test apparatuses as determined from recent round robins

				Peak HRR		Total HRR	
Apparatus	Year	Labs	Levels	r (%)	R (%)	r (%)	R (%)
Cone calorimeter	2000	4	16	17	23	8	15
ICAL	1999	3	8	56	67	72	118
SBI	1997	16	30	38	54	47	71
Room calorimeter	1994	12	5	65	79	25	41

2. Random error, sometimes termed 'precision uncertainty.'

Bias is properly minimized by use of calibration standards; for HRR testing this often comprises a metered flow of a calibration gas of high purity. Another source of bias that can be minimized, when appropriate, is specific to oxygen-consumption calorimetry bases measurements. For most testing, a standard oxygen consumption constant value of 13.1 MJ per kg of oxygen consumed is used. A small number of substances of fire-safety interest show oxygen consumption constants substantially different from this standard value. If the molecular composition of the substance is known, a correction can always be made to eliminate this source of bias.

Most of the instruments in which the HRR measurements are made have been subjected to round robins ("inter-laboratory trials") to quantify the magnitude of random error that can be expected. Comparative values have been compiled by Janssens [241], as shown in Table 26.35. For a number of them, several round robins have been conducted, thus the data shown are identified by year. SBI denotes the European Single Burning Item test [242], which is a regulatory HRR test for building products that uses two wall panels in a corner configuration, without ceiling. The values tabulated refer to the 95 % confidence intervals; standard deviations can be obtained by dividing the figures shown by 2.8.

References

1. Babrauskas, V., and Peacock, R. D., Heat Release Rate: The Single Most Important Variable in Fire Hazard, *Fire Safety J.* **18**, 255-272 (1992).
2. Babrauskas, V., Lawson, J. R., Walton, W. D., and Twilley, W. H., Upholstered Furniture Heat Release Rates Measured with a Furniture Calorimeter (NBSIR 82-2604), U. S. Natl. Bur. Stand. (1982).
3. Heskestad, G., A Fire Products Collector for Calorimetry into the MW Range (FMRC J. I. OC2El.RA), Factory Mutual Research Corp., Norwood (1981).
4. Standard Test Method for Fire Testing of Real Scale Upholstered Furniture Items (ASTM E 1537), ASTM, West Conshohocken PA.
5. Standard Test Method for Fire Testing of Real Scale Mattresses (ASTM E 1590), ASTM, West Conshohocken PA.
6. Pipe Insulation: Fire Spread and Smoke Production--Full-scale Test (NT FIRE 036), NORDTEST, Espoo (1988).
7. Upholstered Furniture: Burning Behaviour--Full Scale Test (NT FIRE 032), 2nd ed., NORDTEST, Espoo, Finland (1991).
8. Standard Fire Test of Limited-Smoke Cables (UL 1685), Underwriters Laboratories, Northbrook, IL (1991).
9. Hirschler, M. M., Use of Heat Release Calorimetry in Standards, pp. 69-80 in Fire Calorimetry (DOT/FAA/CT-95/46), Federal Aviation Administration, Atlantic City Intl. Airport, NJ (1995).
10. Sundström, B., ed., Fire Safety of Upholstered Furniture--The Final Report on the CBUF Research Programme (Report EUR 16477 EN). Directorate-General Science, Research and Development (Measurements and Testing). European Commission. Distributed by Interscience Communications Ltd, London (1995).
11. Babrauskas, V., and Wickström, U. G., Thermoplastic Pool Compartment Fires, *Combustion and Flame* **34**, 195-201 (1979).
12. Dahlberg, M., Error Analysis for Heat Release Rate Measurement With the SP Industry Calorimeter (SP Report1994:29), Swedish National Testing and Research Institute, Borås (1994).
13. Cooper, L. Y., Some Factors Affecting the Design of a Calorimeter Hood and Exhaust, *J. Fire Prot. Engineering* **6**, 99-112 (1994).
14. Fisher, F. L., and Williamson, R. B., Intralaboratory Evaluation of a Room Fire Test Method (NBS-GCR-83-421), U.S. Natl. Bur. Stand. (1983).

15. Lee, B.T., Standard Room Fire Test Development at the National Bureau of Standards, pp. 29-44 in Fire Safety: Science and Engineering (ASTM STP 882), T. Z. Harmathy, ed., American Society for Testing and Materials, Philadelphia (1985).
16. Sundström, B., Room Fire Test in Full Scale for Surface Products (Rapport SP-RAPP 1984:16). Statens Provningsanstalt, Borås, Sweden (1984).
17. Surface Products: Room Fire Tests in Full Scale (NORDTEST Method NT FIRE 025). NORDTEST, Espoo, Finland (1986).
18. International Standard--Fire Tests--Full scale room test for surface products. ISO 9705:1993(E). International Organization for Standardization, Geneva (1993).
19. Standard Test Method for Room Test of Wall and Ceiling Materials Assemblies (ASTM E 2257), ASTM Intl., West Conshohocken PA.
20. Babrauskas, V., Development of the Cone Calorimeter--A Bench Scale Heat Release Rate Apparatus Based on Oxygen Consumption, *Fire and Materials* 8, 81-95 (1984).
21. Standard Test Method for Heat and Visible Smoke Release Rates for Materials and Products using an Oxygen Consumption Calorimeter (ASTM E 1354), ASTM, West Conshohocken PA.
22. International Standard -- Fire Tests -- Reaction to Fire -- Part 1: Rate of Heat Release from Building Products (Cone Calorimeter method). ISO 5660-1:1993(E). International Organization for Standardization, Geneva (1993).
23. Babrauskas, V., and Grayson, S. J., eds., Heat Release in Fires, Elsevier Applied Science Publishers, London (1992).
24. Urbas, J., and Luebbers, G. E., The Intermediate Scale Calorimeter Development, *Fire and Materials* 19, 65-70 (1995).
25. Standard Test Method for Determining of Fire and Thermal Parameters of Materials, Products, and Systems using an Intermediate Scale Calorimeter (ICAL), (ASTM E 1623), ASTM, West Conshohocken PA.
26. Babrauskas, V., A Closed-Form Approximation for Post-Flashover Compartment Fire Temperatures, *Fire Safety J.* 4, 63-73 (1981).
27. Kokkala, M., Göransson, U., and Söderbom, J., Five Large-Scale Room Fire Experiments. Project 3. EUREFIC Fire Research Program (VTT Publications 104), VTT-Technical Research Center of Finland, Espoo (1992).
28. Schleich, J.-B., and Cajot, L.-G., Natural Fire Safety for Buildings, pp. 359-367 in *Interflam 2001—Proc. 9th Intl. Conf.*, Interscience Communications Ltd., London (2001).
29. Simonson, M., Blomqvist, P., Boldizar, A., Möller, K., Rosell, L., Tullin, C., Stripple, H., and Sundqvist, J. O., Fire-LCA Model: TV Case Study, Swedish National Testing and Research Institute, Borås (2000).
30. Tests for Flammability of Plastic Materials for Parts in Devices and Appliances (UL 94), Underwriters Laboratories, Northbrook IL.
31. Dembsey, N. A., Compartment Fire Measurements and Analysis for Near Field Entrainment, Model Validation and Wall Lining Fire Growth (Ph.D. dissertation), Univ. California, Berkeley (1995).
32. Sherratt, J., and Drysdale, D. D., The Effect of the Melt-Flow Process on the Fire Behaviour of Thermoplastics, pp. 149-159 in *Interflam 2001—Proc. 9th Intl. Conf.*, Interscience Communications Ltd., London (2001).
33. Parker, W. J., Prediction of the Heat Release Rate of Wood (Ph.D. dissertation). George Washington University, Washington, DC (1988).
34. Hirata, T., Kashiwagi, T., and Brown, J. E., Thermal and Oxidative Degradation of Poly (methylmethacrylate): Weight Loss, *Macromolecules* 18, 1410-1418 (1984).
35. Kashiwagi, T., Hirata, T., and Brown, J. E., Thermal and Oxidative Degradation of Poly (methylmethacrylate): Molecular Weight, *Macromolecules* 18, 131-138 (1985).
36. Vovelle, C., Delfau, J. L., Reuillon, M., Bransier, J., and Laraqui, N., Experimental and Numerical Study of the Thermal Degradation of PMMA, pp. 43-66 in *Papers of ITSEMAP International Meeting of Fire Research and Test Centers*, Avila, Spain (October 7-9, 1986).
37. Holland, K. A., and Rae, I. D., Thermal Degradation of Polymers. Part 3. Thermal Degradation of a Compound Which Models the Head-to-Head Linkage in Poly(Methyl Methacrylate), *Australian J. Chemistry* 40, 687-692 (1987).
38. Manring, L. E., Thermal Degradation of Saturated Poly(methylmethacrylate), *Macromolecules* 21, 528-530 (1988).
39. Inaba, A., Kashiwagi, T., and Brown, J. E., Effects of Initial Molecular Weight on Thermal Degradation of Poly(methyl methacrylate). Part 1, *Polymer Degradation and Stability* 21, 1-20 (1988).
40. Steckler, K. D., Kashiwagi, T., Baum, H. R., and Kanemaru, K., Analytical Model for Transient Gasification of Noncharring Thermoplastic Materials, pp 895-904 in *Fire Safety Science—Proc. 3rd Intl. Symp.*, International Association for Fire Safety Science. Elsevier Applied Science, New York, (1991).
41. McGrattan, K., Hostikka, S., McDermott, R., Floyd, R., Weinschenk, C., and overholt, K., Fire Dynamics Simulator Technical Reference G uide. Vol. 1: Mathematical Model (NISTSP 1018) NIST, Gaithersburg MD (2013).
42. Babrauskas, V., Specimen Heat Fluxes for Bench-scale Heat Release Rate Testing, *Fire and Materials* 19, 243-252 (1995).
43. Basic Considerations in the Combustion of Hydrocarbon Fuels in Air (NACA Report 1300), National

Advisory Committee for Aeronautics, Washington (1957).
44. Babrauskas, V., Ignition Handbook, Fire Science Publishers/Society of Fire Protection Engineers, Issaquah WA (2003).
45. Babrauskas, V., and Krasny, J. F., Fire Behavior of Upholstered Furniture (NBS Monograph 173), U.S. Natl. Bur. Stand. (1985).
46. Kokkala, M., and Heinilä, M., Flame Height, Temperature, and Heat Flux Measurements on a Flame in an Open Corner of Walls, Project 5 of the EUREFIC fire research programme, Valtion Teknillinen Tutkimuskeskus, Espoo, Finland (1991).
47. Quintiere, J. G., A Simulation Model for Fire Growth on Materials Subject to a Room-Corner Test, *Fire Safety J*. 20, 313-339 (1993).
48. Parker, A. J., Wenzel, A. B., and Al-Hassan, T., Evaluation of Passive Fire Protection by Jet Fire Test Procedure, paper 4-d in *29th Loss Prevention Symp*., American Institute of Chemical Engineers, New York (1995).
49. Söderbom, J., EUREFIC--Large Scale Tests according to ISO DIS 9705. Project 4 of the EUREFIC fire research programme (SP Report 1991:27). Statens Provningsanstalt, Borås, Sweden (1991).
50. Lee, B.T., Standard Room Fire Test Development at the National Bureau of Standards, pp. 29-44 in *Fire Safety: Science and Engineering* (ASTM STP 882), T. Z. Harmathy, ed., American Society for Testing and Materials, Philadelphia (1985).
51. Hasemi, Y., Experimental Wall Flame Heat Transfer Correlations for the Analysis of Upward Wall Flame Spread, *Fire Science and Technology* 4, 75-90 (1984).
52. Quintiere, J. G., The Application of Flame Spread Theory to Predict Material Performance, *J. of Research of the National Bureau of Standards* 93, 61-70 (1988).
53. **53.,** Kulkarni, A. K., Kim, C. I., and Kuo, C.H., Turbulent Upward Flame Spread for Burning Vertical Walls Made of Finite Thickness (NIST-GCR-91-597), Natl. Inst. Stand. and Technol., Gaithersburg, MD (1991).
54. Fang, J. B., and Breese, J. N., Fire Development in Residential Basement Room (NBSIR 80-2120), U.S. Natl. Bur. Stand., Gaithersburg, MD (1980).
55. Babrauskas, V., and Williamson, R. B., The Historical Basis of Fire Resistance Testing, Part I, *Fire Technology* 14, 184-194, 205 (1978). Part II, *Fire Technology* 14,304-316 (1978).
56. Rhodes, B. T., Burning Rate and Flame Heat Flux for PMMA in the Cone Calorimeter (M.S. thesis, University of Maryland). NIST-GCR-95-664. Natl. Inst. Stand. and Technol., Gaithersburg (1994).
57. Hopkins, D. jr., and Quintiere, J. G., Material Fire Properties and Predictions for Thermoplastics, *Fire Safety J*. 26, 241-268 (1996).
58. Gore, J., Klassen, M., Hamins, A., and Kashiwagi, T., Fuel Property Effects on Burning Rate and Radiative Transfer from Liquid Pool Flames, pp. 395-404 in *Fire Safety Science—Proc. 3rd Intl. Symp*., Elsevier Applied Science, London (1991).
59. Janssens, M., Cone Calorimeter Measurements of the Heat of Gasification of Wood, pp. 549-558 in *Interflam '93: Sixth Intl. Fire Conf. Proc*., Interscience Communications Ltd., London (1993).
60. Sorathia, U., Dapp, T., Kerr, J., and Wehrle, J., Flammability Characteristics of Composites (DTRC SME 89/90), US Navy, David Taylor Research Center, Bethesda MD (1989).
61. Rowen, J. W., and Lyons, J. W., The Importance of Externally Imposed Heat Flux on the Burning Behavior of Materials, *J. Cellular Plastics* 14, 25-32 (1978).
62. Paul, K., unpublished data, RAPRA Technology, Shawbury, England.
63. Elliot, P., Whiteley, R. H., and Staggs, J. E., Steady State Analysis of Cone Calorimeter Data, pp. 35-42 in *Proc. 4th IIntl. Fire and Materials Conf*., Interscience Communications Ltd., London (1995).
64. Tsantaridis, L., Reaction to Fire Performance of Wood and Other Building Products (Ph.D. dissertation), Kungliga Tekniska Högskolan, Stockholm (2003).
65. Cleary, T. G., and Quintiere, J. G., Flammability Characterization of Foam Plastics (NISTIR 4664), Natl. Inst. Stand. Technol., Gaithersburg, MD (1991).
66. Nussbaum, R. M., and Östman, B. A.-L., Larger Specimens for Determining Rate of Heat Release in the Cone Calorimeter, *Fire and Materials* 10, 151-160 (1986); and 11, 205 (1987).
67. Janssens, M., and Urbas, J., Comparison of Small and Intermediate Scale Heat Release Data, pp. 285-294 in *Interflam '96*, Interscience Communications Ltd, London (1996).
68. Orloff, L., Modak, A. T., and Alpert, R. L., Burning of Large-Scale Vertical Wall Surfaces, pp. 1345-54 in *16th Symp. (Intl.) on Combustion*, The Combustion Institute, Pittsburgh (1976).
69. Babrauskas, V., Cone Calorimeter Annotated Bibliography, 2003 edition, Fire Science Publishers, Issaquah WA (2004).
70. Beard, A., and Goebeldecker, S., Fire Behaviour of Household Appliances towards External Ignition, European Fire Retardants Assn., Brussels (2007).
71. Ohlemiller, T. J., Shields, J. R., McLane, R. A., and Gann, R. G., Flammability Assessment Methodology for Mattresses (NISTIR 6497), Nat. Inst. Stand. and Technol., Gaithersburg MD (2000).
72. Bwalya, A. C., Characterization of Fires in Multi-Suite Residential Dwellings: Phase 1 – Room Fire Experiments with Individual Furnishings (IRC-RR-302), National Research Council Canada, Ottawa (2010).

73. Klitgaard, P. S., and Williamson, R. B., The Impact of Contents on Building Fires, *J. Fire and Flammability/Consumer Product Flammability Supplement* 2, 84-113 (1975).
74. White, J. A. jr, Western Fire Center, Inc., Kelso WA, unpublished test results (2003).
75. Huczek, J. P., Southwest Research Institute, San Antonio TX, unpublished test results (2003).
76. Tu, K. M., and Davis, S., Flame Spread of Carpet Systems Involved in Room Fires (NBSIR 76-1013), U. S. Natl. Bur. Stand., Washington (1976).
77. Vandevelde, P., and Van Hees, P., Wind Aided Flame Spread of Floor Coverings, Development and Evaluation of Small and Large Scale Tests, pp. 57-67 in *Interflam '96*, Interscience Communications Ltd., London (1996).
78. Ames, S., Colwell, R., and Shaw, K., The Fire Behaviour and Fire Testing of Carpet Used as a Stair Covering, pp. 69-77 in *Interflam '96*, Interscience Communications Ltd., London (1996).
79. Williamson, R. B., and Dembsey, N. A., Advances in Assessment Methods for Fire Safety, *Fire Safety J.* 20, 15-38 (1993).
80. Stroup, D. W., DeLauter, L., Lee, J., and Roadarmel, G., Fire Tests of Men's Suits on Racks (FR 4013), Nat. Inst. Stand. and Technol., Gaithersburg MD (2001).
81. Satoh, H., and Mizuno, T., Fire Source Model Based on the Ignited Material and Its Burning Property in the Early Stages of Fire in Residential Accommodation, *Fire Science & Technology* 25, 163-188 (2006).
82. Simonson, M., Report for the Fire Testing of One Printer and Two CPUs, (P008664), Swedish National Testing and Research Institute, Borås (2000).
83. Bundy, M., and Ohlemiller, T., Full-Scale Flammability Measures for Electronic Equipment (Tech. Note 1461), Nat. Inst. Stand. and Technol., Gaithersburg MD (2004).
84. Edenburn, D., Burning Mouse, Albemarle Corp. [n. p.] (2003).
85. Bliss, D., and Simonson, M., Fire Performance of IT Equipment Studied in the Furniture Calorimeter, pp. 171-179 in *Interflam 2001—Proc. 9th Intl. Conf.*, Interscience Communications Ltd., London (2001).
86. Steel, J. S., unpublished data, Natl. Inst. Stand. and Technol., Gaithersburg (1985).
87. Zicherman, J. and Stevanovic, A., unpublished test results, Fire Cause Analysis, Inc., Richmond CA, (20035).
88. Babrauskas, V., Harris, R. H., Jr., Gann, R. G., Levin, B. C., Lee, B. T., Peacock, R. D., Paabo, M., Twilley, W., Yoklavich, M. F., and Clark, H. M., Fire Hazard Comparison of Fire-Retarded and Non-Fire-Retarded Products (NBS Special Publication SP 749), U. S. Natl. Bur. Stand. (1988).
89. Mangs, J., and Keski-Rahkonen, O., Full Scale Experiments on Electronic Cabinets (VTT Publications 186), Valtion Teknillinen Tutkimuskeskus, Espoo, Finland (1994).
90. Mangs, J., and Keski-Rahkonen, O., Full Scale Experiments on Electronic Cabinets II (VTT Publications 269), Valtion Teknillinen Tutkimuskeskus, Espoo, Finland (1996).
91. Keski-Rahkonen, O., and Mangs, J., Maximum and Minimum Rate of Heat Release during Flashover in Electronic Cabinets of NPPs. Paper presented at *Fire Safety in Power Plants and Industrial Installations, SMiRT 13 Post Conference Seminar No. 6*, Gramado, Brazil. Valtion Teknillinen Tutkimuskeskus, Espoo, Finland (1995).
92. Rigollet, L., and Mélis, S., Fires of Electrical Cabinets, Paper no. 023 in *11th Intl. Topical Meeting on Nuclear Reactor Thermal-Hydraulics (NURETH-11)*, Avignon, France; publ. by American Nuclear Society, LaGrange Park, IL (2005).
93. Folke, F., Experiments in Fire Extinguishment, *NFPA Quarterly* 31, 115 (1937).
94. Nilsson, L., The Effect of Porosity and Air Flow on the Rate of Combustion of Fire in an Enclosed Space (Bulletin 18), Lund Institute of Technology, Lund, Sweden (1971).
95. Yamashika, S., and Kurimoto, H, Burning Rate of Wood Crib, *Rept. of Fire Res. Inst. Japan,* No. 41, 8 (1976).
96. Harmathy, T.Z., Experimental Study on the Effect of Ventilation on the Burning of Piles of Solid Fuels, *Combustion and Flame* 31, 259 (1978).
97. Quintiere, J.G., and McCaffrey, B.J., The Burning of Wood and Plastic Cribs in an Enclosure, Vol. 1 (NBSIR 80-2054), [U.S.] Natl. Bur. Stand., Washington (1980).
98. Fons, W.L., Clements, H.B., and George, P.M., Scale Effects on Propagation Rate of Laboratory Crib Fires, in *9th Symp. (Intl.) on Combustion,* The Combustion Institute, Pittsburgh (1962).
99. Delichatsios, M.A., Fire Growth Rates in Wood Cribs, *Combustion and Flame* 27, 267 (1976).
100. Moore, L. D., Full-scale Burning Behavior of Curtains and Drapes (NBSIR 78-1448), [U.S.] Nat. Bur. Stand., Washington (1978).
101. Wetterlund, I., and Göransson, U., A Full Scale Fire Test Method for Free-Hanging Curtain and Drapery Textiles (SP Report 1988:45),Swedish National Testing Institute, Borås (1988).
102. Yamada, T., Yanai, E., and Naba, H., A Study of Full-Scale Flammability of Flame Retardant and Non-Flame Retardant Curtains, pp. 463-473 in *Proc. 4th Asia-Oceania Symp. on Fire Science & Technology*, Asia-Oceania Assn. for Fire Science & Technology/Japan Assn. for Fire Science & Engineering, Tokyo (2000).
103. Urban Wildland Interface Building Test Standards (12-7A-5), Fire Resistive Standards for Decks and

Other Horizontal Ancillary Structures, California Office of State Fire Marshal, Sacramento (2004).
104. Chow, W. K., Han, S. S., Dong, H., Gao, Y., and Zou, G. W., Full-Scale Burning Tests on Heat Release Rates of Furniture, *Intl. J. of Engineering Performance-Based Fire Codes* 6, 168-180 (2004).
105. Hietaniemi, J., Mangs, J., and Hakkarainen, T., Burning of Electrical Household Appliances—An Experimental Study (VTT Research Notes 2084), Valtion Teknillinen Tutkimuskeskus, Espoo, Finland (2001).
106. NIST, unpublished data.
107. Tewarson, A., Lee, J.L., and Pion, R.F., Categorization of Cable Flammability. Part I. Experimental Evaluation of Flammability Parameters of Cables Using Laboratory-scale Apparatus, EPRI Project RP 1165-1, Factory Mutual Research Corp., Norwood (1979).
108. Sumitra, P.S., Categorization of Cable Flammability. Intermediate-Scale Fire Tests of Cable Tray Installations, Interim Report NP-1881, Research Project 1165-1, Factory Mutual Research Corp., Norwood (1982).
109. Lee, B.T., Heat Release Rate Characteristics of Some Combustible Fuel Sources in Nuclear Power Plants, NBSIR 85-3195, [U.S.] Nat. Bur. Stand., Washington (1985).
110. Arvidson, M., Potato Crisps and Cheese Nibbles Burn Fiercely, *Brandposten* [SP] No. 32, 10-11 (2005).
111. Madrzykowski, D., unpublished test results (2012).
112. Persson, H., Evaluation of the RDD-measuring Technique. RDD-Tests of the CEA and FMRC Standard Plastic Commodities (SP Report 1991:04), SP, Borås, Sweden (1991).
113. Babrauskas, V., unpublished test results (1997).
114. Heskestad, G., Flame Heights of Fuel Arrays with Combustion in Depth, pp. 427-438 in *Fire Safety Science—Proc. 5th Intl. Symp.,* Intl. Assn. for Fire Safety Science (1997).
115. Heskestad, G., Flame Heights of Fuel Arrays with Combustion in Depth, FMRC J.I. 0Y0J3.RU (2), Factory Mutual Research Corp., Norwood MA (1995).
116. Dean, R. K., Stored Plastics Test Program (FMRC Serial No. 20269), Factory Mutual Research Corp., Norwood MA (1975).
117. Yu, H.-Z., and Kung, H.-C., Strong Buoyant Plumes of Growing Rack Storage Fires, pp. 1547-1554 in *20th Symp. (Intl.) on Combustion*, Combustion Institute, Pittsburgh PA (1984).
118. Yu, H.-Z., and Kung, H.-C., Strong Buoyant Plumes of Growing Rack Storage Fires, FMRC J.I. 0G2E7.RA(1), Factory Mutual Research Corp., Norwood MA (1984).
119. Commodities and Storage Arrangements, *Record* 66:3, 13-18 (May/June 1989).
120. Guide for Smoke and Heat Venting (NFPA 204), National Fire Protection Assn., Quincy MA (1998).
121. Kung, H.-C., Spaulding, R. D., and You, H.-Z., Response of Sprinkler Links to Rack Storage Fires. FMS J.I.0G2E7.RA(2). FMRC (1984).
122. Chicarello, P. J., and Troup, J. M. A., Fire Collector Test Procedure for Determining the Commodity Classification of Ordinary Combustible Products. FMRC J.I. 0R0E5.RR. FMRC (1990).
123. Yu, H.-Z., and Stavrianidis, P., The Transient Ceiling Flows of Growing Rack Storage Fires. FMRC J.I. 0N1J0.RA(3). FMRC (1989).
124. Yu, H.-Z., A Sprinkler-Response-Prediction Computer Program for Warehouse Applications. FMRC J.I. 0R2E1.RA. FMRC (1992).
125. Newman, J., and Troup, J. M. A., The Building Calorimeter: FM Global's Novel Approach to Large-Scale Fire Testing, NFPA World Safety Conf. and Expo., Las Vegas (2005).
126. Yu, H.-Z., RDD and Sprinklered Fire Tests for Expanded Polystyrene Egg Crates, FMRC J.I. 0R2E3.RA(1), Factory Mutual Research Corp., Norwood MA (1990).
127. Sleights, J. E., SPRINK 1.0—A Sprinkler Response Computer Program for Warehouse Storage Fires (M.S. thesis), Worcester Polytechnic Institute, Worcester MA (1993).
128. Lee, J. L., and Dean, R. K., Fire Products Collector Tests of Polyethylene Terephthalate (PET) Plastic Bottles in Corrugated Carton, FMRC J.I. 0N0J6. RA070(A), Factory Mutual Research Corp., Norwood MA (1986).
129. Lee, J. L., Combustibility Evaluation of Shredded Newsprint Commodity and an Improved Polyurethane Foam Packaging Product Using the Fire Products Collector, FMRC J.I. 0K0E6.RANS, Factory Mutual Research Corp., Norwood MA (1984).
130. Khan, M. M., Evaluation of the Fire Behavior of Packaging Materials, presented at Defense Fire Protection Symp., Annapolis (1987).
131. Hasegawa, H., Alvares, N. J., and White, J. A., Fire Tests of Packaged and Palletized Computer Products, *Fire Technology* 35, 294-307 (1999).
132. Hasegawa, H., private communication (2000).
133. Dillon, S. E., Janssens, M. L., and Garabedian, A. S., A Comparison of Building Code Classifications and Results of Intermediate-Scale Fire Testing of Stored Plastic Commodities, pp. 593-604 in *Interflam 2001—Proc. 9th Intl. Conf.*, Interscience Communications Ltd., London (2001).
134. Roberts, T. A., Merrifield, R., and Tharmalingam, S., Thermal Radiation Hazards from Organic Peroxides, *J. Loss Prevention in the Process Industries* 3, 244-252 (1990).
135. Babrauskas, V., unpublished test data (1997).
136. Yu, H.-Z., and Stavrianidis, P., The Transient Ceiling Flows of Growing Rack Storage Fires, FMRC J.I. 0N1J0.RA(3), Factory Mutual Research Corp., Norwood MA (1989).

137. Mitler, H. E., Input Data for Fire Modeling, pp. 187-199 in Thirteenth Meeting of the UJNR Panel on Fire Research and Safety, March 13-20, 1996 (NISTIR 6030, vol. 1), Nat. Inst. Stand. and Technol., Gaithersburg MD (1997).
138. Messa, S., Designing Fires for FIRESTARR, LSF Fire Laboratories, Montano Lucino, Italy (2000).
139. Chow, W. K., Zou, G., Dong, H., and Gao, Y., Necessity of Carrying out Full-Scale Burning Tests for Post-Flashover Retail Shop Fires, *Intl. J. on Engineering Performance-Based Fire Codes* 5, 20-27 (2003).
140. Madrzykowski, D., and Kerber, S, Fire Fighting Tactics under Wind Driven Conditions: Laboratory Experiments (TN 1618), Nat. Inst. Stand & Technol., Gaithersburg MD (2009).
141. Babrauskas, V., Bench-Scale Predictions of Mattress and Upholstered Chair Fires, pp. 50-62 in *Fire and Flammability of Furnishings* (ASTM STP 1233). American Society for Testing and Materials, Philadelphia (1994).
142. Damant, G. H., and Nurbakhsh, S., Heat Release Tests of Mattresses and Bedding Systems, State of California, Bureau of Home Furnishings and Thermal Insulation, North Highlands, CA (1991).
143. Holmstedt, G., and Kaiser, I., Brand I vårdbäddar (SP-RAPP 1983:04), Swedish National Testing and Research Institute, Borås, Sweden (1983).
144. Andersson, B., Fire Behaviour of Beds and Upholstered Furniture--An Experimental Study (LUTVDG/ISSN 0282-3756),Lund University, Dept. of Fire Safety Engineering, Lund, Sweden (1985).
145. Babrauskas, V., Baroudi, D., Myllymäki, J., and Kokkala, M., The Cone Calorimeter Used for Predictions of the Full-scale Burning Behaviour of Upholstered Furniture, *Fire and Materials* 21, 95-105 (1997).
146. Hansen, R., and Ingason, H., Heat Release Rate Measurements of Burning Mining Vehicles in an Underground Mine, *Fire Safety J.* 61, 12-25 (2013).
147. Walton, W. D., and Budnick, E. K., Quick Response Sprinklers in Office Configurations: Fire Test Results (NBSIR 88-3695), [U. S.] Natl. Bur. Stand., Gaithersburg, MD (1988).
148. Madrzykowski, D., and Vettori, R. L., Sprinkler Fire Suppression Algorithm for the GSA Engineering Fire Assessment System (NISTIR 4833), Natl. Inst. Stand. Technol., Gaithersburg, MD (1992).
149. Madrzykowski, D., Office Work Station Heat Release Rate Study: Full Scale vs. Bench Scale, pp. 47-55 in *Interflam '96*, Interscience Communications Ltd., London (1996).
150. Madrzykowski, D., and Walton, W. D. Cook County Administration Building Fire, 69 West Washington, Chicago, Illinois, October 17, 2003: Heat Release Rate Experiments and FDS Simulations (NIST SP 1021), Nat. Inst. Stand. & Technol., Gaithersburg MD (2004).
151. Kakegawa, S., et al., Design Fires for Means of Egress in Office Buildings Based on Full-scale Fire Experiments, pp. 975-986 in *Fire Safety Science—Proc. 7th Intl. Symp.*, International Association for Fire Safety Science (2003).
152. Krasner, L. M., Burning Characteristics of Wooden Pallets as a Test Fuel (Serial 16437), Factory Mutual Research Corp., Norwood (1968).
153. Babrauskas, V., Pillow Burning Rates, *Fire Safety J.* 8, 199-200 (1984/85).
154. Pipe Insulation: Fire Spread and Smoke Production--Full-scale Test (NT FIRE 036), NORDTEST, Espoo, Finland (1988).
155. Wetterlund, I., and Göransson, U., A New Test Method for Fire Testing of Pipe Insulation in Full Scale (SP Report 1986:33), Swedish National Testing Institute, Borås (1986).
156. Babrauskas, V., Toxic Fire Hazard Comparison of Pipe Insulations: The Realism of Full-scale Testing Contrasted with Assessments from Bench-scale Toxic Potency Data Alone, pp. 439-452 in *Asiaflam '95*, Interscience Communications Ltd, London (1995).
157. Ahonen, A., Kokkala, M. and Weckman, H., Burning Characteristics of Potential Ignition Sources of Room Fires (Research Report 285), Valtion Teknillinen Tutkimuskeskus, Espoo, Finland (June 1984).
158. Damant, G., and Nurbakhsh, S., Christmas Trees--What Happens When They Ignite? *Fire and Materials* 18, 9-16 (1994).
159. Babrauskas, V., Chastagner, G., and Stauss, E., Flammability of Cut Christmas Trees, IAAI Annual General Meeting and Conference, Atlantic City NJ (2001).
160. Evans, D. D., Rehm, R. G., Baker, E. S., McPherson, E. G., and Wallace, J. B., Physics-Based Modeling of Community Fires, pp. 1065-1076 in *Interflam 2004*, Interscience Communications Ltd., London (2004).
161. Stroup, D. W., DeLauter, L., Lee, J., and Roadarmel, G., Scotch Pine Christmas Tree Fire Tests (FR 4010), Nat. Inst. Stand. and Technol., Gaithersburg MD (1999).
162. Madrzykowski, D., Impact of a Residential Sprinkler on the Heat Release Rate of a Christmas Tree Fire (NISTIR 7506), Nat. Inst. Stand & Technol., Gaithersburg MD (2008).
163. Jackman, L., Finegan, M., and Campbell, S., Christmas Trees: Fire Research and Recommendations (LPR 17:2000), Loss Prevention Council, London (2000).
164. Stephens, S. L., Gordon, D. A., and Martin, R. E., Combustibility of Selected Domestic Vegetation Subjected to Desiccation, pp. 565-571 in *Proc. 12th Intl. Conf. on Fire and Forest Meteorology*, Society of American Foresters, Bethesda MD (1994).

165. Etlinger, M. G., Fire Performance of Landscape Plants (M.S. thesis), Univ. California, Berkeley (2000).
166. Outline of Investigation for Artificial Christmas Trees (Subject 411), 2nd ed., Underwriters Laboratories Inc., Northbrook IL (1991).
167. Babrauskas, V., to be published.
168. McCaffrey, B., Flame Height, pp. 2-1 to 2-8 in SFPE Handbook of Fire Protection Engineering, 2nd ed., National Fire Protection Assn., Quincy MA (1995).
169. McCaffrey, B. J. Momentum Implications for Buoyant Diffusion Flames, *Combustion and Flame 52*, 149-167 (1983).
170. Särdqvist, S., Initial Fires: RHR, Smoke Production and CO Generation from Single Items and Room Fire Tests (LUTVDG/TVBB-3070-SE), Lund University, Dept. of Fire Safety Engineering, Lund, Sweden (1993).
171. Blinov, V. I., and Khudiakov, G. N., Diffusion Burning of Liquids. U.S. Army Translation. NTIS No. AD296762 (1961).
172. Hottel, H.C., Review Certain Laws Governing Diffusive Burning of Liquids, by V. I. Blinov and G. N. Khudiakov, *Fire Research Abstracts and Reviews* 1, 41-44 (1958).
173. Babrauskas, V., Tables and Charts, pp. A-1 to A-17 in Fire Protection Handbook, 18th ed., National Fire Protection Assn., Quincy, MA (1997).
174. Babrauskas, V., Estimating Large Pool Fire Burning Rates, *Fire Technology* 19, 251-261 (1983).
175. Gosse, A., BG Technologies Ltd., private communication (2000).
176. Putorti, A. D. jr., Flammable and Combustible Liquid Spill/Burn Patterns (NIJ 604-00), National Institute of Justice, U.S. Department of Justice, Washington (2001).
177. Modak, A. T., Ignitability of High-Fire-Point Liquid Spills (EPRI NP-1731), Electric Power Research Inst., Palo Alto, CA (1981).
178. Gottuk, D. T., Scheffey, J. L., Williams, F. W., Gott, J. E., and Tabet, R. J., Optical Fire Detection (OFD) for Military Aircraft Hangars: Final Report on OFD Performance to Fuel Spill Fires and Optical Stresses (NRL/MR/6180--00-8457), Naval Research Lab., Washington (2000).
179. DeHaan, J. D., The Dynamics of Flash Fires Involving Flammable Hydrocarbon Liquids, *Amer. J. Forensic Medicine and Pathology* 17, 24-31 (1996).
180. Babrauskas, V., COMPF2—A Program for Calculating Post-Flashover Fire Temperatures (Tech Note 991), [U. S.] Natl. Bur. Stand., Gaithersburg MD (1979).
181. Gore, J. P., Klassen, M., Hamins, A., and Kashiwagi, T., Fuel Property Effects on Burning Rate and Radiative Transfer From Liquid Pool Flames, pp. 395-404 in *Fire Safety Science—Proc. 3rd Intl. Symp.*, International Association for Fire Safety Science, Elsevier Applied Science, New York (1991).
182. Hamins, A., Fischer, S. J., Kashiwagi, T., Klassen, M. E., and Gore, J. P., Heat Feedback to the Fuel Surface in Pool Fires, *Combustion Science and Technology* 97, 37-62 (1994).
183. Adiga, K. C., Ramaker, D. E., Tatem, P. A., and Williams, F. W., Modeling Pool-Like Gas Flames of Propane, *Fire Safety J.* 14, 241-250 (1989).
184. Adiga, K. C., Ramaker, D. E., Tatem, P. A., and Williams, F., Modeling Thermal Radiation in Open Liquid Pool Fires, pp. 241-250 in *Fire Safety Science—Proc. 2nd Intl. Symp.*, International Association for Fire Safety Science, Hemisphere Publishing Corp., New York (1989).
185. Koseki, H., and Mulholland, G. W., Effect of Diameter on the Burning of Crude Oil Pool Fires, *Fire Technology* 27, 54-65 (1991).
186. Koseki, H., Boilover and Crude Oil Fire, *J. Applied Fire Science* 3, 243-272 (1993/1994).
187. Chow, W. K., Necessity of Testing Combustibles under Well-developed Fires, *J. Fire Sciences* (2005).
188. Troitzsch, J. H., Flammability and Fire Behaviour of TV Sets, pp. 979-990 in *Fire Safety Science—Proc. 6th Intl. Symp.*, Intl. Assn. of Fire Safety Science (2000).
189. Nam, D.-G., Hasemi, Y., and Kamikawa, D., Investigation of an Apartment Fire—Experiments for Estimating the Cause and Mechanism of the Fire, pp. 389-400 in *Fire & Materials 2005*, Interscience Communications Ltd., London (2005).
190. Hoffmann, J. M., Hoffmann, D. J., Kroll, E. C., and Kroll, M. J., Full Scale Burn Tests of Television Sets and Electronic Appliances, *Fire Technology* 39, 207-224 (2003).
191. Shipp, M., and Spearpoint, M., Measurements of the Severity of Fires Involving Private Motor Vehicles, *Fire and Materials* 19, 143-151 (1995).
192. Mangs, J., and Keski-Rahkonen, O., Characterization of the Fire Behaviour of a Burning Passenger Car. Part I: Car Fire Experiments, *Fire Safety J.* 23, 17-35 (1994).
193. Steinert, C., Experimentelle Untersuchhungen zum Abbrand-und Feuerubersprungsverhalten von Personenkraftwagen, *VFDB-Zeitschrift*, No. 4, 63-172 (2000).
194. Ingason, H., Gustavsson, S., and Werling, P., Brandförsök i en bergtunnel—Naturlig ventilation. Delrapport II (SP AR 1995:45), Swedish National Testing and Research Institute, Borås (1995).
195. Okamoto, K., Watanabe, N., Hagimoto, Y., Chigira, T., Masano, R., Miura, H., Ochiai, H., Tamura, Y., Hayano, K., Maeda, Y., and Suzuki, J., Burning Behavior of Sedan Passenger Cars, *Fire Safety J.* 44, 301-310 (2009).
196. Okamoto, K., Otake, T., Miyamoto, H., Honma, M., and Watanabe, N., Burning Behavior of Minivan Passenger Cars, *Fire Safety J.* 62, 272-280 (2013).
197. Ohlemiller, T. J., and Shields, J. R., Burning Behavior of Selected Automotive Parts from a Minivan

(NISTIR 6143), Nat. Inst. Stand. & Technol., Gaithersburg MD (1998).
198. Ohlemiller, T. J., Influence of Flame-Retarded Resins on the Burning Behavior of a Heating, Ventilating and Air Conditioning Unit from a Sports Coupe (NISTIR 6748), Nat. Inst. Stand. & Technol., Gaithersburg MD (2003).
199. Ingason, H., Gustavsson, S., and Dalhberg, M., Heat Release Rate Measurements in Tunnel Fires (SP Report 1994:08), Swedish National Testing & Research Institute, Borås (1994).
200. Steinert, C., Smoke and Heat Production in Tunnel Fires, pp. 123-137 in *Proc. Intl. Conf. on Fires in Tunnels* (SP Report 1994:54), Swedish National Testing & Research Institute, Borås (1994
201. Göransson, U., and Lundqvist, A., Fires in Buses and Trains: Fire Test Methods (SP Report 1990:45). Swedish National Testing and Research Institute, Borås (1990).
202. Peacock, R. D., Reneke, P. A., Averill, J. D., Bukowski, R. W., and Klote, J. H., Fire Safety of Passenger Trains. Phase II: Application of Fire Hazard Analysis Techniques (NISTIR 6525), Nat. Inst. Stand. & Technol., Gaithersburg MD (2002).
203. Hansen, P. A., Fire in Tyres: Heat Release Rate and Response of Vehicles (STF25 A95039). SINTEF NBL, Norwegian Fire Research Laboratory, Trondheim (1995).
204. Shipp, M. P., Fire Spread in Tyre Dumps, pp. 79-88 in Interflam '96. Interscience Communications Ltd., London (1996).
205. Murrell, J., and Briggs, P., Developments in European and International Fire Test Methods for Composites Used in Building and Transport Applications, pp. 21-32 in *Proc. 2nd Intl. Conf. on Composites in Fire*, Conference Design Consultants, Newcastle upon Tyne, England (2001).
206. Ingason, H., and Lönnermark, A., Heat Release Rates from Heavy Goods Vehicle Trailer Fires in Tunnels, *Fire Safety J*. 40, 646-668 (2005).
207. Fires in Transport Tunnels. Report on Full-Scale Tests (EUREKA Project EU 499: FIRETUN), Studiengesellschaft Stahlanwendung e.V., Düsseldorf, Germany (1995).
208. Proceedings of the International Conference on Fires in Tunnels, SP - Swedish National Testing and Research Institute, Borås (1994). Distributed by Interscience Communications Ltd, London.
209. Ingason, H., An Overview of Vehicle Fires in Tunnels, pp. 425-434 in *Intl. Conf. on Tunnel Fires and Escape from Tunnels*, Madrid (2001).
210. Mehaffey, J. R., Craft, S. T., Richardson, L. R., and Batista, M., Fire Experiments in Furnished Houses, pp. 163-174 in *Proc. 4th Intl. Symp. on Fire and Explosion Hazards*, FireSERT, Univ. Ulster, Northern Ireland (2004).
211. Stroup, D. W., and Madrzykowski, D., Heat Release Rate Tests of Plastic Trash Containers (FR 4018), Nat. Inst. Stand. & Technol., Gaithersburg MD (2003).
212. Zicherman, J. B., Fire Cause Analysis, Berkeley CA; unpublished tests conducted at the Western Fire Center, Inc. (2008).
213. Fire Tests for Foamed Plastics Used for Decorative Purposes (UL 1975), Underwriters Laboratories Inc., Northbrook IL.
214. Babrauskas, V., Upholstered Furniture Heat Release Rates: Measurements and Estimation, *J. Fire Sciences* 1, 9-32 (1983).
215. Flammability Information Package (Contains Technical Bulletins 116, 117, 121, 133, 106 and 26). Bureau of Home Furnishings, Dept. of Consumer Affairs, State of California, North Highlands (1987).
216. Babrauskas, V., Full-Scale Burning Behavior of Upholstered Chairs (Tech Note 1103), [U. S.] Natl. Bur. Stand., Gaithersburg MD (1979).
217. Mitler, H. E., and Tu, K.-M., Effect of Ignition Location on Heat Release Rate of Burning Upholstered Furniture, pp. 121-122 in Annual Conf. on Fire Research. Book of Abstracts. October 17-20, 1994 (NISTIR 5499), Nat. Inst. Stand. & Technol., Gaithersburg MD (1994).
218. Collier, P. C. R., and Whiting, P. N., Timeline for Incipient Fire Development (Study Report 194), BRANZ, Judgeford, New Zealand (2008).
219. Babrauskas, V., Lawson, J. R., Walton, W. D., and Twilley, W. H., Upholstered Furniture Heat Release Rates Measured with a Furniture Calorimeter (NBSIR 82-2604), [U. S.] Natl. Bur. Stand., Gaithersburg MD (1982).
220. Janssens, M. L., Gomez, C., Huczek, J. P., Overholt, K. J., Ewan, D. M., Hirschler, M. M., Mason, R. L., and Sharp, J. M., Reducing Uncertainty of Quantifying the Burning Rate of Upholstered Furniture (SwRI Project No. 01.15998), Prepared for National Institute of Justice, Southwest Research Institute, San Antonio TX (2012).
221. Medford, R. L., and Ray, D. R., Upholstered Furniture Flammability: Fires Ignited by Small Open Flames and Cigarettes, CPSC, Washington (Oct. 24, 1997).
222. Babrauskas, V., Blum, A., Daley, R., and Birnbaum, L., Flame Retardants in Furniture Foam: Benefits and Risks, pp. 265-278 in *Fire Safety Science—Proc. 10th Intl. Symp.*, Intl. Assn. for Fire Safety Science, London (2011).
223. Babrauskas, V., and Walton, W. D., A Simplified Characterization for Upholstered Furniture Heat Release Rates, *Fire Safety J*. 11, 181-192 (1986).
224. Standard Test Method for Determining the Heat Release Rate of Upholstered Furniture and Mattress Components or Composites Using a Bench-Scale Oxygen Consumption Calorimeter (E 1474-96a). American Society for Testing and Materials, Philadelphia (1996).
225. Edenburn, D., Burning Video Game System (Technical Report), Albemarle Corp., [n.p.] (2003).

226. Babrauskas, V., Bench-Scale Methods for Prediction of Full-Scale Fire Behavior of Furnishings and Wall Linings, SFPE Technical Report 84-10, Society of Fire Protection Engineers, Boston (1984).
227. Wickström, U., and Göransson, U., Prediction of Heat Release Rates of Surface Materials in Large-Scale Fire Tests Based on Cone Calorimeter Results, *J. Testing and Evaluation* 15, 364-370 (1987).
228. Proceedings of the International EUREFIC Seminar 1991, Interscience Communications Ltd, London (1991).
229. Göransson, U., Model, Based on Cone Calorimeter Results, for Explaining the Heat Release Rate Growth of Tests in a Very Large Room, pp. 39-47 in *Interflam '93: Sixth Intl. Fire Conf. Proc.*, Interscience Communications Ltd., London (1993).
230. Sumathipala, K., Kim, A. K., and Lougheed, G. D., A Comparison of ASTM and ISO Full-scale Room Fire Test Methods, pp. 101-110 in *Proc. Fire and Materials, 2nd Intl. Conf.*, Interscience Communications Ltd, London (1993).
231. Sumathipala, K., Kim, A. K., and Lougheed, G. D., Configuration Sensitivity of Full-scale Room Fire Tests, pp. 237-246 in *Proc. Fire and Materials, 3rd Intl. Conf.*, Interscience Communications Ltd, London (1994).
232. Karlsson, B., and Magnusson, S.-E., An Example Room Fire Model, pp. 159-171 in Heat Release in Fires, *op cit.*
233. Karlsson, B., Models for Calculating Flame Spread on Wall Lining Materials and the Resulting Heat Release Rate in a Room, *Fire Safety J.* 23, 365-386 (1994).
234. Magnusson, S. E., and Sundström, B., Combustible linings and room fire growth – A first analysis, pp. 45-69 in Fire Safety Science and Engineering (ASTM STP 882), American Society for Testing and Materials, Philadelphia (1985).
235. Cleary, T. G., and Quintiere, J. G., A Framework for Utilizing Fire Property Tests, pp. 647-656 in *Fire Safety Science--Proc. of the 3rd Intl. Symp.*, Elsevier Applied Science, London (1991).
236. Quintiere, J. G., A Simulation Model for Fire Growth on Materials Subject to a Room-Corner Test, *Fire Safety J.* 20, 313-339 (1993).
237. Quintiere, J. G., Haynes, G., and Rhodes, B. T., Applications of a Model to Predict Flame Spread over Interior Finish Materials in a Compartment, *J. Fire Prot. Engineering* 7, 1013 (1995).
238. Janssens, M., Grexa, O., Dietenberger, M., and White, R., Predictions of ISO 9705 Room/corner Test Using a Simple Model, pp. 73-83 in *Proc. 4th Intl. Fire and Materials Conf.*, Interscience Communications Ltd., London (1995).
239. Lawson, J. R., Walton, W. D., and Twilley, W. H., Fire Performance of Furnishings as Measured in the NBS Furniture Calorimeter. Part 1 (NBSIR 83-2787), U.S. Natl. Bur. Stand., Gaithersburg MD (1983).
240. Peacock, R. D., Reneke, P. A., Averill, J. D., Bukowski, R. W., and Klote, J. H., Fire Safety of Passenger Trains, Phase II: Application of Fire Hazard Analysis Techniques (NISTIR 6525), Nat. Inst. Stand. and Technol., Gaithersburg MD (2002).
241. Janssens, M. L., Heat Release Rate, FORUM Workshop on Measurement Needs for Fire Safety, Nat. Inst. Stand. and Technol., Gaithersburg MD (2000).
242. Smith, D. A., and Shaw, K., Single Burning Item (SBI) Test: The Euroclasses and Transitional Arrangements, pp. 1-9 in *Interflam '99*, Interscience Communications Ltd., London (1999).

Dr. Vytenis Babrauskas is the President of Fire Science and Technology Inc., Issaquah, WA, a company specializing in fire safety research, fire testing issues, and fire science applications to fire investigations and litigations.